

CALIFORNIA AIR RESOURCES BOARD



**CONTRACT NO. A832-128**  
**FINAL REPORT**  
**JANUARY 1991**

# **Spatial Inhomogeneities in SCAQ5 Filters**

**State of California**  
**AIR RESOURCES BOARD**  
**Research Division**



Spatial Inhomogeneities  
in SCAQS Filters

Final Report

Contract No. A832-128

Submitted to:

Research Division  
California Air Resources Board  
1102 Q Street  
P.O. Box 2815  
Sacramento, CA 95812

Submitted by:

Air Quality Group, Crocker Nuclear Lab  
University of California, Davis  
Davis, Ca 95616

Prepared by:

Robert J. Matsumura  
and  
Thomas A. Cahill  
Principal Investigators

January 1991



## ABSTRACT

The PM 10 and PM 2.5 teflon filters collected by the SCAQS sampler during the entire extent of 1987 Southern California Air Quality Study (SCAQS) were non-uniform in deposit due to an error in sampler design. For this reason, the elemental values measured by the EPA (and others), though correct for the area they analyzed, could not be used to establish aerosol concentrations in  $\text{ng}/\text{m}^3$ . To establish the conversion factors needed to convert EPA XRF values into aerosol concentrations, selected filters were laterally scanned by the PIXE proton milliprobe at Davis. These calculated factors ranged from corrections of less than 25% (PM 2.5 sulfur; carbon soot) to over 200% (PM 10 soils). Difficulties were encountered for copper and zinc due to contamination of the filters by brass shavings in the samplers.

#### DISCLAIMER

The statements and conclusions in this report are those of the contractor and not necessarily those of the California Air Resources Board. The mention of commercial products, their source or their use in connection with material reported herein is not to be construed as either an actual or implied endorsement of such products.

#### ACKNOWLEDGMENTS

The authors wish to gratefully acknowledge the support of the the California Air Resources Board, with special thanks to Eric Fujita and Lowell Ashbaugh. We are also grateful for support from ENSR Consulting and Engineering, John Collins. Finally, we wish to thank the students and staff (Brian Perley, Paul Wakabayashi, Jennifer Geerts, etc.) at the Air Quality Group, University of California, Davis who worked on this project.

This report was submitted in fulfillment of ARB Contract #A832-128, UCD-CNL Report #90-102, Spatial Inhomogeneities in SCAQS Filter by Crocker Nuclear Lab, University of California, Davis under the sponsorship of the California Air Resources Board. Work was completed as of January 10, 1991.

## EXECUTIVE SUMMARY

The PM 10 and PM 2.5 filters collected by the SCAQS aerosol sampler during the 1987 Southern California Air Quality Study (SCAQS) were found to have non-uniform particulate deposition. The major non-uniformity was a radially symmetric central peaking, with center/edge ratios that were species dependent. We hypothesize that this was caused by an inadequate transition between the cyclone (1/2" tube x 3/8" pipe) and the filter media, which were 47mm (diameter) stretched teflon filters.

Approximately 80 filters were analyzed at UC Davis on the PIXE milliprobe, which could handle such non-uniformity at the expense of trace sensitivity, with typically 16 separate analyses per filter. Results for PM 10 filters showed mean center/edge ratios that averaged  $5.3 \pm 0.8$  for soils,  $1.24 \pm 0.04$  for sulfur, and  $2.4 \pm 0.4$  for most trace elements. Corresponding values for PM 2.5 were  $2.8 \pm 0.7$  for soils,  $1.15 \pm 0.02$  for sulfur, and  $2.2 \pm 0.2$  for most trace elements, and  $1.5 \pm 0.2$  for lead. Soot was quite uniform across the filter, with a ratio of less than 1.1, PM 10 and PM 2.5.

Other types of non-uniformity were seen, especially correlated Cu/Zn particles, circular annular areas of low deposition, and occasionally a linear slope, edge to edge. However, no systematic behavior was seen between sites, or summer to fall.

These non-uniformities made prior XRF analyses highly uncertain, since the results would depend critically upon the exact shape and location of the x-ray source on each filter. This varied from element to element on the wavelength dispersive system used for most analyses. Factors were derived to convert the prior XRF values to their uniform filter equivalent values. This was required to obtain "correct" atmospheric concentrations in  $\text{ng}/\text{m}^3$ . Tables were developed from statistical studies and correlation plots, presented below:

Global Conversion Factors (XRF/PIXE Scan) as  
Derived from Correlation Plots and Ratios

	Correlations	Ratios
1. XRF/PIXE Standards	1.038	1.038
2. PM 10 Soils, (Na, Mg, Al, Si)	1.13	$1.21 \pm 0.10$
PM 10 Soils, (K, Ca, Ti, Fe, Sr, Zn)	2.09	$2.06 \pm 0.28$
3. PM 10 Sulfur	1.22	$1.25 \pm 0.04$
4. PM 10 Combustion-derived aerosols (Mn, Cu, Zn, Br, Pb, V, Ni)	1.30	$1.39 \pm 0.31$
5. PM 2.5 Soils, (Na, Mg, Al, Si)	1.14	$1.30^* \pm 0.44$
PM 2.5 Soils, (K, Ca, Ti, Fe, Sr, Zr)	1.56	$1.30^* \pm 0.44$
6. PM 2.5 Sulfur	1.30	$1.22 \pm 0.07$
7. PM 2.5 Combustion-derived aerosols (Mn, Cu, Zn, Br, Pb, V, Ni)	1.30	$1.63 \pm 0.33$
* All Soils: $0.82 \pm 0.23$ Summer		
$1.55 \pm 0.21$ Fall		

RECOMMENDATIONS

It is our opinion that the values derived from correlation plots are the most reliable, since individual outlying points and extreme behavior such as seen in Cu (and to a lesser extent, Zn and other trace elements), can be evaluated. On the other hand, the mean ratios (XRF/PIXE scan) give uncertainties that show the high degree of variability between some of the filter results.

However, statistically - speaking, one can derive a global average for the XRF vs PIXE integrated scan comparisons. Only PM 10 soils (K, Ca, Ti, Fe) and chlorine (sea salt) are inconsistent with a global correction factor,  $1.31 \pm 0.17$ , for all secondary aerosols (sulfur) and combustion derived trace elements. For the PM 10 soils (K and heavier) and sea salt, a value of  $2.1 \pm 0.28$  is preferred. Light PM 10 soils have a value of  $1.21 \pm 0.10$  consistent with fine aerosols, despite the strong central peak of coarse aerosols. The reason for this is unknown to us. All corrections factors were calculated ignoring the slight difference in calibration, XRF/PIXE scans =  $1.038 \pm 0.045$ .

It is not our contention that application of such factors will solve the dauntingly complex spatial uniformity and contamination problems of the SCAQS filters. But application of these factors, plus a dose of skepticism about "outlier" values such as seen in Cu and Zn, will result in an improved data set.

TABLE OF CONTENTS

ABSTRACT . . . . .	ii
DISCLAIMER . . . . .	iii
ACKNOWLEDGMENTS . . . . .	iii
EXECUTIVE SUMMARY . . . . .	iv
RECOMMENDATIONS . . . . .	v
TABLE OF CONTENTS . . . . .	vi
LIST OF FIGURES . . . . .	viii
LIST OF TABLES . . . . .	xii
INTRODUCTION . . . . .	1
EXPERIMENTAL TECHNIQUES . . . . .	4
Standards and XRF/PIXE Comparisons . . . . .	4
Visual Description of Samples . . . . .	4
Optical Scans of Absorption . . . . .	5
CONVERSION OF SCANS TO CONCENTRATIONS . . . . .	6
ELEMENTAL SCANS OF CONCENTRATIONS . . . . .	7
PM 10 ELEMENTAL SCANS - SUMMER . . . . .	9
Soil-Like Elements - Si, K, Ca, Ti, Fe . . . . .	9
Sulfur . . . . .	9
Trace Elements - K, Mn, Cu, Zn, Br, Pb . . . . .	9
PM 10 CORRELATION PLOTS, XRF VS PIXE - SUMMER . . . . .	16
Soil-Like Elements - Si, K, Ca, Ti, Fe . . . . .	16
Sulfur . . . . .	16
Trace Elements - Mn, Cu, Zn, Br, Pb . . . . .	16
PM 10 ELEMENTAL SCANS - FALL . . . . .	20
Soil-Like Elements - Si, K, Ca, Ti, Fe . . . . .	20
Sulfur . . . . .	20
Trace Elements - Cl, Mn, Cu, Zn, Br, Pb . . . . .	20
PM 10 CORRELATION PLOTS, XRF VS PIXE - FALL AND SUMMER . . . . .	29
PM 2.5 ELEMENTAL SCANS - SUMMER . . . . .	34
Soil-Like Elements - Si, K, Ca, Ti, Fe . . . . .	34
Sulfur . . . . .	34
Trace Elements - K, Mn, Cu, Zn, Br, Pb . . . . .	34

PM 2.5 CORRELATION PLOTS, XRF VS PIXE - SUMMER . . . . .	43
Soil-Like Elements - Si, K, Ca, Ti, Fe . . . . .	43
Sulfur . . . . .	43
Trace Elements - Mn, Cu, Zn, Br, Pb . . . . .	43
PM 2.5 ELEMENTAL SCANS - FALL . . . . .	47
Soil-Like Elements - Si, K, Ca, Ti, Fe . . . . .	47
Sulfur . . . . .	47
Trace Elements . . . . .	47
Chlorine . . . . .	47
Titanium . . . . .	47
Vanadium . . . . .	55
Manganese . . . . .	55
Copper and Zinc . . . . .	55
Bromine and Lead . . . . .	55
PM 2.5 CORRELATION PLOTS, XRF VS PIXE - FALL AND SUMMER PLUS FALL . . . . .	65
Soil-Like Elements - Si, K, Ca, Ti, Fe . . . . .	65
Sulfur . . . . .	65
Trace Elements . . . . .	65
Chlorine, Titanium, Vanadium . . . . .	65
Manganese . . . . .	65
Copper and Zinc . . . . .	72
Bromine and Lead . . . . .	72
STATISTICAL REDUCTION OF THE DATA . . . . .	77
INTERPRETATION . . . . .	80
SELECTED REFERENCES . . . . .	83

## LIST OF FIGURES

Figure 1:	Hypothetical flow characteristics of particles in SCAQS sampler filter cassettes . . . . .	1
Figure 2:	Soil and sulfur profiles for typical SCAQS filters . . . . .	2
Figure 3:	XRF versus AQS PIXE scan excitation/analysis area . . . . .	3
Figure 4:	Lateral scans of absorption by laser integrating plate method (LIPM) of typical PM 10 and PM 2.5 SCAQS filters . . .	5
Figure 5:	Weighting factors for integration of Gaussian fits for SCAQS PIXE scans . . . . .	6
Figure 6:	Downtown Los Angeles, 06/25/87, period 3 SCAQS PIXE Scans for PM 10: S, K, Ca . . . . .	10
Figure 7:	Downtown Los Angeles, 06/25/87, period 3 SCAQS PIXE Scans for PM 10: Ti, Fe Gaussian fits for PM 10 . . . . .	11
Figure 8:	Gaussian fits for PM 10 Rubidoux, 7/14/87, period 3 Downtown Los Angeles, 08/28/87, period 3 Long Beach, 09/03/87, period 3 . . . . .	12
Figure 9:	SCAQS PIXE Scans for PM 10 Pb: Burbank, 7/14/87, period 3 Pb: Azusa, 7/14/87, period 3 Cr: Burbank, 7/14/87, period 3 . . . . .	13
Figure 10:	Downtown Los Angeles, 9/3/87, period 3 SCAQS PIXE Scans for PM 10: Zn, Cu, Br . . . . .	15
Figure 11:	XRF vs. PIXE Scan correlation plots PM 10: Si, K, Ca, Fe for summer . . . . .	17
Figure 12:	XRF vs. PIXE Scan correlation plot PM 10: S for summer . . . . .	18
Figure 13:	XRF vs. PIXE Scan correlation plot PM 10: Zn for summer . . . . .	19
Figure 14A:	Downtown Los Angeles, 11/12/87, period 5 SCAQS PIXE Scans for PM 10: Si, K, Ca . . . . .	21
Figure 14B:	Downtown Los Angeles, 11/12/87, period 5 SCAQS PIXE Scans for PM 10: Ti, Fe . . . . .	22

Figure 15:	Gaussian fits for PM 10 Rubidoux, 12/10/87, period 3 Burbank, 11/12/87, period 3 Downtown Los Angeles, 11/12/87, period 5 . . . . .	23
Figure 16:	SCAQs PIXE scans for PM 10: S Anaheim, 11/12/87, period 3 . . . . .	24
Figure 17:	SCAQs PIXE scans for PM 10: Cl, Mn Downtown Los Angeles, 11/12/87, period 5 . . . . .	25
Figure 18:	SCAQs PIXE scans for PM 10 Zn, Cu: Hawthorne, 11/12/87, period 3 Cu, Zn: Burbank, 11/12/87, period 3 . . . . .	26
Figure 19:	SCAQs PIXE scans for PM 10 Cu, Zn: Long Beach, 12/11/87, period 3 . . . . .	27
Figure 20:	SCAQs PIXE scans for PM 10 Pb: Hawthorne, 11/12/87, period 3 Br, Pb: Downtown Los Angeles, 11/12/87, period 3 . . . . .	28
Figure 21:	XRF vs. PIXE Scan correlation plot PM 10: Zn for summer and fall . . . . .	30
Figure 22:	XRF vs. PIXE Scan correlation plot PM 10: Si for summer and fall . . . . .	31
Figure 23:	XRF vs. PIXE Scan correlation plot PM 10: Soils for summer and fall . . . . .	32
Figure 24:	XRF vs. PIXE Scan correlation plots for PM10 Cu, Mn, Zn, Pb for summer and fall . . . . .	33
Figure 25:	SCAQs PIXE scans for PM 2.5: Si, K, Ca, Fe Downtown Los Angeles, 07/14/87, period 3 . . . . .	35
Figure 26A:	SCAQs PIXE scans for PM 2.5: Si, K, Ca Azusa, 07/14/87, period 3 . . . . .	36
Figure 26B:	SCAQs PIXE scans for PM 2.5 Ti, Fe: Azusa, 07/14/87, period 3 Fe: Rubidoux, 07/14/87, period 3 . . . . .	37
Figure 27:	SCAQs PIXE scans for PM 2.5: Si, K, Ca Rubidoux, 07/14/87, period 3 . . . . .	38
Figure 28:	SCAQs PIXE scans for PM 2.5: S Downtown Los Angeles, 07/14/87, period 3 Azusa, 07/14/87, period 3 Rubidoux, 07/14/87, period 3 . . . . .	39

Figure 29:	Gaussian fits for PM 2.5 Azusa, 07/14/87, period 3 Downtown Los Angeles, 07/14/87, period 3 Rubidoux, 07/14/87, period 3 . . . . .	40
Figure 30:	SCAQs PIXE scans for PM 2.5: Cu, Zn Downtown Los Angeles, 07/14/87, period 3 . . . . .	41
Figure 31:	SCAQs PIXE scans for PM 2.5: Cu, Zn, Br: Downtown Los Angeles, 08/28/87, period 3 Br: Downtown Los Angeles, 08/27/87, period 3 . . . . .	42
Figure 32:	XRF vs. PIXE Scan correlation plots PM 2.5: Si, K, Ca, Fe for summer . . . . .	44
Figure 33:	XRF vs. PIXE Scan correlation plot PM 2.5: S for summer . . . . .	45
Figure 34:	XRF vs. PIXE Scan correlation plots PM 2.5: Cu, Zn, Br for summer . . . . .	46
Figure 35:	SCAQs PIXE scans for PM 2.5: Si, K, Ca, Fe: Downtown Los Angeles, 11/12/87, period 3 . . . . .	48
Figure 36:	SCAQs PIXE scans for PM 2.5: Si, K, Ca, Fe: Long Beach, 11/12/87, period 1 . . . . .	49
Figure 37:	SCAQs PIXE scans for PM 2.5: Si, Fe, K, Ca: Burbank, 11/12/87, period 3 . . . . .	50
Figure 38:	SCAQs PIXE scans for PM 2.5: S Downtown Los Angeles, 11/12/87, period 3 Long Beach, 11/12/87, period 1 Burbank, 11/12/87, period 3 . . . . .	51
Figure 39:	Gaussian fits for PM 2.5 Downtown Los Angeles, 11/12/87, period 3 Long Beach, 11/12/87, period 1 Burbank, 11/12/87, period 3 . . . . .	52
Figure 40:	SCAQs PIXE scans for PM 2.5: Cl Anaheim, 12/10/87, period 3 . . . . .	53
Figure 41:	SCAQs PIXE scans for PM 2.5: Ti Downtown Los Angeles, 11/12/87, period 5 Long Beach, 11/12/87, period 1 Downtown Los Angeles, 12/11/87, period 3 Anaheim, 12/11/87, period 3 . . . . .	54
Figure 42:	SCAQs PIXE scans for PM 2.5: V Hawthorne, 11/12/87, period 3 . . . . .	56

Figure 43:	SCAQs PIXE scans for PM 2.5: Mn Long Beach, 11/12/87, period 1 Downtown Los Angeles, 11/12/87, period 2 Downtown Los Angeles, 11/12/87, period 5 . . . . .	57
Figure 44:	SCAQs PIXE scans for PM 2.5 Cu, Zn: Downtown Los Angeles, 11/12/87, period 1 Cu, Zn: Downtown Los Angeles, 11/12/87, period 2 . . . . .	58
Figure 45:	SCAQs PIXE scans for PM 2.5 Cu, Zn: Downtown Los Angeles, 11/12/87, period 3 Cu, Zn: Downtown Los Angeles, 11/12/87, period 5 . . . . .	59
Figure 46:	SCAQs PIXE scans for PM 2.5 Cu, Zn: Downtown Los Angeles, 12/11/87, period 3 Cu, Zn: Anaheim, 12/11/87, period 3 . . . . .	60
Figure 47:	SCAQs PIXE scans for PM 2.5 Br, Pb: Downtown Los Angeles, 11/12/87, period 5 Br: Long Beach, 11/12/87, period 5 Br: Long Beach, 11/12/87, period 1 . . . . .	61
Figure 48:	SCAQs PIXE scans for PM 2.5 Br, Pb: Downtown Los Angeles, 11/12/87, period 1 Br, Pb: Anaheim, 12/10/87, period 3 . . . . .	63
Figure 49:	SCAQs PIXE scans for PM 2.5: Pb Burbank, 11/12/87, period 3 Long Beach, 11/12/87, period 1 Downtown Los Angeles, 11/12/87, period 3 . . . . .	64
Figure 50:	XRF vs. PIXE Scan correlation plots PM 2.5: Si, K, Ca, Fe for fall . . . . .	66
Figure 51:	XRF vs. PIXE Scan correlation plots PM 2.5: Si, K, Ca, Fe for summer and fall . . . . .	67
Figure 52:	XRF vs. PIXE Scan correlation plots PM 2.5: Soils, Ti for summer and fall . . . . .	68
Figure 53:	XRF vs. PIXE Scan correlation plots PM 2.5: S for fall PM 2.5: S for summer and fall PM 2.5 and PM 10: S for summer and fall . . . . .	69
Figure 54:	XRF vs. PIXE Scan correlation plot PM 2.5: Ti for fall . . . . .	70
Figure 55:	XRF vs. PIXE Scan correlation plot PM 2.5: Mn for summer and fall . . . . .	71

Figure 56:	XRF vs. PIXE Scan correlation plots	
	PM 2.5: Cu for fall	
	PM 2.5: Zn for fall . . . . .	73
Figure 57:	XRF vs. PIXE Scan correlation plots	
	PM 2.5: Cu for summer and fall	
	PM 2.5: Zn for summer and fall . . . . .	74
Figure 58:	XRF vs. PIXE Scan correlation plot	
	PM 2.5 and PM 10: Zn for summer and fall . . . . .	75
Figure 59:	XRF vs PIXE Scan correlation plots	
	PM 2.5: Br for fall	
	PM 2.5: Pb for fall . . . . .	76

LIST OF TABLES

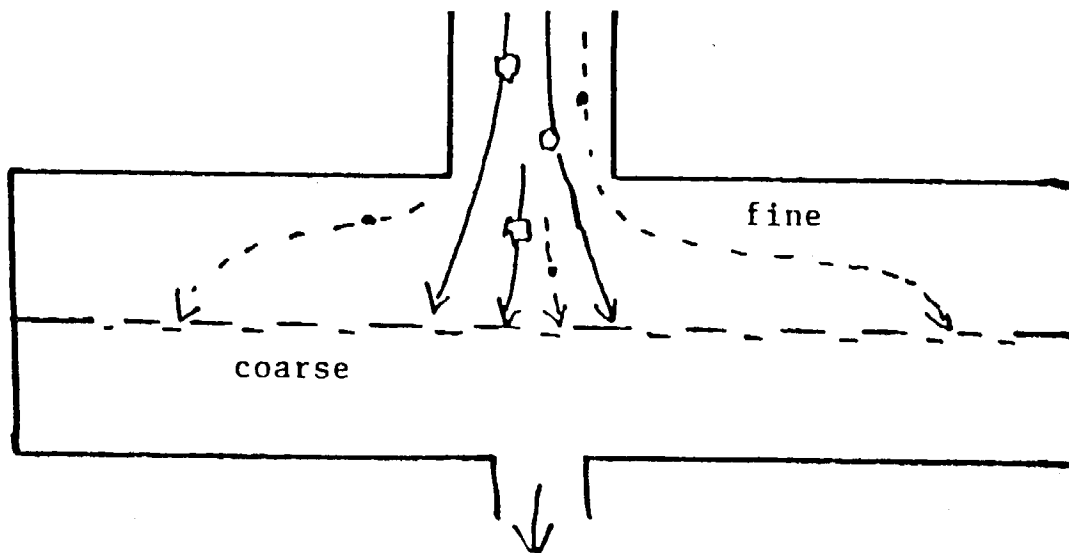
Table 1:	Degree of Central Peaking of PM 10 Filters	
	[ (average of 2 highest / average of 3 lowest) ] . . . . .	77
Table 2:	Mean ratios of XRF to PIXE Scan Concentrations for PM 10 Filters	78
Table 3:	Degree of Central Peaking of PM 2.5 Filters	
	[ (average of 2 highest / average of 3 lowest) ] . . . . .	78
Table 4:	Mean ratios of XRF to PIXE Scan Concentrations for PM 2.5 Filters	79
Table 5:	Conversion Factors (XRF/PIXE Scan)	
	as Derived from Correlation Plots . . . . .	80
Table 6:	Global Conversion Factors (XRF/PIXE Scan)	
	as Derived from Correlation Plots and Ratios . . . . .	81



## INTRODUCTION

The SCAQS aerosol samplers were used at up to 11 sites to collect air filters for subsequent elemental analysis by X-Ray Fluorescence (XRF). One assumption used in these XRF analyses to convert from areal density of an element ( $\text{ng}/\text{cm}^2$ ) to an aerosol concentration ( $\text{ng}/\text{m}^3$ ) is that the deposit is uniform across the filter. Unfortunately, the samples delivered by the SCAQS sampler were not uniform, and routinely exhibited a higher concentration of mass in the center of the filter. This was due to a poor coupling between the aerosol intake and the filter, shown schematically below<sup>1</sup> (and described in Appendix A).

Figure 1. Hypothetical flow characteristics of particles in SCAQS sampler filter cassettes.



Larger particles were unable to make the sharp bend, and were impacted on the center of the filter. Most fine particles made it to the edge of the filter. The result was a filter deposit with a profile as shown in Figure 2.

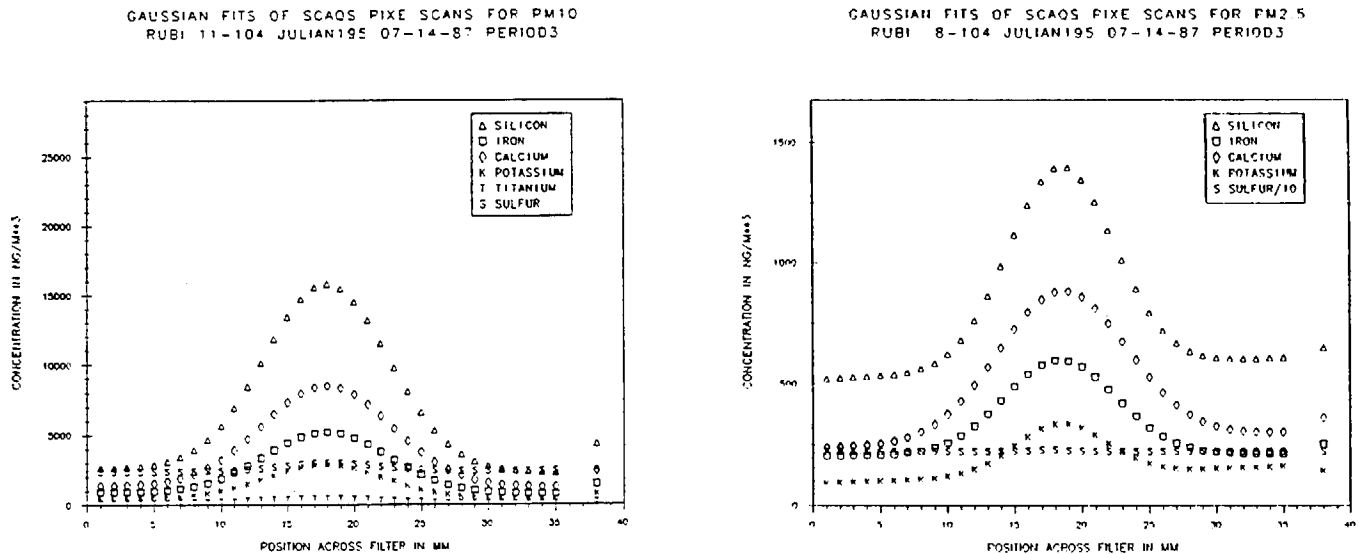


Figure 2: Soil and sulfur profiles for typical SCAQS filter (PM 10 and PM 2.5)

Clearly, if the XRF analysis system analyzed only the very center of the filter, it would see a mixture of coarse soil particles plus fine sulfur and soot particles (as an example). Conversely, analysis of an edge would not show as much soil. Multiplication of either XRF value ( $\text{ng}/\text{cm}^2$ ) by the conversion factor (filter area / volume of air) would then give an incorrect measure of concentration ( $\text{ng}/\text{m}^3$ ) and an incorrect ratio of elements present, confounding chemical mass balance (CMB) analyses and other interpretive models. Note that such an error would not occur for analyses that dissolve or burn material off the filter, such as ion chromatography (ions) or combustion techniques (carbon species).

Since the filters appeared by eye to be uniform, the error was not detected until XRF elemental analyses by different but credible laboratories showed differences outside the uncertainty units of each group<sup>2</sup>. After discussions between the California Air Resources Board (CARB) and members of the Air Quality Group, Crocker Nuclear Laboratory, UC Davis (AQG), it was decided to use the AQG external proton milliprobe to confirm the problem and develop correction factors to convert Environmental Protection Agency (EPA) XRF values into ambient concentrations. The reason the AQG could do this was that the proton beam used

in its Proton Induced X-ray Emission (PIXE) analyses could be made 2mm wide by 4.2mm high<sup>3,4</sup> (Appendix B). Each filter could be stepped across the beam in typically 16 steps, analyzing from edge to center to edge. This is shown below in Figure 3.

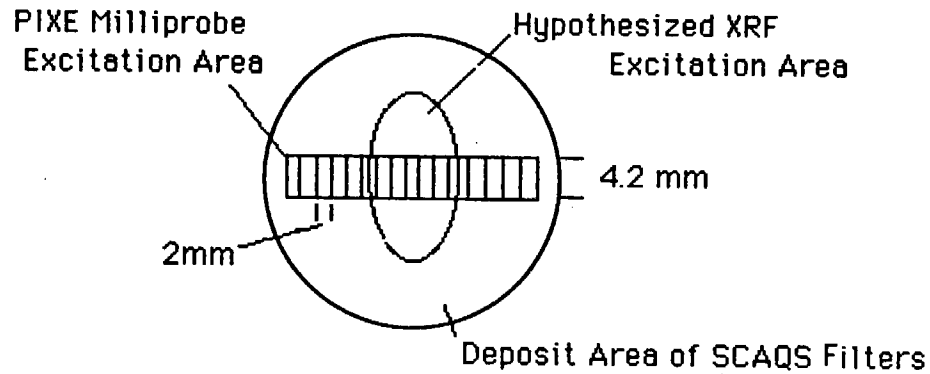


Figure 3: XRF versus AQG PIXE scan excitation/analysis area

The resulting elemental analyses, when folded into an area function, gave a true mean areal density ( $\text{ng}/\text{cm}^2$ ) for direct conversion into correct ambient concentrations ( $\text{ng}/\text{m}^3$ ). The result of this exercise is a conversion factor that divides each XRF value, element by element, to calculate correct ambient concentrations ( $\text{ng}/\text{m}^3$ ).

## EXPERIMENTAL TECHNIQUES

### Standards and XRF/PIXE Comparisons

The standards used in this program included the thin single or dual-element foils provided by Micromatter, Inc., of Washington, and a number of NBS multiple element standards. Each group maintained independent calibration standards for their analyses, but a selected set was analyzed twice during the PIXE milliprobe scans at Davis.

The samples included seven Micromatter foils, NBS 997 and NBS 1417 multielemental standards, and several EPA filters. The mean result of each sample type, in two different analytical periods, was

$$\frac{\text{XRF}}{\text{PIXE}} = 1.038 \pm 0.045.$$

Since these samples were uniform, this represents a small analytical offset, most visible in the Ti-V region. Full analyses are included in Appendix C.

### Visual Description of Samples

Each filter was examined visually upon receipt at Davis. Full descriptions of a few of them are included as Appendix D, and these were typical of the entire set.

There appeared to be two sets of relevant observations about the filters:

1. Those features that appeared to be due to the sampling.
2. Those features that were most likely generated after sampling.

The features that were probably due to sampling included a series of white arcs on the filters, sometimes faint, sometimes strong. We judged that these were caused by lightly loaded areas in which air flow was hindered by some sort of circular support grid behind the filter: Since any analysis that included part of such an arc would have less mass than a uniform area, we carefully aligned all PIXE scans to avoid them, but we could not be sure we missed the faint arcs in all cases. It is not certain, however, that prior XRF analyses took these into account. No documentation we received even mentioned this problem. Our estimate is that for a 1 cm<sup>2</sup> analysis area, the arcs could reduce the results by 20 to 30%, at most.

The second feature was small holes at the edge of a few of the filters. If these holes were present during sampling, air would preferentially pass through them, reducing collected mass on the rest of the filter. Such holes are rare in 25mm and 37mm filters, but much more common in 47mm filters (stretched teflon with ring support). Such holes would reduce the measured mass, but we have no quantitative estimate of the effect.

The features that appeared to date from after sampling included a browning of the center of lightly loaded filters (so that the color change could be seen, especially on the back or clean side of the filter). We have studied such effects, and anticipate negligible problems from them.

There were also a number of large contamination particles on the filters (see Appendix D) which we tried to avoid with our PIXE scans. This may be relevant to our Cu/Zn values, as shown later, but could also affect other species.

### Optical Scans of Absorption

The filters appeared to be uniformly grey, other than the problems mentioned earlier. The color was consistent with soot, normally present in a very fine particle.

To perform quantitative analyses of the filter absorption, scans were made with a modification of the AQG laser integrating plate method (LIPM) system<sup>5,6</sup>. The scans, since they are insensitive to scattering, are most likely dominated by carbon soot. Figure 4 gives two examples, one for PM 10 and one for PM 2.5. Others were made, and they will be found in Appendix E. There is a modest degree of central peaking in the PM 10, but essentially none for PM 2.5. This is to be expected, since both PM 10 and PM 2.5 absorptions are caused by particles that may be as small as  $D_p = 0.1\mu\text{m}$ , or even less.

LONG BEACH JULIAN 195 07/25/90 PERIOD 3 PM 10 & PM 2.5 FILTERS

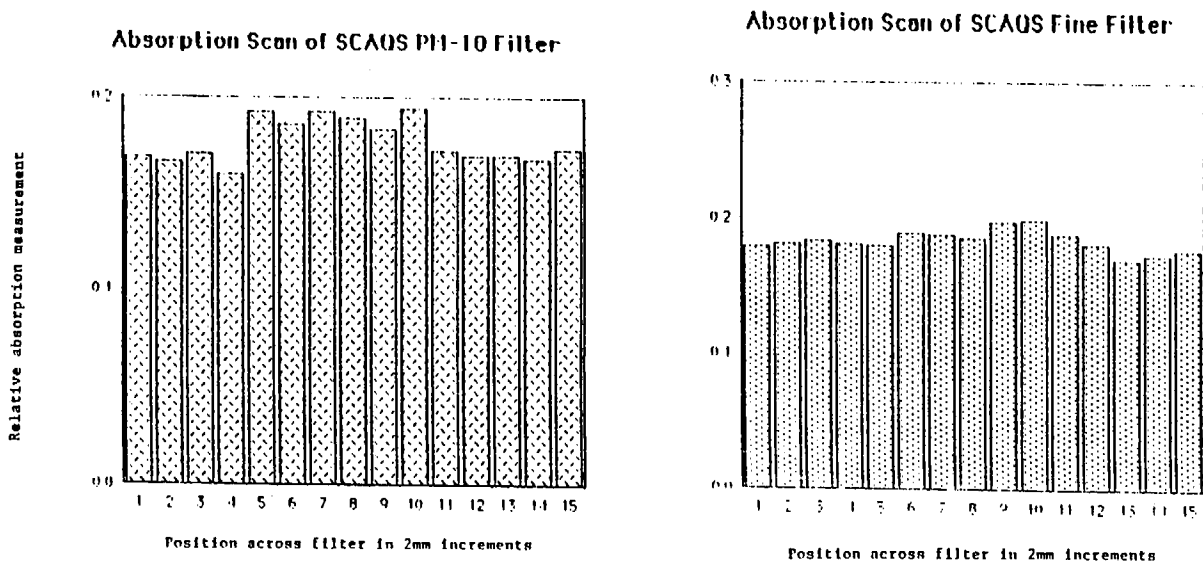


Figure 4: Lateral scans of absorption by laser integrating plate method (LIPM) of typical PM 10 and PM 2.5 SCAQS filters

### CONVERSION OF SCANS TO CONCENTRATIONS

The PIXE scans described above can be characterized in a number of ways. The most obvious is the ratio of central maximum to edge concentrations. A better way, however, is a fit to a central gaussian plus a linear component. This was done for all scans, and yielded the width (full width, half-maximum of the Gaussian, or FWHM) of the central peak.

These data can then be integrated azimuthally around the filter, using a weighting function for the area of each concentric ring. This is shown below in Figure 5. The area of the outer edges of the filter dominate the weighting function since the central region contains little area. This has an unfortunate impact on any analysis that has a small area of excitation centered on the middle of the filter, as is often the case. The result of such an analysis would represent only the central area of the filter and therefore the central maximum of the deposit area, so the conversion to  $\text{ng}/\text{m}^3$  would be in gross error.

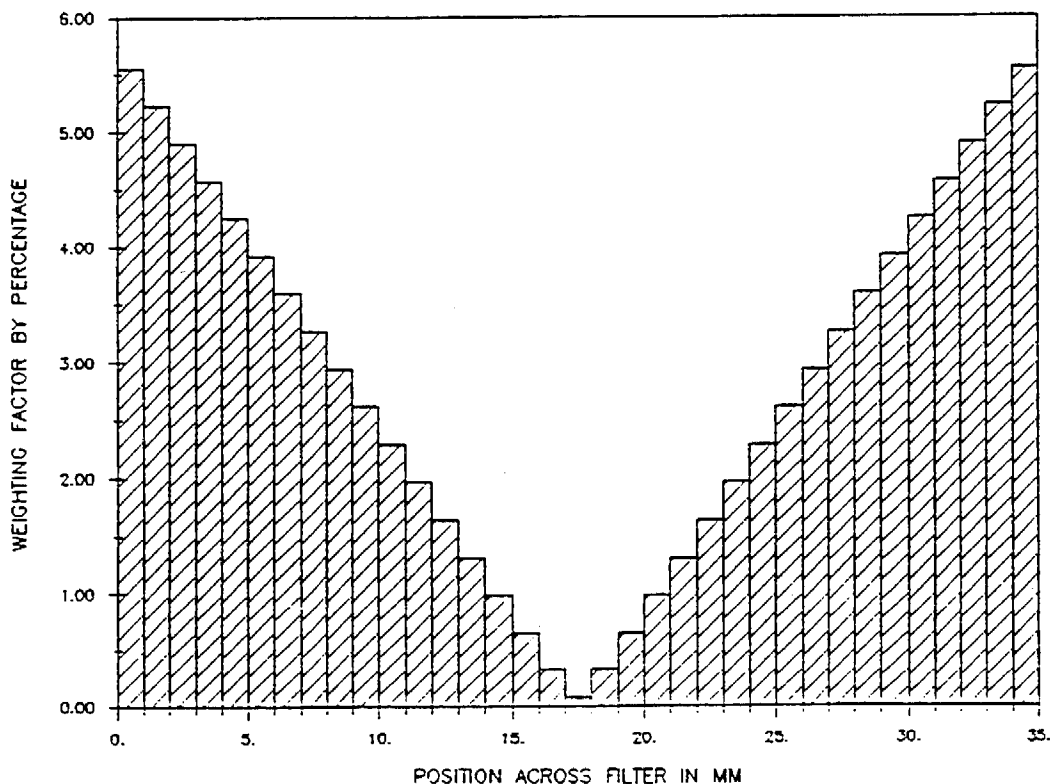


Figure 5: SCAQS PIXE Scans Weighting Factors for Integration of Gaussian Fits

In PM 10 samples, center to edge ratios of 6 have been seen, resulting in a value that could be high by as much as 300%. In practice, analytical areas are usually larger than  $2\text{mm} \times 4.2\text{mm}$ , and such extreme ratios were not found in the actual results. However, this is the reason that the AQG has always magnetically scanned its proton beam to cover 50 to 80% of the diameter of each filter, covering 40 to 65% of the filter area.

## ELEMENTAL SCANS OF CONCENTRATIONS

Scans were made of elemental concentrations across SCAQS filters in order to establish concentration profiles. For this purpose, the new PIXE milliprobe beam line, normally used for Davis Rotating-Drum Unit for Monitoring<sup>4</sup> (DRUM) scans, was modified to analyze SCAQS filters. For descriptions of milliprobes, and XRF and PIXE analyses, please refer to Appendix F. Quality assurance protocols were developed, using the Micromatter™ thin foil standards used in our normal scanned-beam PIXE set-up. However, this was a new protocol, and has not yet the extensive track record of our existing system.

Once the selected filter had been mounted, it was positioned so that the first scan was just inside the polyolefin ring. The beam spot was 2mm x 3mm, but since the filter was at a 45° angle, the effective area was 2mm x 4.2mm. Scans were then made every 2mm across the diameter of the filter chosen to have the least non-uniformities visible by eye. Typically 16 to 18 valid locations could be scanned. The ones closest to each edge were often rejected due to increased blank thickness (plastic from the ring support) or, occasionally, large elemental spikes often seen at the very edge of filters. Since this location was also the site of many of the visible particles (contamination), and since no XRF analyses would have ever seen them, these results were deleted from the plots.

The sensitivity of the scans, in terms of minimum detectable limits for each element, was reduced by the desire not to damage the samples already fragile from prior handling and analysis. Some of the first batch of samples sent to Davis were damaged in transit, and thus great care had to be exercised with further handling and ion beam intensity. The beam area used for each scan, 0.084 cm<sup>2</sup>, is much less than that used for normal analyses, 0.5 cm<sup>2</sup>, and the beam current had to be reduced. It would not do to have the filter fail half-way through an analysis. In fact, none failed during these tests, but detectable limits were much higher than our normal ones.

With the advice of the Research Division, California Air Resources Board (Eric Fujita) filters were selected to test hypotheses concerning filter non-uniformity. Since scanning each individual filter required 15 to 18 PIXE analyses, only a limited number of filters could be scanned. Therefore, filters to be analyzed were selected to be representative of factors which could affect filter non-uniformity such as season (summer vs fall), particle size (PM 10 vs PM 2.5), site (filters from all sites and SCAQS samplers were analyzed), sample period (day vs night), SCAQS sampling episodes, etc. After the selection of filters, the prime question of our work was the following:

Could factors be developed to convert the extensive EPA XRF data set for the non-uniformity of the samples?

This was made more complex by the nature of the wavelength dispersive EPA XRF system. It uses a series of fixed channels and a variable (wavelength scanned) channel to cover a wide elemental range<sup>7</sup>. The shape, location, profile, and effective area of excitation, for each element and detection channel, was not recorded. Therefore, no first principle correction factors can be calculated to compare with the true values measured by the filter scans. Thus, we must mainly

rely upon the slope of correlation plots between XRF and PIXE integrated scan values. Fortunately, most of these are highly linear, and correction factors have been developed for many elements.

The number of data points generated in this exercise was very large. Altogether, almost 80 scans were made in this project, each scan averaged 16 analyses, plus numerous quality assurance tests. Typically, between 10 and 20 elements were examined for each analysis. Many such examples are given in Appendix G (PM 10) and Appendix H (PM 2.5), but many more were never plotted on hard copy if they were consistent with other analyses. All valid SCAQS data scans (54) were used for the correlation plots that established correction factors. The ones presented in the next sections are examples chosen as typical.

## PM 10 ELEMENTAL SCANS - SUMMER

### Soil-Like Elements - Si, K, Ca, Ti, Fe

The aerodynamics of the SCAQS sampler were such that a well developed velocity profile was doubtless established across the duct between the PM 10 intake and the filter. Thus, large particles such as soil particles, which occur above  $D_p = 5\mu\text{m}$  in Los Angeles aerosols should impact on the filter center. Therefore, it was no surprise to find soil elements (Al, Si, K, Ca, Ti, Mn, Fe, ...) peaked on the center of the filter, summer and fall, at every SCAQS site. Figure 6 shows the profile for Downtown Los Angeles (DOLA) for 6/25/87, period 3, for silicon, potassium, and calcium. Figure 7 shows the profile for Ti, Fe, and a summary of the above, plus sulfur. Each plot includes the data, a simple smoothing of the data, and a Gaussian fit to the data with a linear component. On the right hand edge of the plot is found the average of the smoothed PIXE results, the integration of the actual data with the radial weighing factor of Figure 5, and the quoted XRF value. Since the XRF excitation/analysis area did not extend to the edge of the filter, it weighted the central maximum more heavily than the edge, giving a result generally higher than the true value of the weighted or integrated scan. Thus, the ratio of these two values is the correction factor to bring the XRF values into a "uniform filter" equivalency necessary for conversion into  $\text{ng}/\text{m}^3$ .

The last graph of Figure 7 also shows sulfur, which is much more uniform across the filter.

Several points should be noted. The width of the distributions is approximately constant, a great aid in the analysis. The plots are generally centered the same way also, close to the geometrical center of the filter. However, the plots are not exactly scaled to each other, and the linear (flat) component is lower for calcium than other soil-like elements. The linear component could represent a fine particle, non-soil component in the aerosol that behaves like sulfur and carbon soot.

Figure 8 shows similar summaries for Rubidoux (RUBI), 7/14/87, period 3; DOLA, 8/28/87, period 3; and Long Beach (LOBE), 9/3/87, period 3. Soils at each site behave in a similar fashion, but the ratios and the flat non-gaussian (fine particle) component varies.

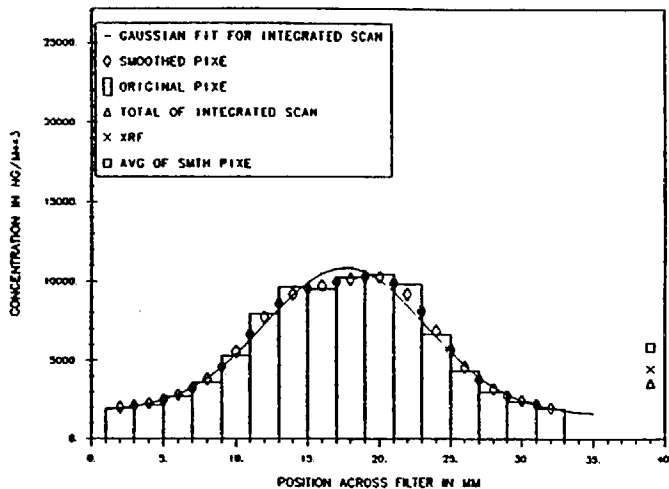
### Sulfur

Sulfur varies both in amount and in profile, with some central peaking (coarse particle component) visible in many samples such as DOLA, 8/28/87, period 3 (Figure 8).

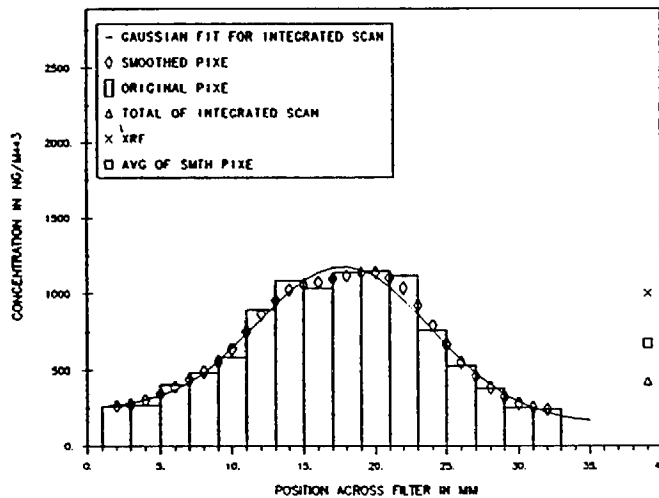
### Trace Elements - K, Mn, Cu, Zn, Br, Pb

Potassium could have both a fine component (smoke tracer) and coarse component (soil). Generally, in these samples potassium had no more fine component than iron or calcium, both of which were overwhelmingly soil derived, and thus we can assign it to soils.

SCAQ5 PIXE SCANS FOR PM10 SI; CHISO = 0.81  
DOLA 11-207 JULIAN176 06-25-87 PERIOD3



SCAQ5 PIXE SCANS FOR PM10 K; CHISO = 0.44  
DOLA 11-207 JULIAN176 06-25-87 PERIOD3



SCAQ5 PIXE SCANS FOR PM10 CA; CHISO = 1.79  
DOLA 11-207 JULIAN176 06-25-87 PERIOD3

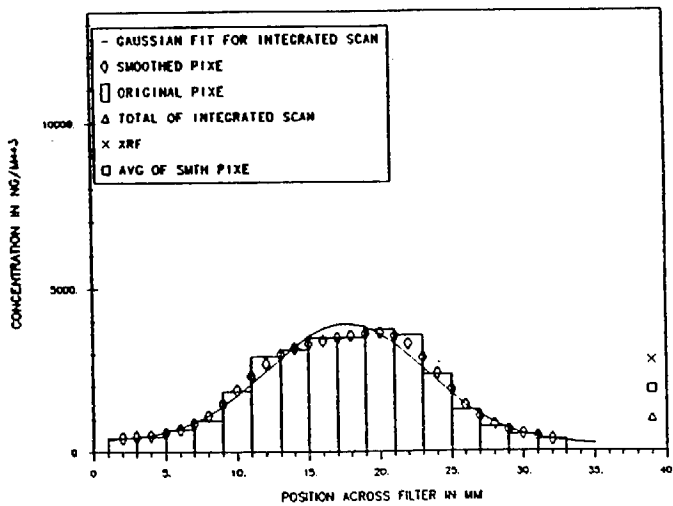
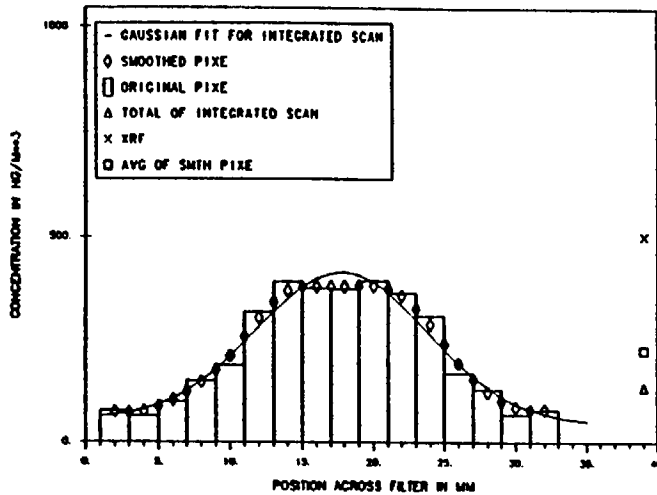
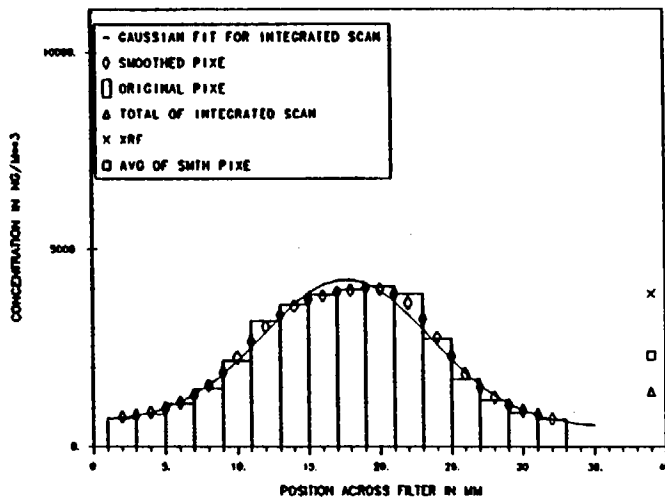


Figure 6

SCAQ5 PIXE SCANS FOR PM10 TI; CHISQ = 0.46  
 DOLA 11-207 JULIAN176 06-25-87 PERIOD3



SCAQ5 PIXE SCANS FOR PM10 FE; CHISQ = 0.79  
 DOLA 11-207 JULIAN176 06-25-87 PERIOD3



GAUSSIAN FITS OF SCAQ5 PIXE SCANS FOR PM10  
 DOLA 11-207 JULIAN176 06-25-87 PERIOD3

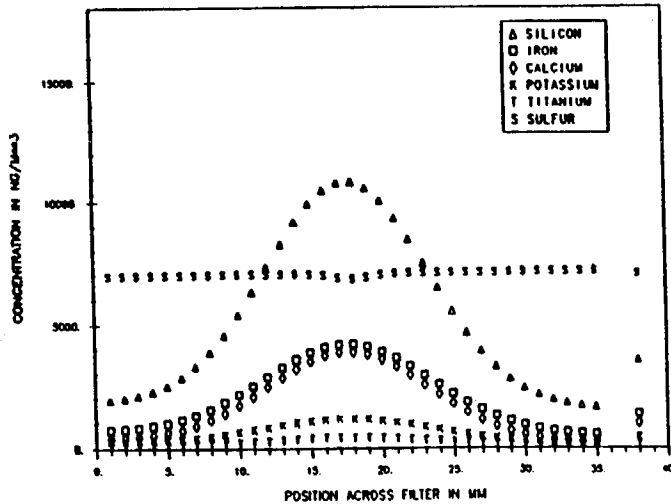
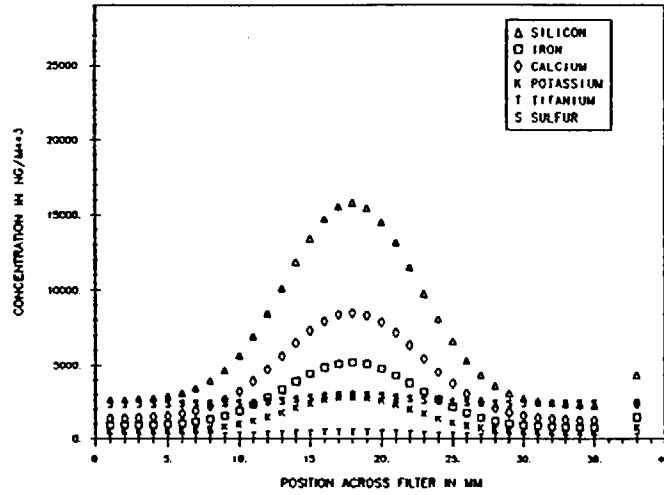
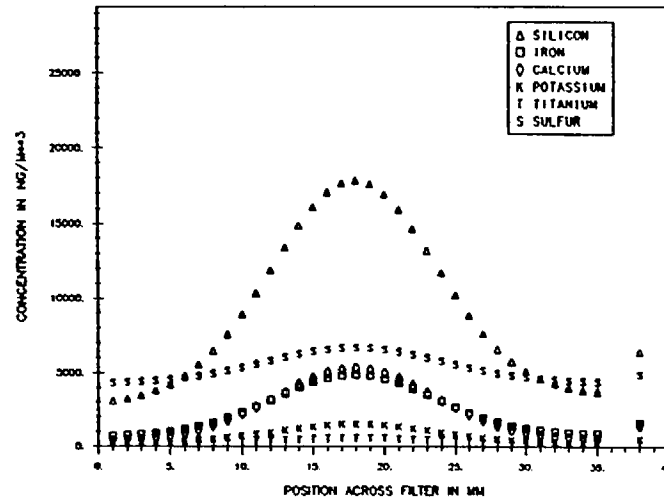


Figure 7

GAUSSIAN FITS OF SCAQS PIXE SCANS FOR PM10  
RUBI 11-104 JULIAN195 07-14-87 PERIOD3



GAUSSIAN FITS OF SCAQS PIXE SCANS FOR PM10  
DOLA 11-450 JULIAN240 08-28-87 PERIOD3



GAUSSIAN FITS OF SCAQS PIXE SCANS FOR PM10  
LOBE 11-575 JULIAN246 09-03-87 PERIOD3

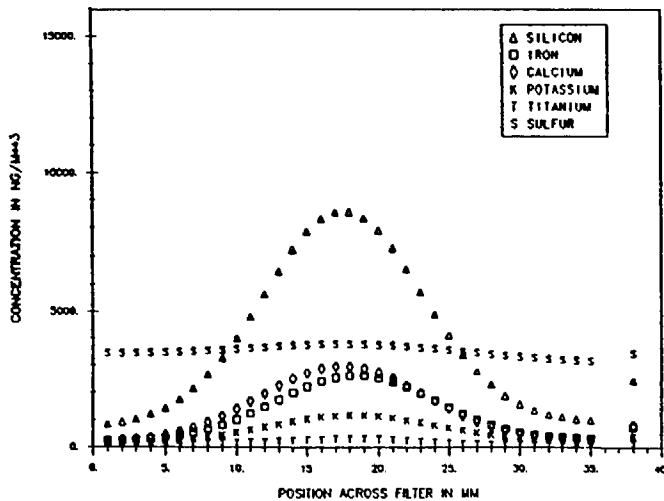
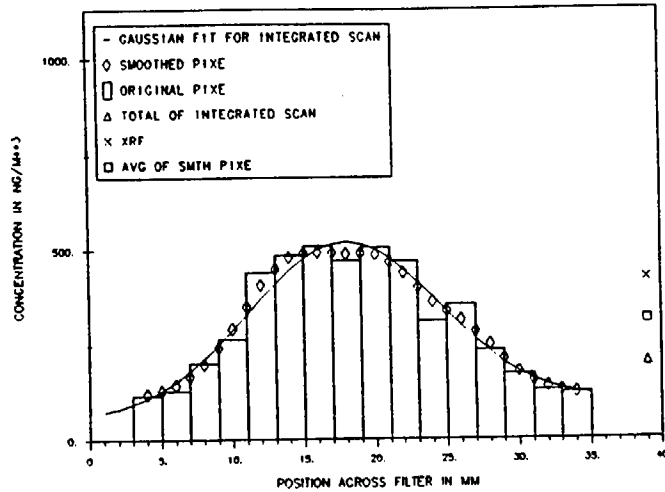
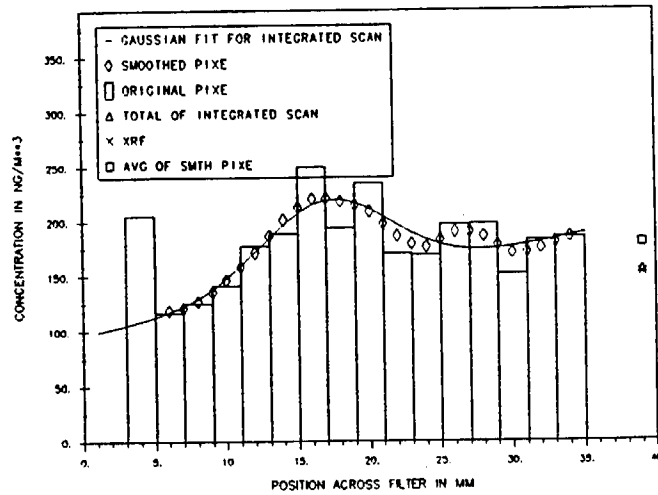


Figure 8

SCAQ5 PIXE SCANS FOR PM10 PB: CHISQ = 0.48  
 BURB 11-088 JULIAN195 07-14-87 PERIOD3



SCAQ5 PIXE SCANS FOR PM10 PB: CHISQ = 0.10  
 AZUS 11-040 JULIAN195 07-14-87 PERIOD3



SCAQ5 PIXE SCANS FOR PM10 CR: CHISQ = 0.15  
 BURB 11-088 JULIAN195 07-14-87 PERIOD3

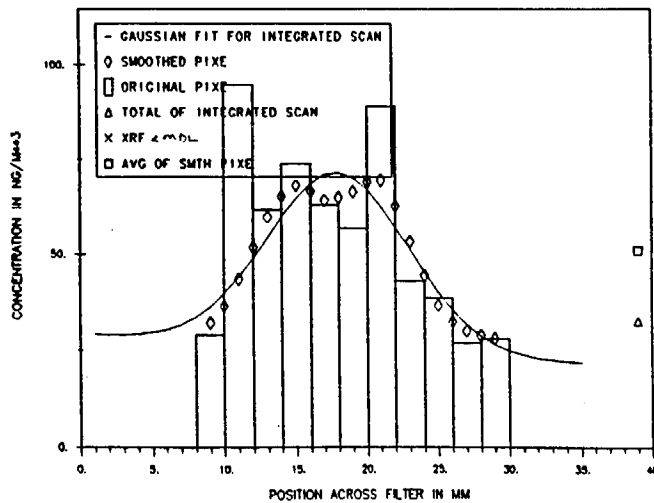
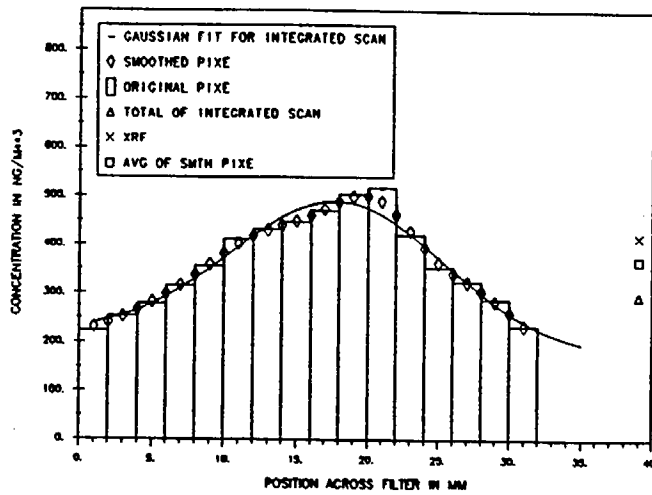


Figure 9

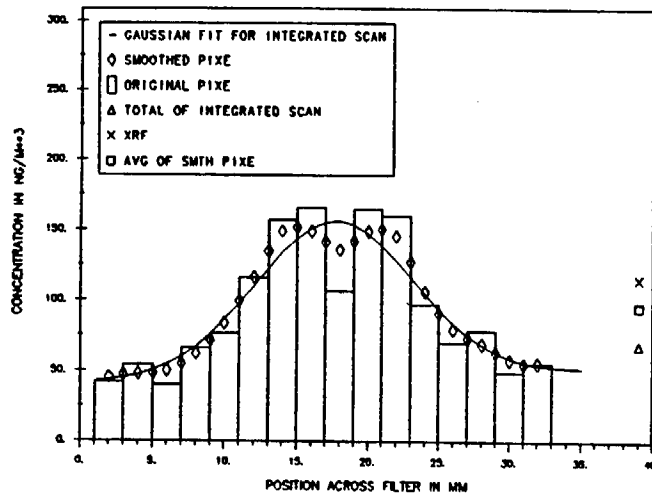
Figure 9 shows scans of PM 10 filters for lead (Pb) on 7/14/87, period 3 at Burbank (BURB) and Azusa (AZUS), as well as chromium (Cr) at Burbank. Note the soil-like profile for BURB, very different than AZUS at the same time which has the much more uniform (though slanted) profile of a fine aerosol like sulfur. Chromium has an intermediate profile. These results challenge simplistic interpretations of particulate size-composition profiles in the South Coast Air Basin, assuming that samples were collected by equivalent samplers. To a reasonable approximation, all sites had similar soil and sulfur profiles during summer. Thus, the variable profiles for trace elements cannot be ascribed to sampler variability.

Figure 10 shows bromine (Br) at Los Angeles, 8/28/87, period 3 with a profile looking more like soil than sulfur, but closely resembling the lead of Burbank in Figure 9. Finally, copper (Cu) and Zinc (Zn) are shown for Los Angeles on 9/3/87, again at period 3. These scans are well behaved, in contrast with many others which show sharp spikes at random locations for Cu and Zn.

SCAQ5 PIXE SCANS FOR PM10 ZN: CHISO = 0.26  
 DOLA 11-543 JULIAN246 09-03-87 PERIOD3



SCAQ5 PIXE SCANS FOR PM10 CU: CHISO = 0.57  
 DOLA 11-543 JULIAN246 09-03-87 PERIOD3



SCAQ5 PIXE SCANS FOR PM10 BR: CHISO = 0.20  
 DOLA 11-450 JULIAN240 08-28-87 PERIOD3

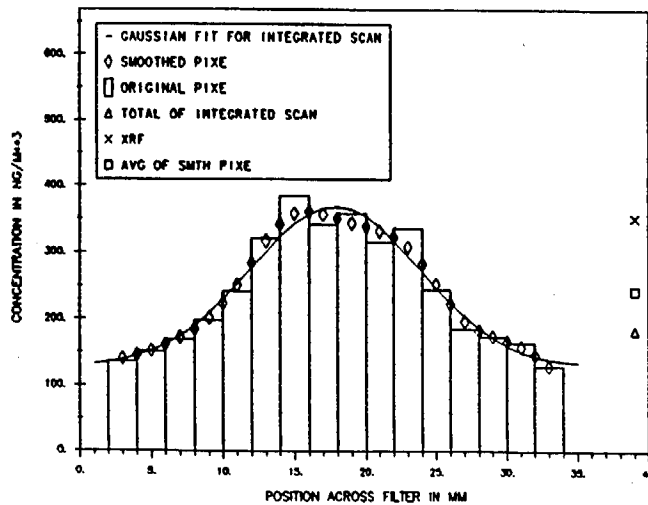


Figure 10

## PM 10 CORRELATION PLOTS, XRF VS PIXE - SUMMER

With the results of the PIXE integrated scans, we now have the true mean areal density and correct ambient concentrations of the filters examined. These can now be compared to the XRF results in order to find the equivalency factors to convert XRF values to  $\text{ng}/\text{m}^3$ .

### Soil-Like Elements - Si, K, Ca, Ti, Fe

Figure 11 shows the results for silicon, potassium, calcium, and iron. The correlation coefficients are high, average  $r^2 = 0.945$ , which is in good accord with the similar shapes of the soil curves at all summer SCAQS sites. The conversion factors, however, varied: XRF/PIXE = 1.14 (Si); 2.07 (K); 2.02 (Ca), 2.61 (Ti) (not shown), and 2.30 (Fe). The reason that silicon (and aluminum - a similar light soil element) have a relatively small correction ratio is not clear. We hypothesize that it may be based on the variable excitation/detection area of the wavelength dispersive EPA system. Nevertheless, whatever the cause, the correction factors are precise, repeatable, and not dependent on site or summer month.

### Sulfur

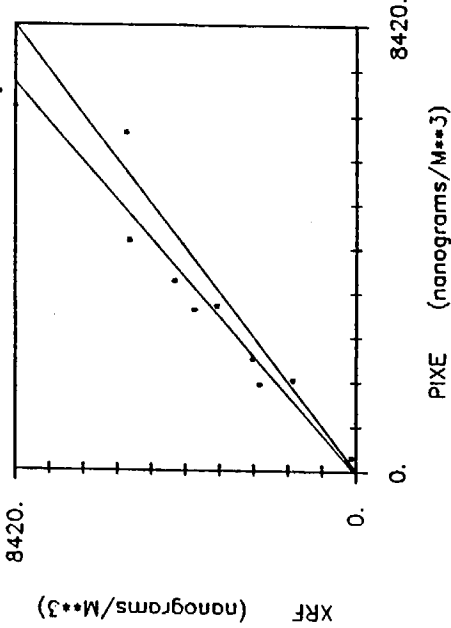
Figure 12 shows an XRF to PIXE sulfur correlation plot for all filter samples scanned, summer 1987. First, an excellent correlation was achieved,  $r^2$  greater than 0.995. This shows that for sulfur all sites and all summer months have an equivalent correction factor, namely XRF = 1.25 times the PIXE values, with an acceptable intercept of about 1.5% full scale. Thus, XRF results must be divided by 1.25 to obtain true values. Recall that for the standards XRF was  $1.038 \pm 0.045$  times PIXE so their calibrations were essentially the same. We will continue to quote the XRF to PIXE scan correction factors assuming the calibrations for the XRF and PIXE scan analyses were the same.

### Trace Elements - Mn, Cu, Zn, Br, Pb

Figure 13 shows the XRF vs PIXE correlation plot for Zn, PM 10, summer, all sites. If the fit is forced through the origin (marked "(CON)"), the  $r^2$  is still about 0.93, while the slope is  $1.18 \pm 0.08$  without an intercept. Other trace elements were more variable, with slopes close to  $1.7 \pm 0.4$ .

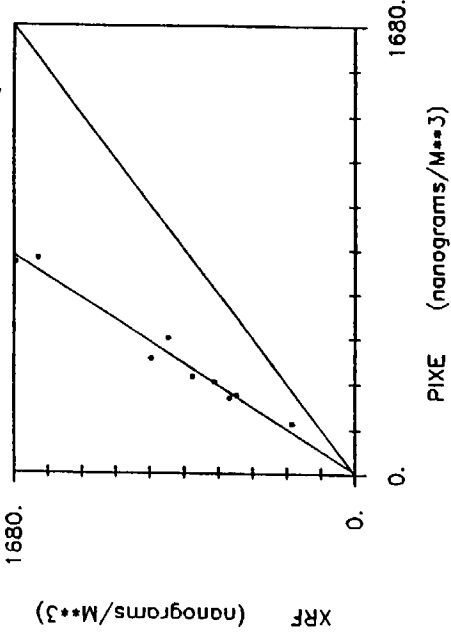
SCAQ5 PM10 : SI FOR SUMMER

N = 10  
 $R = 0.98$   $R^2 = 0.92$   
 $XRF = 1.14 \cdot PIXE + 57.60$   
 $\sigma_x = 0.26$   $\sigma_y = 864.20$   $\sigma_z = 0.087$   $\sigma_w/\sigma_z = 0.211$   
 $\bar{x} = 3312.08$   $\sigma_x = 664.77$   $\sigma_x/\bar{x} = 2102.19$   
 $\bar{y} = 3822.90$   $\sigma_y = 751.77$   $\sigma_y/\bar{y} = 2377.30$   
 $\bar{z} = 510.83$   $\sigma_z = 220.93$   $\sigma_z/\bar{z} = 698.66$   
 $\bar{w}/\bar{z} = 0.154$   $\sigma_w/\sigma_z = 0.087$   $\sigma_w/\bar{z} = 0.211$



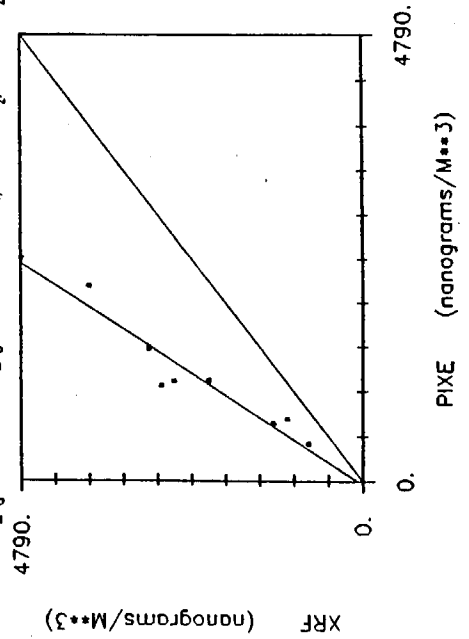
SCAQ5 PM10 : K FOR SUMMER

N = 9  
 $R = 0.98$   $R^2 = 0.97$   
 $XRF = 2.07 \cdot PIXE + -12.83$   
 $\sigma_x = 0.57$   $\sigma_y = 295.11$   $\sigma_z = 1.042$   $\sigma_w/\sigma_z = 0.178$   $\sigma_w/\bar{z} = 0.534$   
 $\bar{x} = 443.80$   $\sigma_x = 73.12$   $\sigma_x/\bar{x} = 219.35$   
 $\bar{y} = 908.33$   $\sigma_y = 149.98$   $\sigma_y/\bar{y} = 449.89$   
 $\bar{z} = 482.33$   $\sigma_z = 79.05$   $\sigma_z/\bar{z} = 237.15$   
 $\bar{w}/\bar{z} = 1.042$   $\sigma_w/\sigma_z = 1.042$   $\sigma_w/\bar{z} = 0.534$



SCAQ5 PM10 : CA FOR SUMMER

N = 9  
 $R = 0.98$   $R^2 = 0.93$   
 $XRF = 2.02 \cdot PIXE + 72.48$   
 $\sigma_x = 0.84$   $\sigma_y = 982.54$   $\sigma_z = 1.077$   $\sigma_w/\sigma_z = 0.197$   $\sigma_w/\bar{z} = 0.592$   
 $\bar{x} = 1188.38$   $\sigma_x = 224.98$   $\sigma_x/\bar{x} = 674.93$   
 $\bar{y} = 2468.44$   $\sigma_y = 443.81$   $\sigma_y/\bar{y} = 1331.42$   
 $\bar{z} = 1280.08$   $\sigma_z = 234.59$   $\sigma_z/\bar{z} = 703.78$   
 $\bar{w}/\bar{z} = 1.077$   $\sigma_w/\sigma_z = 1.077$   $\sigma_w/\bar{z} = 0.592$



SCAQ5 PM10 : FE FOR SUMMER

N = 10  
 $R = 0.98$   $R^2 = 0.96$   
 $XRF = 2.30 \cdot PIXE + 48.62$   
 $\sigma_x = 0.81$   $\sigma_y = 859.45$   $\sigma_z = 1.345$   $\sigma_w/\sigma_z = 0.258$   $\sigma_w/\bar{z} = 0.810$   
 $\bar{x} = 1068.55$   $\sigma_x = 209.49$   $\sigma_x/\bar{x} = 662.48$   
 $\bar{y} = 2500.80$   $\sigma_y = 474.42$   $\sigma_y/\bar{y} = 1500.24$   
 $\bar{z} = 1434.25$   $\sigma_z = 273.09$   $\sigma_z/\bar{z} = 863.59$   
 $\bar{w}/\bar{z} = 1.345$   $\sigma_w/\sigma_z = 1.345$   $\sigma_w/\bar{z} = 0.810$

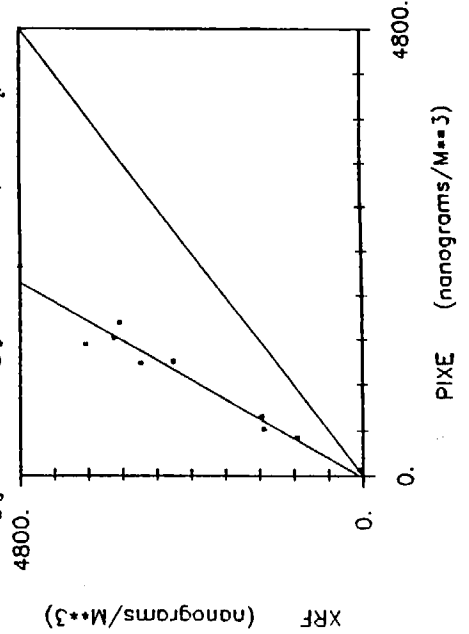


Figure 11

# SCAQs PM10 : S FOR SUMMER

$N = 10$   
 $R = 1.00$   $R^2 = 1.00$   
 $XRF = 1.25 * PIXE + -144.61$   
 $\pm\sigma_a = 0.07$   $\pm\sigma_b = 297.16$   
 $\bar{x} = 4165.44$   $\sigma_{\bar{x}} = 614.52$   $\sigma_x = 1943.30$   
 $\bar{y} = 5065.90$   $\sigma_{\bar{y}} = 768.31$   $\sigma_y = 2429.60$   
 $\bar{z} = 900.46$   $\sigma_{\bar{z}} = 160.84$   $\sigma_z = 508.64$   
 $\bar{z}/\bar{x} = 0.216$   $\sigma_{\bar{z}/\bar{x}} = 0.039$   $\sigma_z/\bar{x} = 0.122$

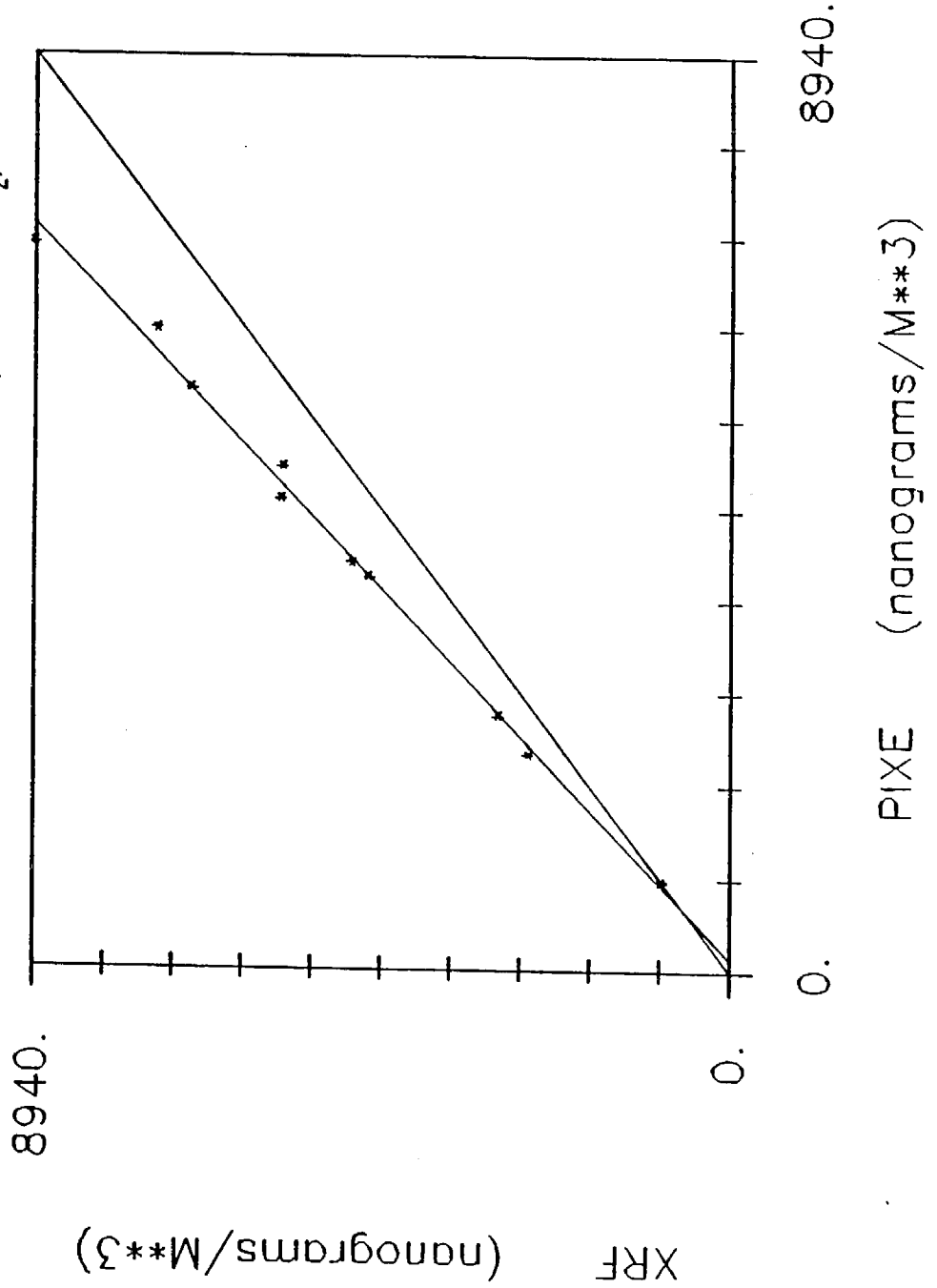


Figure 12

# SCAQs PM10 : ZN FOR SUMMER

$N = 5$   
 $R = 0.98$   $R^2 = 0.96$   
 $XRF = 0.99 * PIXE + 53.64$   
 $\pm\sigma_a = 0.23$   $\pm\sigma_b = 80.38$   
 $\bar{x} = 343.58$   $\sigma_x = 94.89$   $\sigma_x = 212.18$   
 $\bar{y} = 395.00$   $\sigma_y = 94.29$   $\sigma_y = 210.84$   
 $\bar{z} = 51.42$   $\sigma_z = 18.97$   $\sigma_z = 42.42$   
 $\bar{z}/\bar{x} = 0.150$   $\sigma_z/\bar{x} = 0.055$   $\sigma_z/\bar{x} = 0.123$

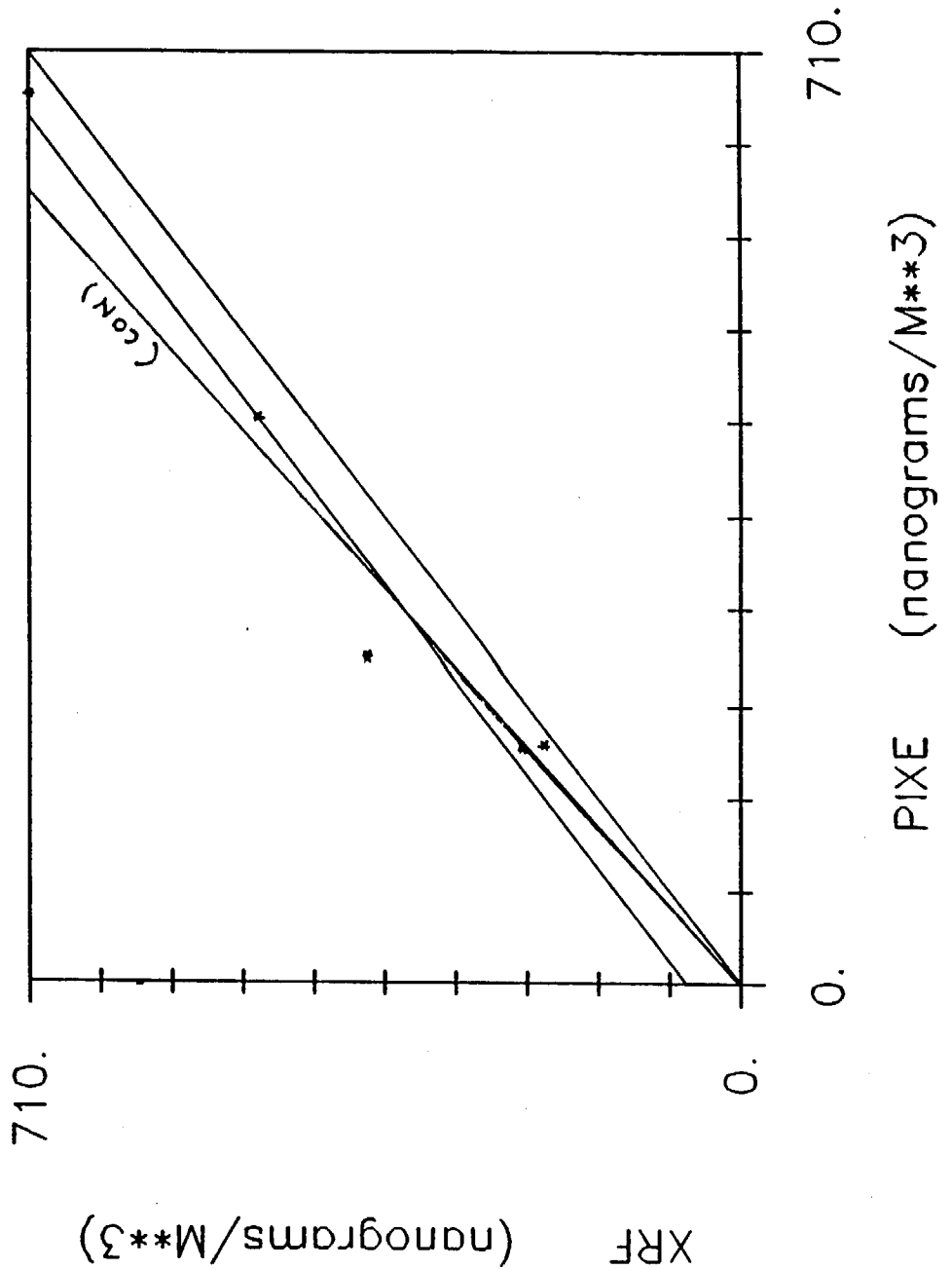


Figure 13

**PM 10 ELEMENTAL SCANS - FALL****Soil-like Elements - Si, K, Ca, Ti, Fe**

Figures 14A and 14B show Si, K, Ca, Ti, and Fe; period 5 for Los Angeles, (DOLA) 11/12/87. Generally, the behavior mimics summer patterns, despite the changed meteorology. Figure 15 shows summaries of soil elements and sulfur for DOLA, 11/12/87, period 3 and Burbank, 11/12/87, period 5. While the patterns are similar, the ratio of elements and the linear (fine particle) component both differ significantly. Iron is much higher than calcium at DOLA, while they are the same at BURB.

**Sulfur**

Sulfur shows only modest (~10%) central peaking, similar to summer, as shown in more detail at Anaheim, 11/12/87, period 3 (Figure 16).

**Trace Elements - Cl, Mn, Cu, Zn, Br, Pb**

Figure 17 shows scans for chlorine (Cl) and manganese (Mn) for DOLA, 11/12/87, period 5. Chlorine clearly possesses a coarse particle profile, not unexpected if the source is sea salt. Manganese, however, while occurring in coarse soil particles, has a flatter profile characteristic of fine aerosols. Thus, most manganese is not from soil.

Figure 18 shows copper and zinc for Hawthorne (for which they are well behaved) and Burbank (for which they are not well behaved). We propose a brass particulate contamination for the Hawthorne results. Clearly, the value recorded by XRF will depend critically on whether it encompasses these spikes or not. Another example is shown in Figure 19 which shows copper and zinc from Long Beach, 12/11/87, period 3. Again, the copper and zinc appear contaminated with brass-like particles. For this reason, all Cu and Zn values from the SCAQS sampler must be used with great caution.

Figure 20 shows lead and bromine scans for fall. Unlike summer, these are characteristic of fine particles. A working hypothesis for the summer coarse particulate peaks might be resuspended lead - contaminated soil near roadways, which might be reduced if there had been rain.

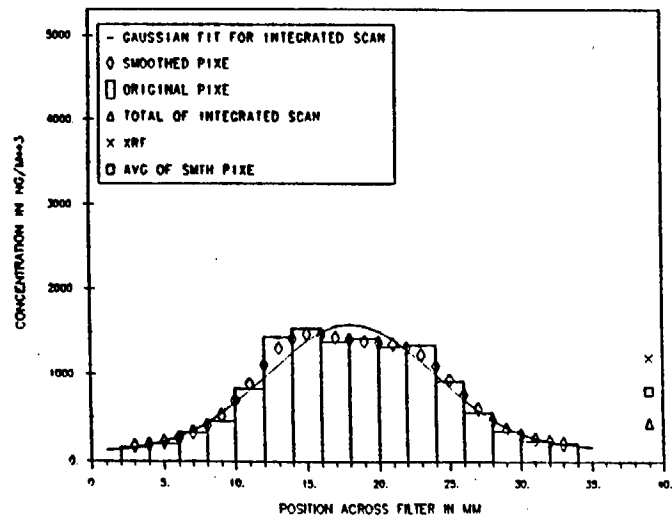
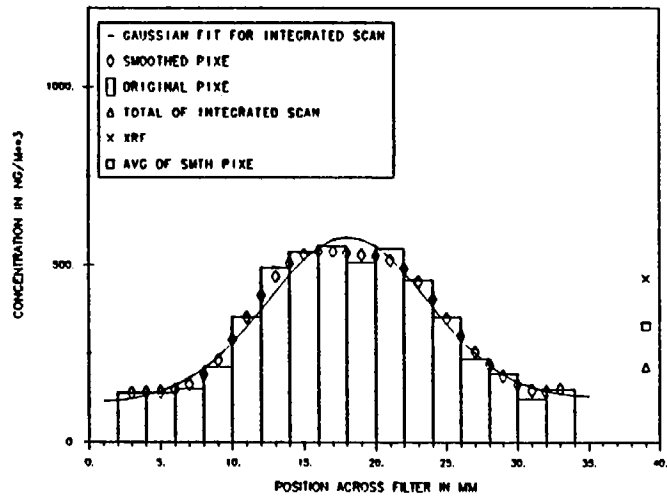
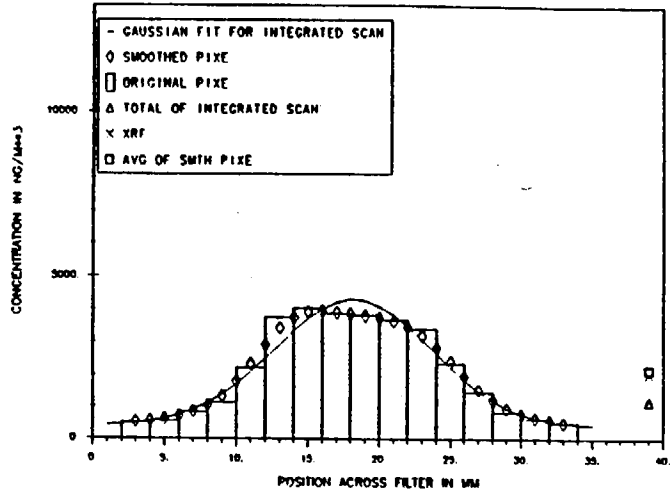
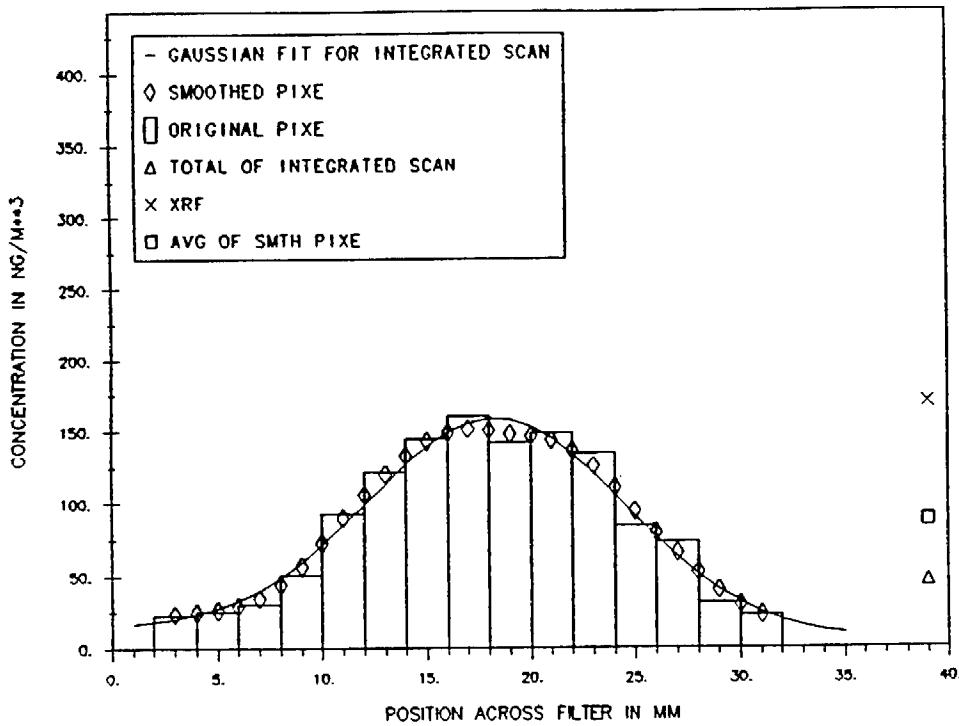


Figure 14A

SCAQ5 PIXE SCANS FOR PM10 TI; CHISO = 0.18  
 DOLA 11-693 JULIAN316 11-12-87 PERIOD5



SCAQ5 PIXE SCANS FOR PM10 FE; CHISO = 1.02  
 DOLA 11-693 JULIAN316 11-12-87 PERIOD5

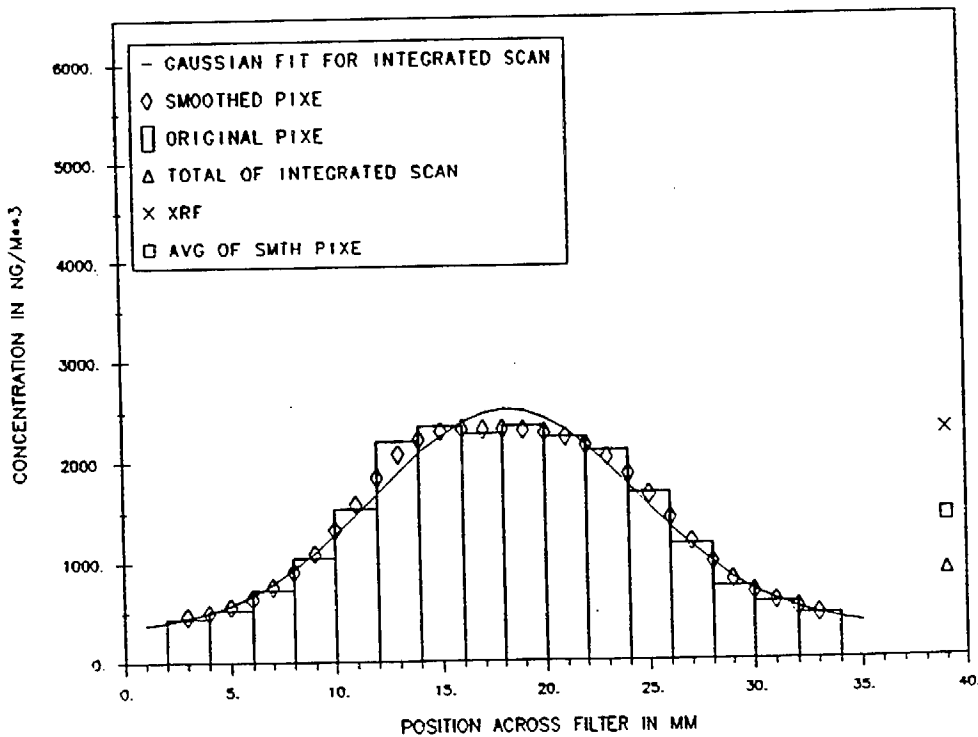
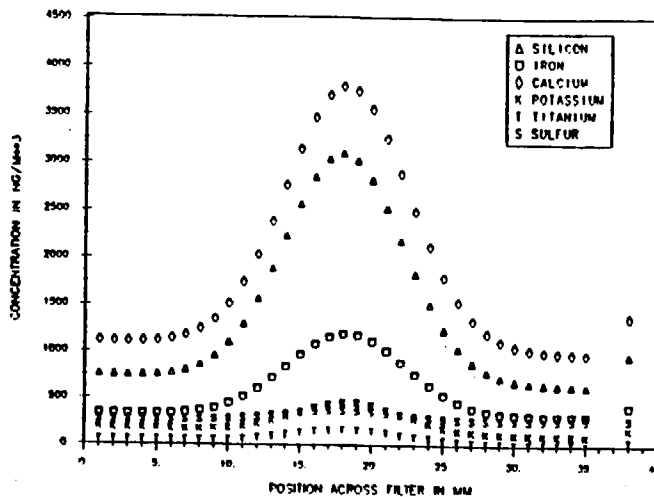
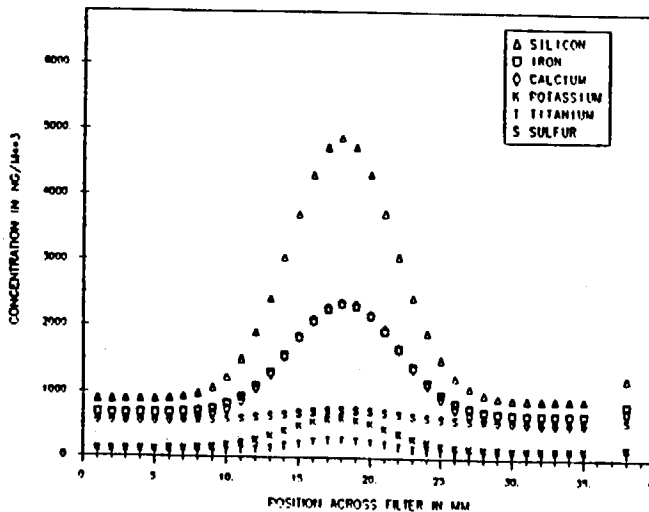


Figure 14B

GAUSSIAN FITS OF SCAQS PIXE SCANS FOR PM10  
 RUBI 11-598 JULIAN344 12-10-87 PERIOD3



GAUSSIAN FITS OF SCAQS PIXE SCANS FOR PM10  
 BURB 11-657 JULIAN318 11-12-87 PERIOD3



GAUSSIAN FITS OF SCAQS PIXE SCANS FOR PM10  
 DOLA 11-693 JULIAN318 11-12-87 PERIOD5

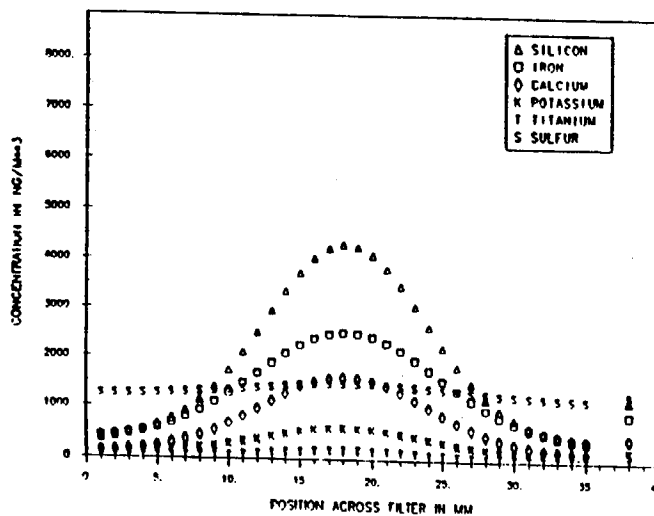


Figure 15

SCAQ5 PIXE SCANS FOR PM10 S ; CHISQ = 0.15  
ANAH 11-625 JULIAN316 11-12-87 PERIOD3

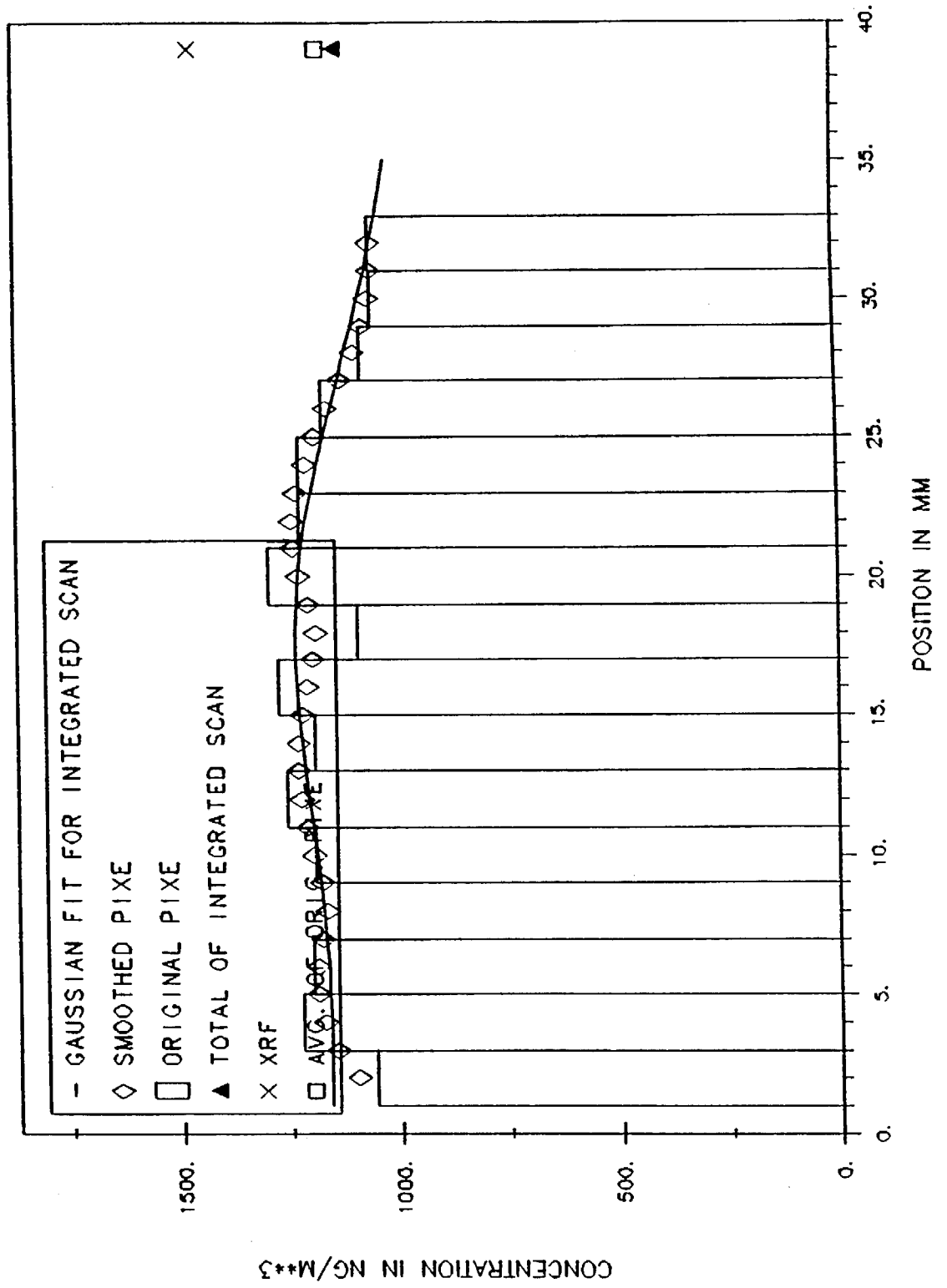
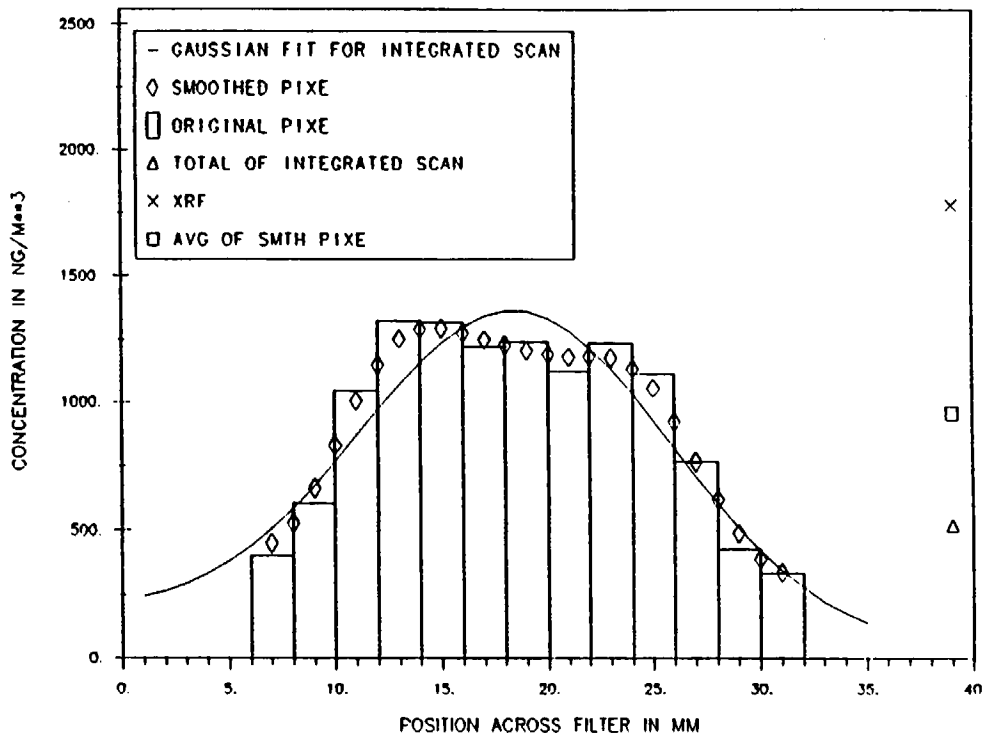


Figure 16

SCAQS PIXE SCANS FOR PM10 CL; CHISQ = 2.94  
 DOLA 11-693 JULIAN316 11-12-87 PERIOD5



SCAQS PIXE SCANS FOR PM10 MN; CHISQ = 0.17  
 DOLA 11-693 JULIAN316 11-12-87 PERIOD5

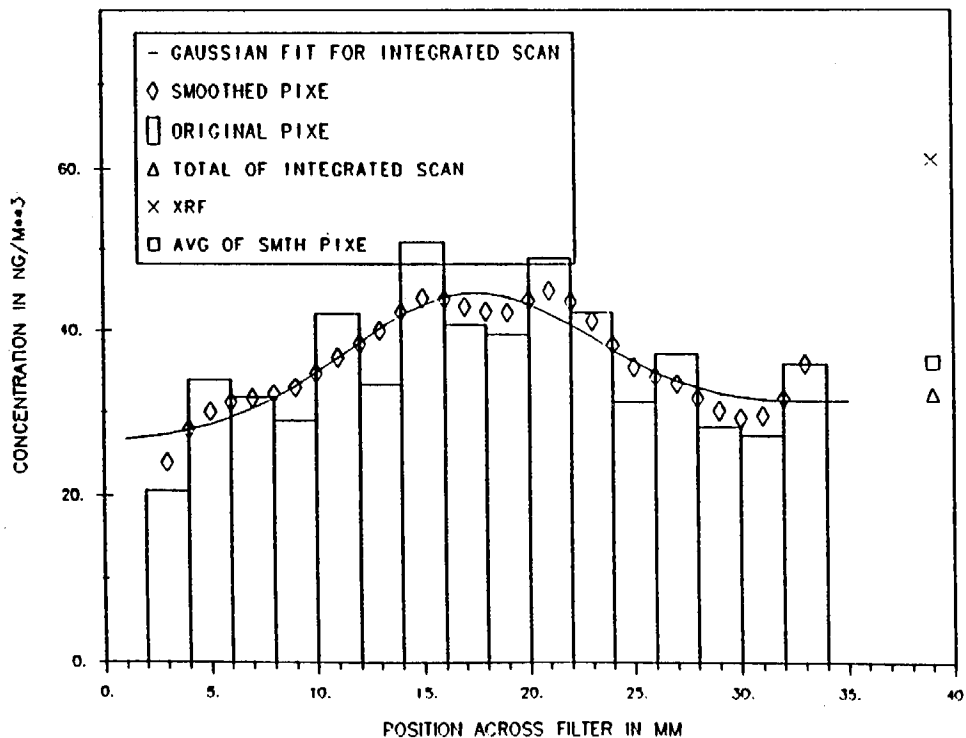
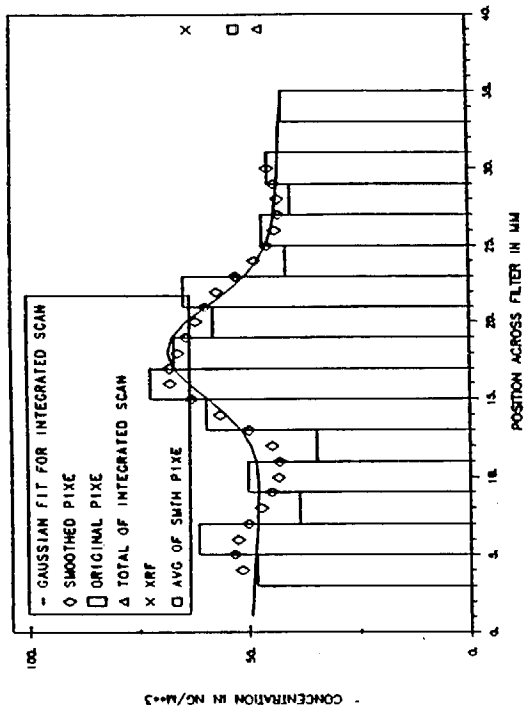
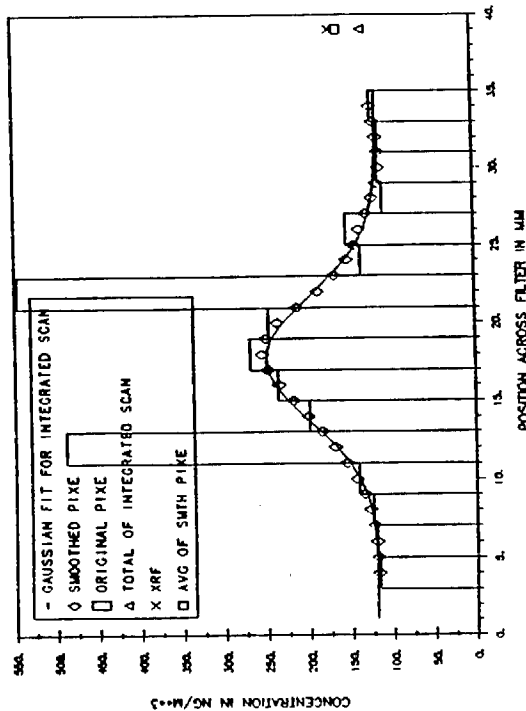


Figure 17

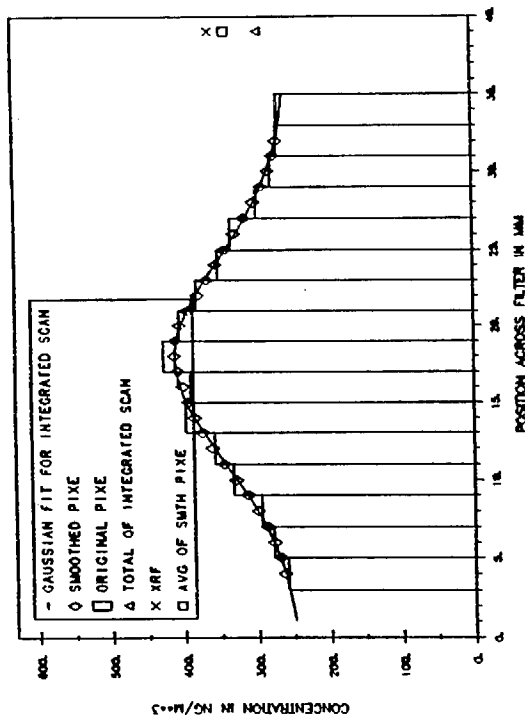
SCAQX PIXE SCANS FOR PM10 CU; CHISO = 0.16  
HAWT 11-724 JULIAN316 11-12-87 PERIOD3



SCAQX PIXE SCANS FOR PM10 ZN; CHISO = 0.11  
BURB 11-657 JULIAN316 11-12-87 PERIOD3



SCAQX PIXE SCANS FOR PM10 ZN; CHISO = 0.01  
HAWT 11-724 JULIAN316 11-12-87 PERIOD3



SCAQX PIXE SCANS FOR PM10 CU; CHISO = 2.80  
BURB 11-657 JULIAN316 11-12-87 PERIOD3

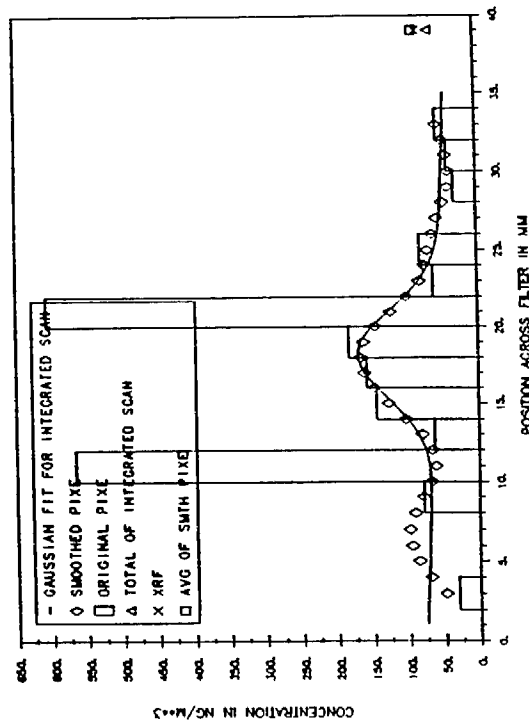
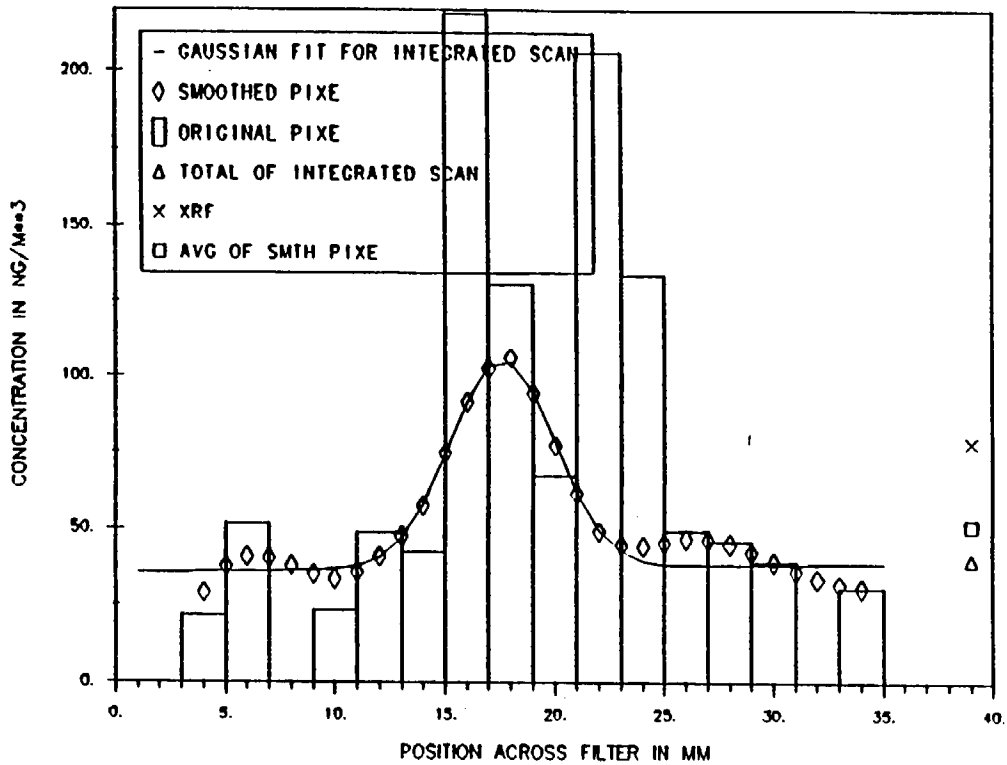


Figure 18

SCAQS PIXE SCANS FOR PM10 CU; CHISO = 0.39  
LOBE 11-515 JULIAN345 12-11-87 PERIOD3



SCAQS PIXE SCANS FOR PM10 ZN; CHISO = 0.35  
LOBE 11-515 JULIAN345 12-11-87 PERIOD3

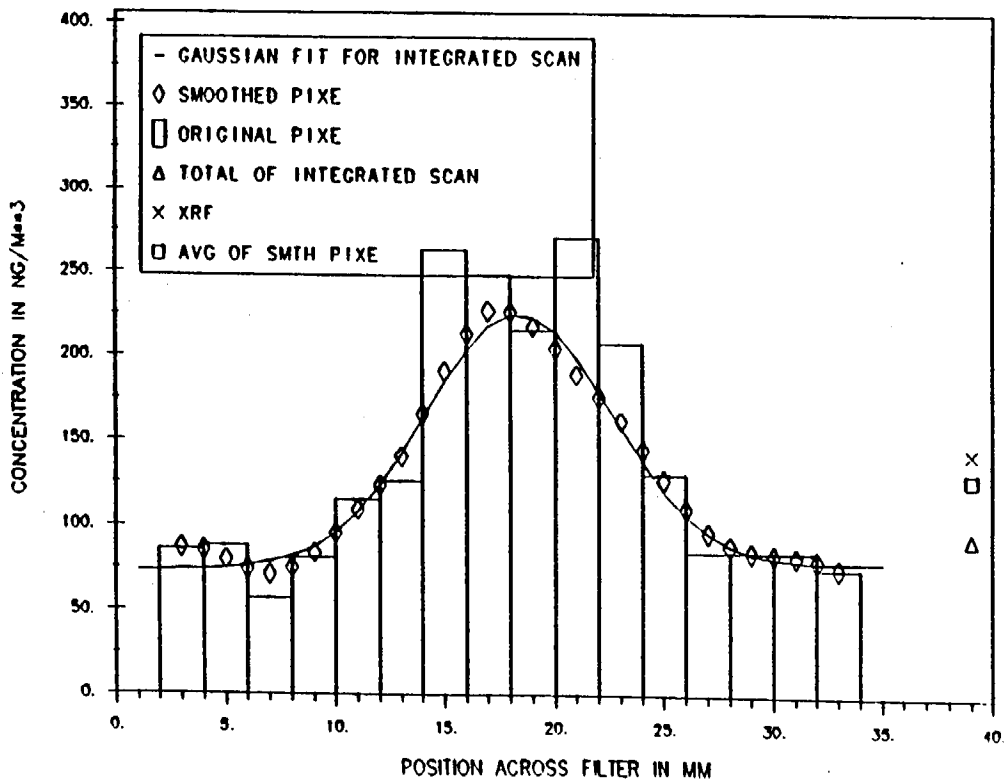
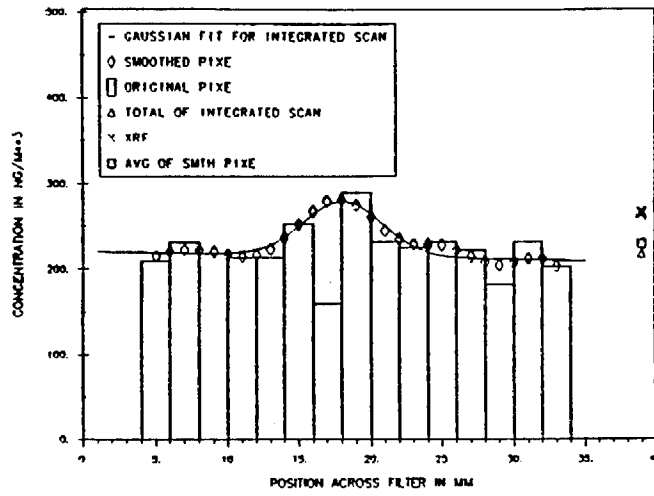
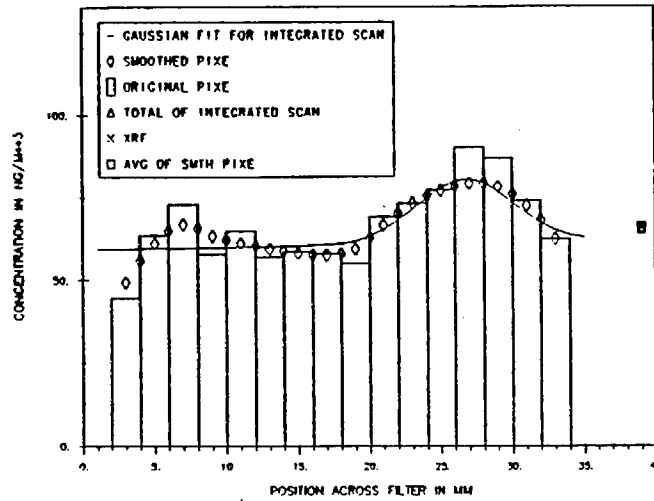


Figure 19

SCAQ5 PIXE SCANS FOR PM10 PB: CHISO = 0.07  
 HAWT 11-724 JULIAN316 11-12-87 PERIOD3



SCAQ5 PIXE SCANS FOR PM10 BP: CHISO = 0.36  
 DOLA 11-693 JULIAN316 11-12-87 PERIOD5



SCAQ5 PIXE SCANS FOR PM10 PB: CHISO = 0.10  
 DOLA 11-693 JULIAN316 11-12-87 PERIOD5

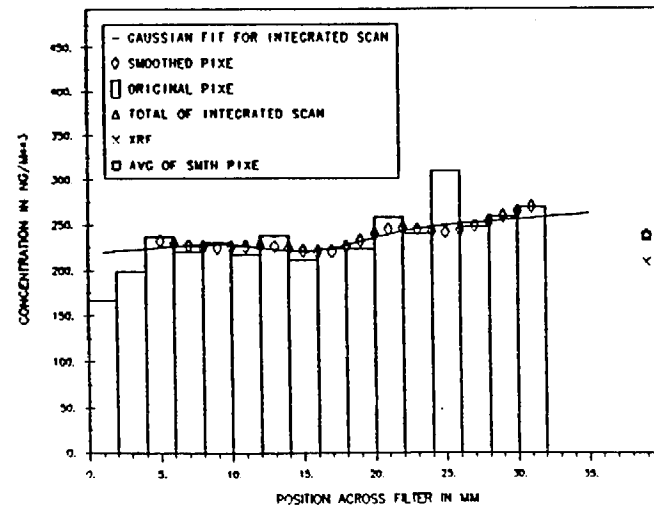


Figure 20

**PM 10 CORRELATION PLOTS, XRF VS PIXE - FALL AND SUMMER**

The seasonal similarities, as seen in the previous scans, encourage us to combine summer and fall PM 10 values in combined XRF vs PIXE correlation plots. Figures 21, 22, and 23 show such plots of sulfur, silicon, and soils (K, Ca, Ti, Fe). The  $r^2$  for sulfur is greater than 0.99, with a slope of 1.22. Silicon also is highly correlated,  $r^2 = 0.94$ , with a slope of 1.13, while all other soils are correlated  $r^2 = 0.94$  but with a slope of 2.09. The insensitivity of the correction factors by season and site is a great aid in correcting the XRF data.

Similar plots combining summer and fall periods were prepared for trace elements. Examples are shown in Figure 24 for Mn, Cu, Zn, Pb, where the "(CON)" gives the least square fit forced through the origin. The calibration factors were thus estimated: Mn, 1.91; Cu, 1.25; Zn, 1.16; Pb, 1.28; and Br, 1.60 (not shown).

# SCAQs PM10 : S FOR SUMMER AND FALL

$N = 23$   
 $R = 1.00$   $R^2 = 1.00$   
 $XRF = 1.22 * PIXE + 32.57$   
 $\pm \sigma_a = 0.04$   $\pm \sigma_b = 94.31$   
 $\bar{x} = 2672.94$   $\sigma_{\bar{x}} = 427.14$   $\sigma_x = 2048.47$   
 $\bar{y} = 3296.89$   $\sigma_{\bar{y}} = 521.47$   $\sigma_y = 2500.88$   
 $\bar{z} = 623.95$   $\sigma_{\bar{z}} = 98.17$   $\sigma_z = 470.79$   
 $\bar{z}/\bar{x} = 0.233$   $\sigma_{\bar{z}/\bar{x}} = 0.037$   $\sigma_z/\bar{x} = 0.176$

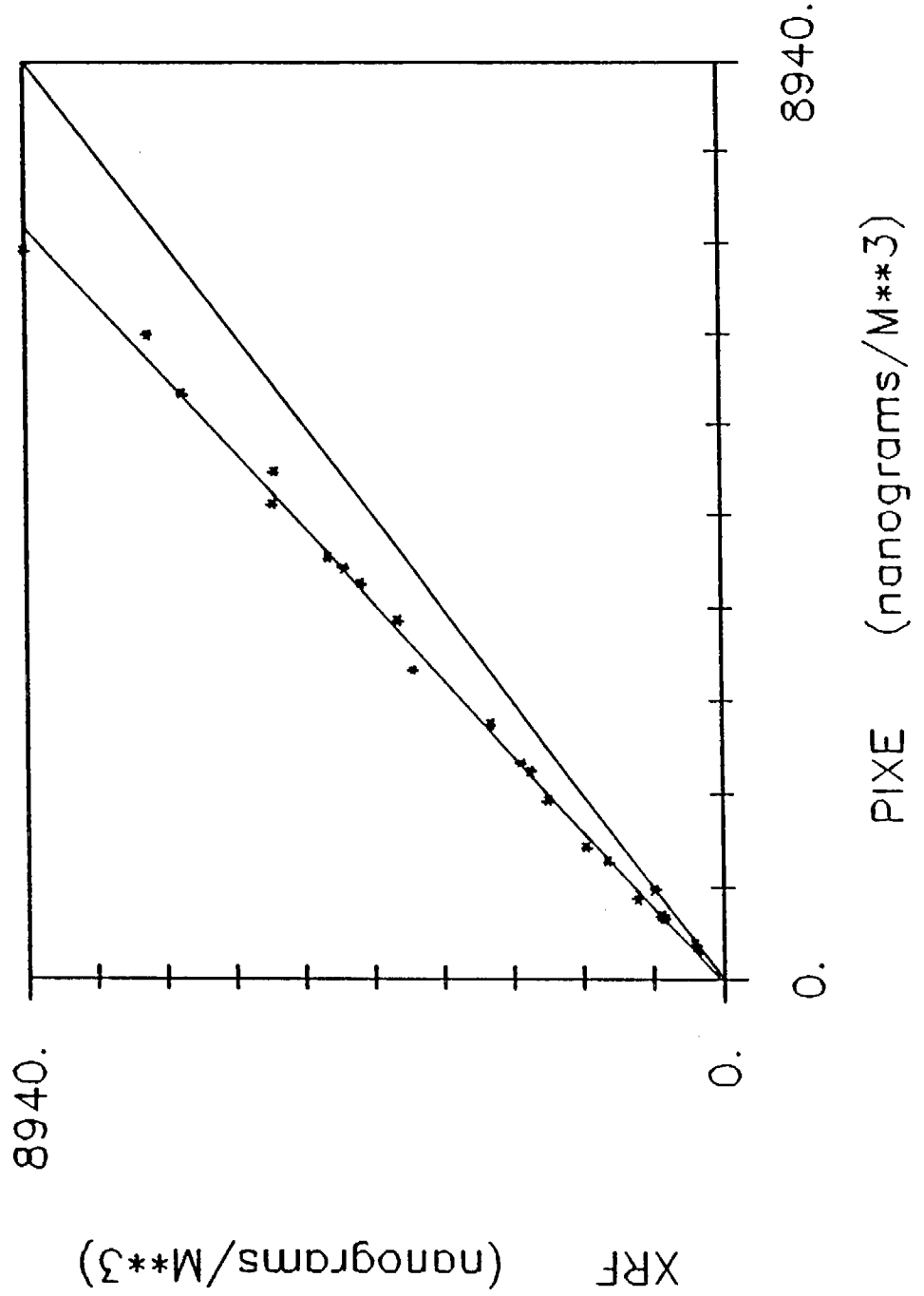


Figure 21

# SCAQs PM10 : SI FOR SUMMER AND FALL

$N = 23$   
 $R = 0.97$   $R^2 = 0.94$   
 $XRF = 1.13 * PIXE + 205.45$   
 $\pm \sigma_a = 0.14$   $\pm \sigma_b = 348.03$   
 $\bar{x} = 2467.06$   $\sigma_{\bar{x}} = 350.05$   $\sigma_x = 1678.77$   
 $\bar{y} = 2995.56$   $\sigma_{\bar{y}} = 394.30$   $\sigma_y = 1890.99$   
 $\bar{z} = 528.50$   $\sigma_{\bar{z}} = 104.95$   $\sigma_z = 503.32$   
 $\bar{z}/\bar{x} = 0.214$   $\sigma_{\bar{z}/\bar{x}} = 0.043$   $\sigma_z/\bar{x} = 0.204$

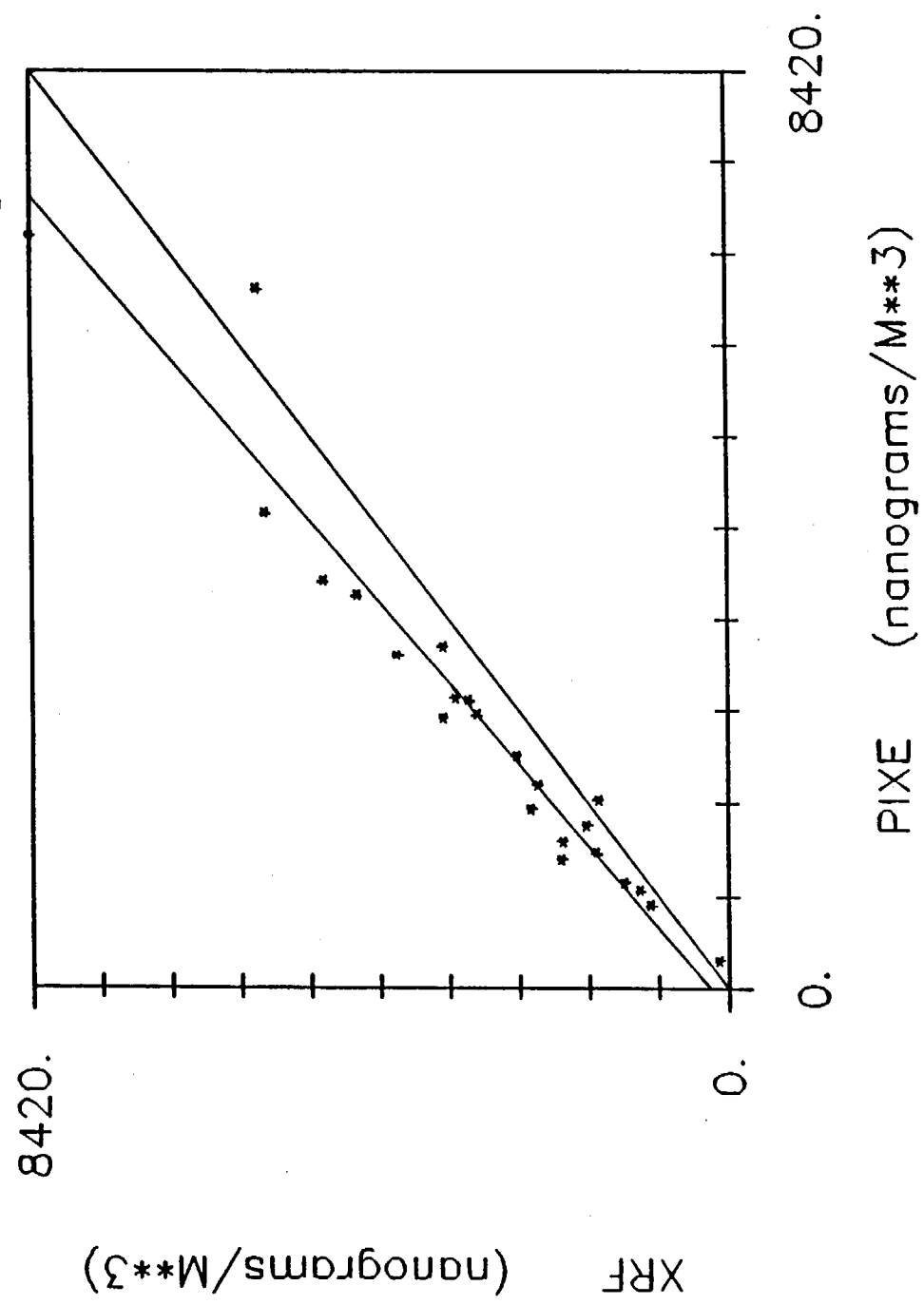


Figure 22

# SCAQs PM10: SOILS FOR SUMMER&FALL

$N = 107$   
 $R = 0.97$   $R^2 = 0.94$   
 $XRF = 2.09 * PIXE + -34.99$   
 $\pm\sigma_a = 0.21$   $\pm\sigma_b = 111:27$   
 $\bar{x} = 532.01$   $\sigma_x = 52.25$   $\sigma_x = 540.52$   
 $\bar{y} = 1077.02$   $\sigma_y = 107.23$   $\sigma_y = 1109.19$   
 $\bar{z} = 545.01$   $\sigma_z = 57.87$   $\sigma_z = 598.62$   
 $\bar{z}/\bar{x} = 1.024$   $\sigma_z/\bar{x} = 0.109$   $\sigma_z/\bar{x} = 1.125$

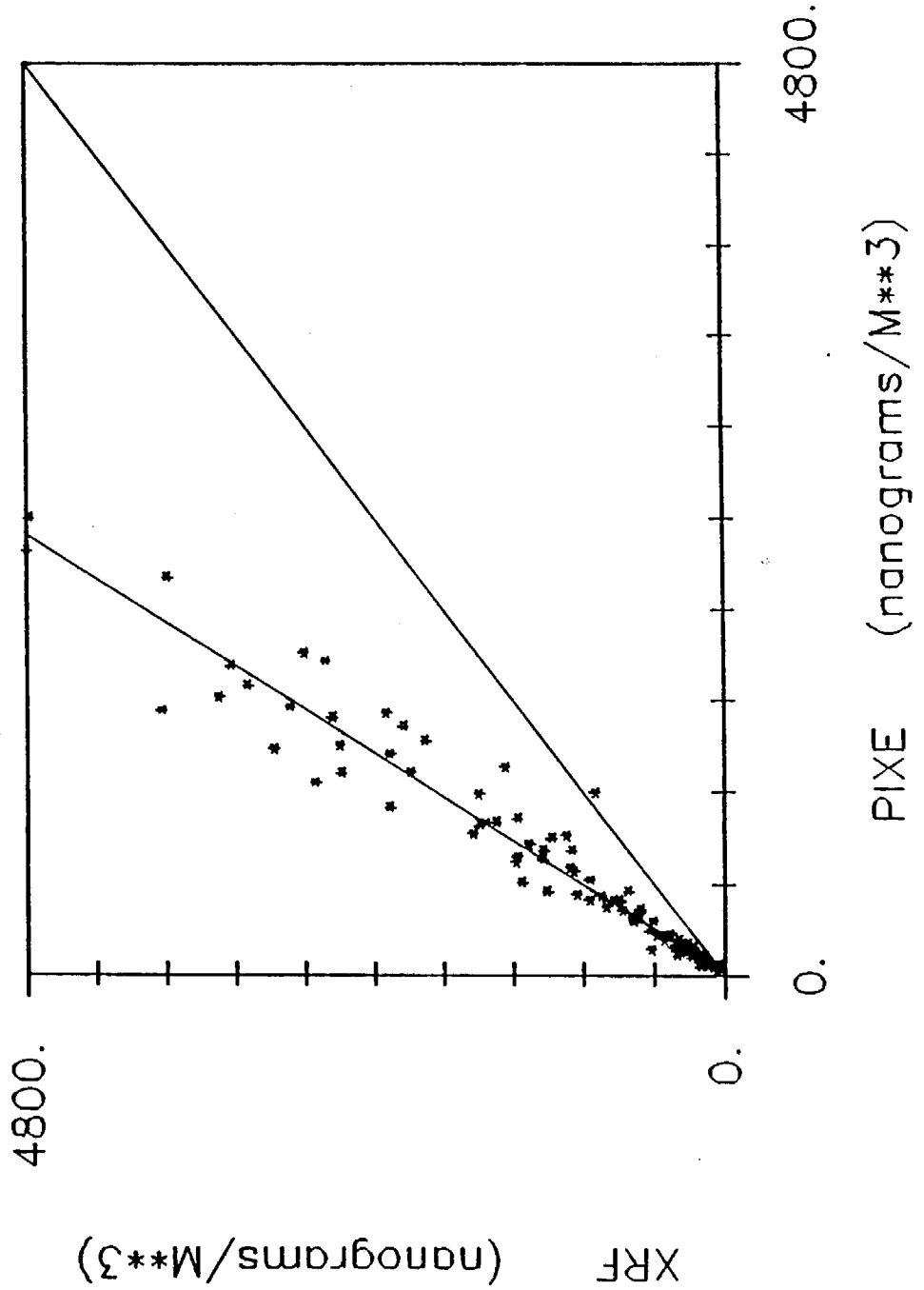
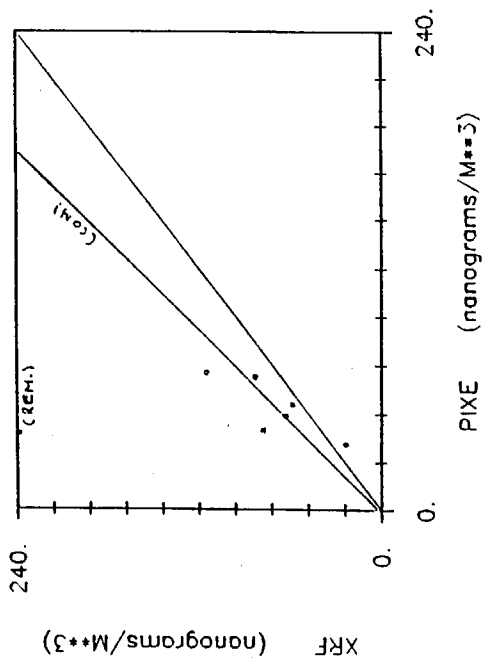
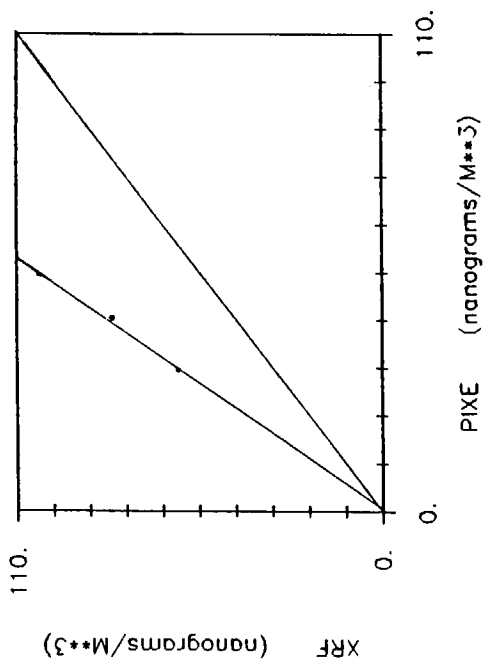


Figure 23

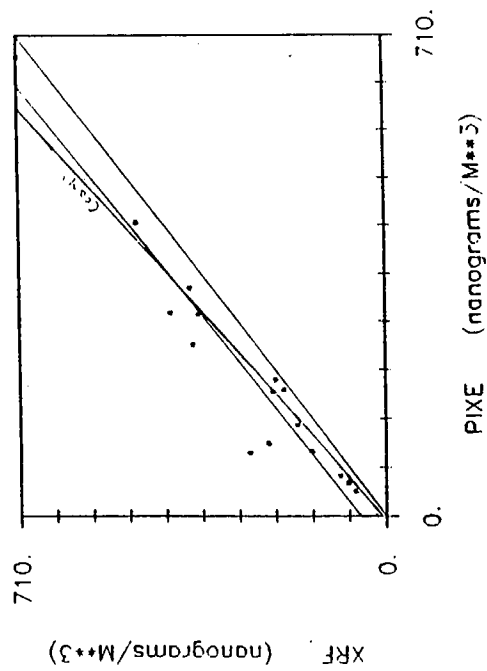
SCAQ5 PM10 : CU FOR SUMMER AND FALL



SCAQ5 PM10 : MN FOR FALL



SCAQ5 PM10 : ZN FOR SUMMER AND FALL



SCAQ5 PM10 : PB FOR SUMMER AND FALL

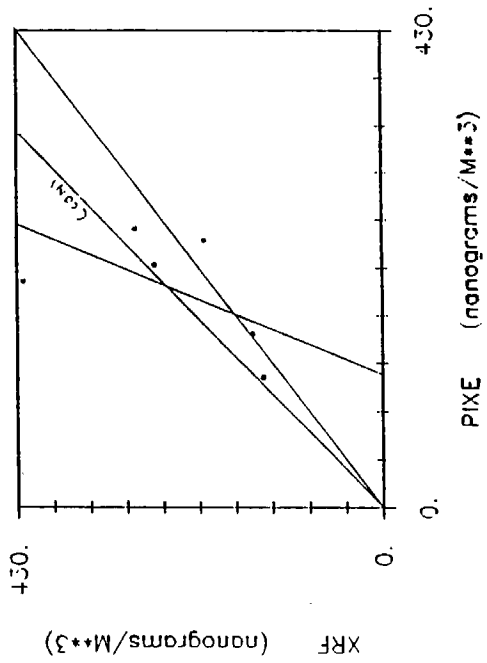


Figure 24

## PM 2.5 ELEMENTAL SCANS - SUMMER

On first principles, one would expect that the lateral scans of PM 2.5 filters would show less central peaking due to the smaller maximum size of the particles. To a degree, this is true, but a major degree of central peaking is still very visible in the soil-like elements; Si, K, Ca, Ti, Mn, Fe, etc.. The central peak to edge ratios are now generally less than 2, versus values of 6 or more seen on occasion in PM 10 samples. A factor of 2 is still a major effect, and correction factors need to be calculated and applied to the XRF data. In addition, scans now show, on occasion, a sloping linear term summed with the central Gaussian. Still, correction factors are somewhat lower for PM 2.5 than PM 10, and correlations among sites and seasons continued to be strong. While almost all major SCAQS episodes were sampled, major emphasis was placed on a summer episode (7/14/87) and a fall episode (11/12/87).

### Soil-Like Elements - Si, K, Ca, Ti, Fe

Figure 25 shows scans of soil-like elements for Downtown Los Angeles (DOLA) for 7/14/87, period 3. The relatively smaller central peak is evident, but there is a good deal of very fine soil-like elements that show no central peak.

Figures 26A, 26B, and 27 show similar fine soils at Azusa and Rubidoux, 7/14/87, period 3. Despite the trend towards drier conditions inland, little change is seen in the central peaking of soils in these scans.

### Sulfur

Figure 28 shows scans of filters at Los Angeles, Azusa, and Rubidoux for 7/14/87, period 3. Very little central peaking is seen, but the XRF values are always about 10 to 15% higher than the PIXE scans. About 4 to 5% of that is accounted for by the difference with standards, a few percent is due to the central peaking, but we have no explanation for the remainder. Figure 29 shows summaries for soils and sulfur/10 for the same samples.

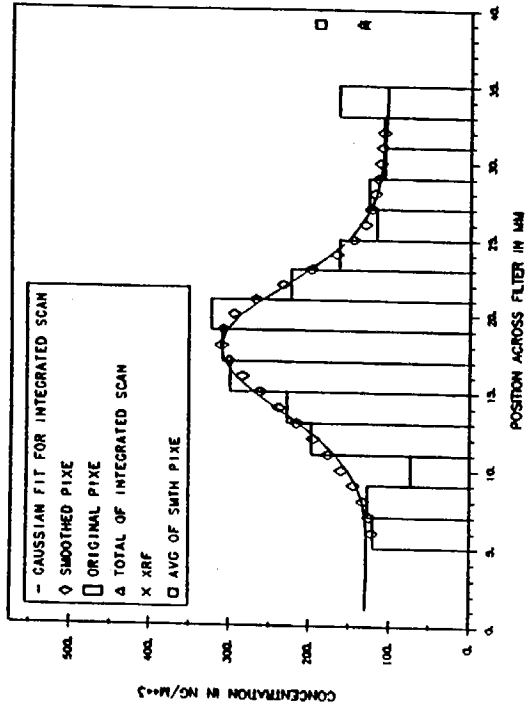
### Trace Elements - K, Mn, Cu, Zn, Br, Pb

We looked for indications of excess fine potassium, an indicator of wood smoke, but found that the lateral scans of potassium had a central peaking similar to calcium, which does not occur in smoke. Therefore, almost all the potassium can be assigned to soils.

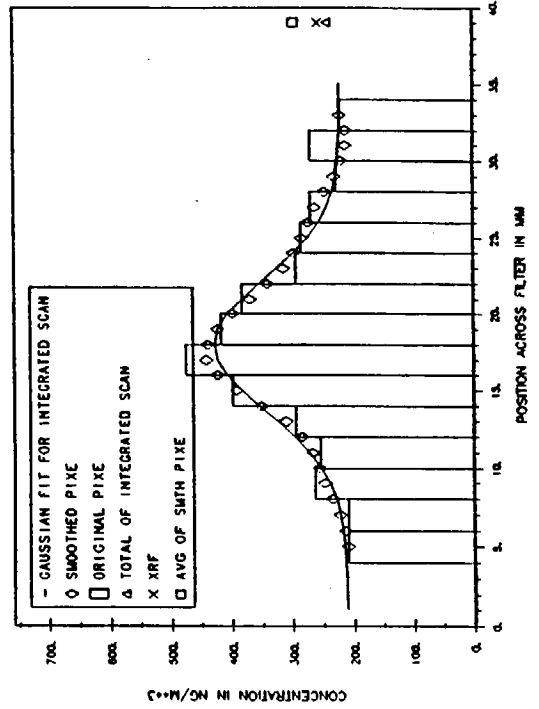
Figure 30 shows copper and zinc at Los Angeles for 7/14/87, period 3. Regretfully, a massive peak indicative of brass, 72% Zn/Cu ratio, is seen close to the center of the filter. Naturally, the XRF value is many times that of the PIXE smoothed filter average for copper, and somewhat larger for zinc. An effort was made to find the central peaking without the brass particle, but these must be considered tentative. Incidentally, the particle's total mass, assuming it was fully covered by the 2mm x 4.2mm PIXE spot, was about 0.9 $\mu$ g. Thus, this is not a brass "chip" and would not be visible to the naked eye. Figure 31 shows similar scans for August at Los Angeles.

More data on trace elements will be given later when we consider all periods.

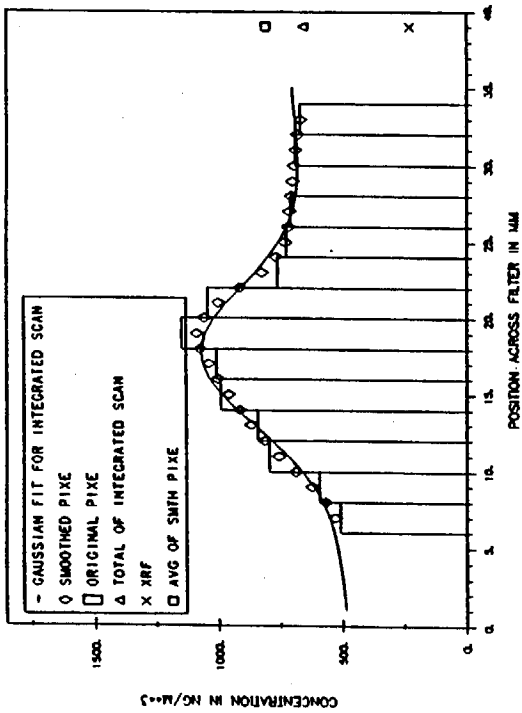
SCAOS PIXE SCANS FOR PM2.5 K; CHISO = 0.05  
 DOLA 8-072 JULIAN195 07-14-87 PERIOD3



SCAOS PIXE SCANS FOR PM2.5 FE; CHISO = 0.36  
 DOLA 8-072 JULIAN195 07-14-87 PERIOD3



SCAOS PIXE SCANS FOR PM2.5 SI; CHISO = 0.19  
 DOLA 8-072 JULIAN195 07-14-87 PERIOD3



SCAOS PIXE SCANS FOR PM2.5 CA; CHISO = 0.25  
 DOLA 8-072 JULIAN195 07-14-87 PERIOD3

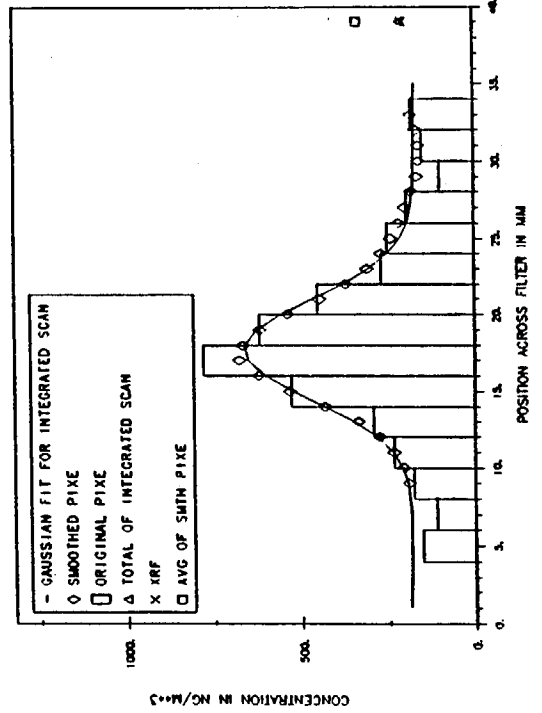
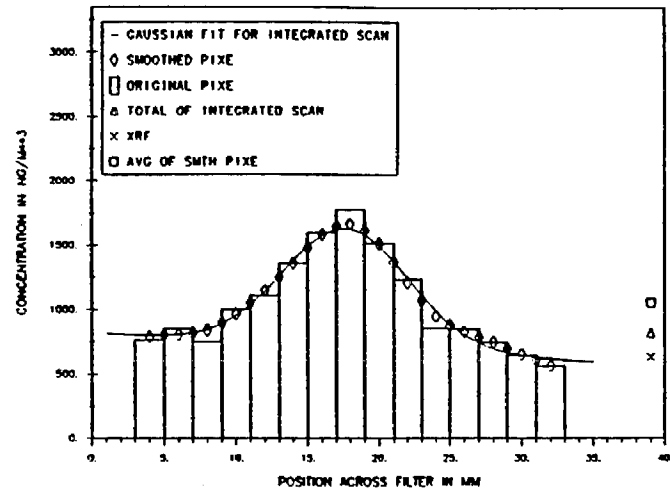
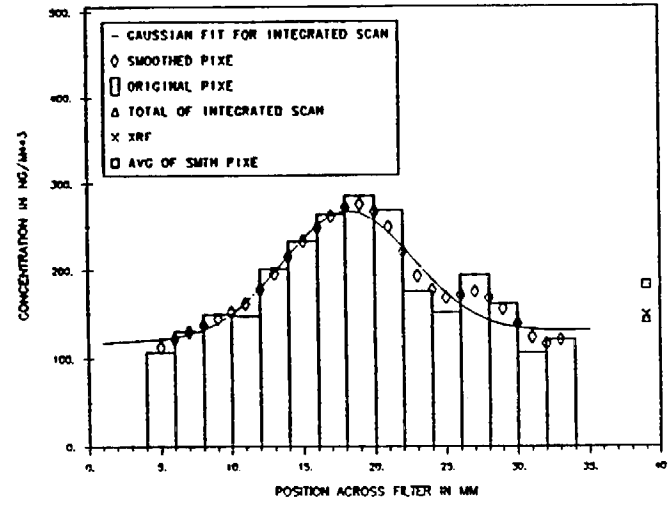


Figure 25

SCAQS PIXE SCANS FOR PM2.5 SI; CHISO = 0.31  
AZUS 8-040 JULIAN195 07-14-87 PERIOD3



SCAQS PIXE SCANS FOR PM2.5 K; CHISO = 0.23  
AZUS 8-040 JULIAN195 07-14-87 PERIOD3



SCAQS PIXE SCANS FOR PM2.5 CA; CHISO = 0.50  
AZUS 8-040 JULIAN195 07-14-87 PERIOD3

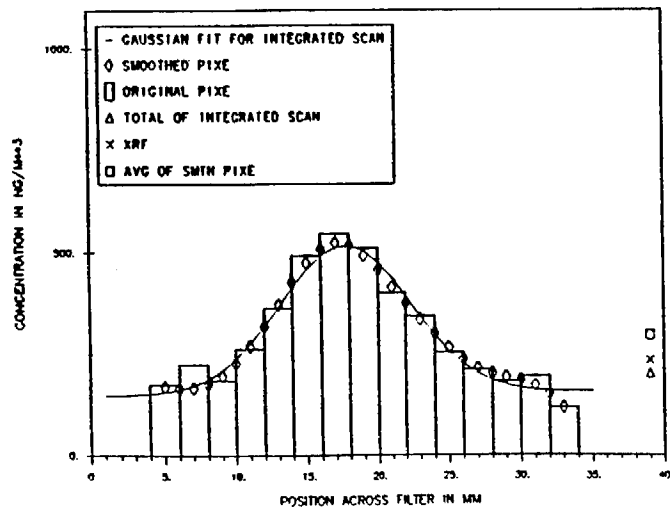


Figure 26A

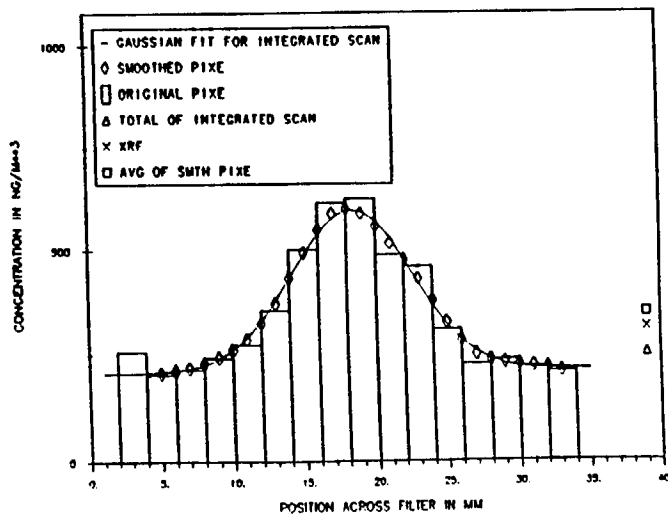
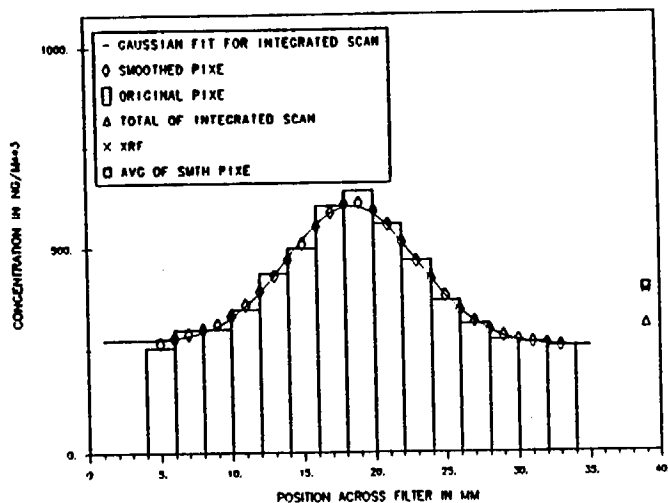
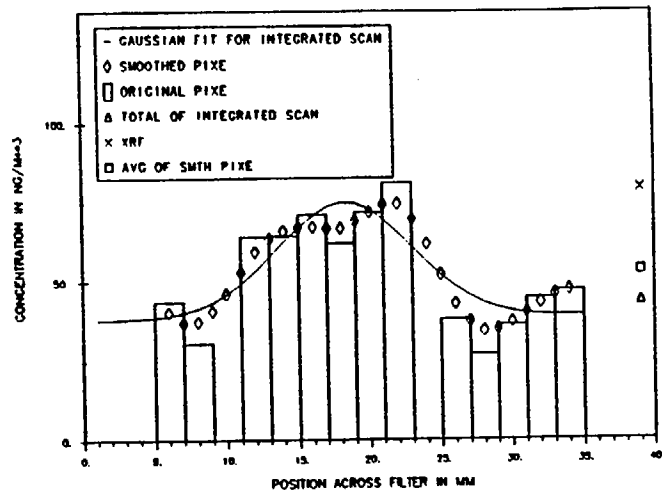
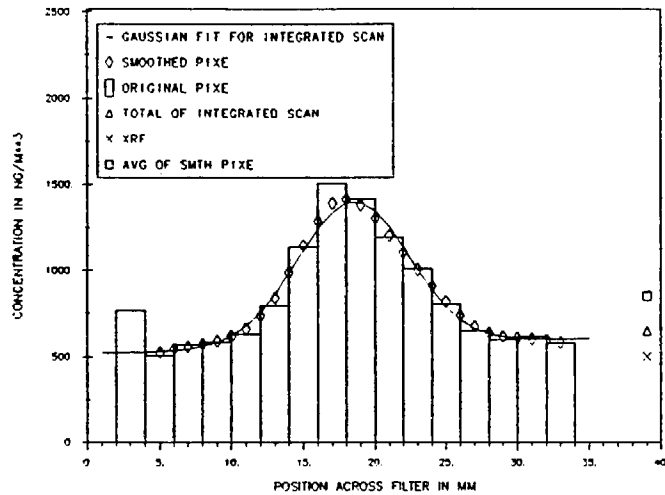
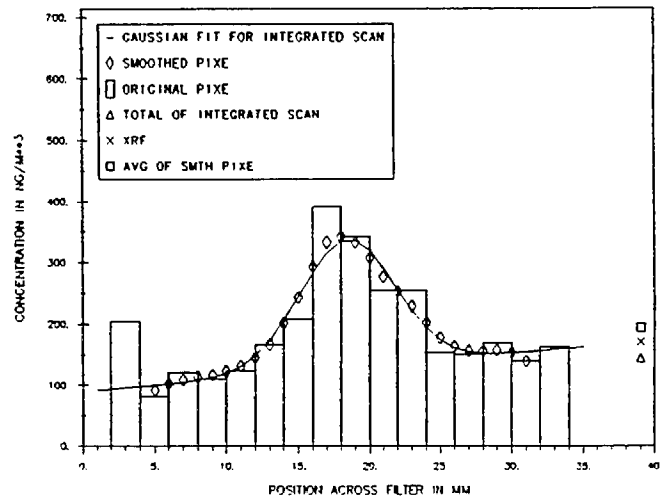


Figure 26B

SCAOS PIXE SCANS FOR PM2.5 SI; CHISO = 0.17  
 RUBI 8-104 JULIAN195 07-14-87 PERIOD03



SCAOS PIXE SCANS FOR PM2.5 K; CHISO = 0.10  
 RUBI 8-104 JULIAN195 07-14-87 PERIOD03



SCAOS PIXE SCANS FOR PM2.5 CA; CHISO = 0.41  
 RUBI 8-104 JULIAN195 07-14-87 PERIOD03

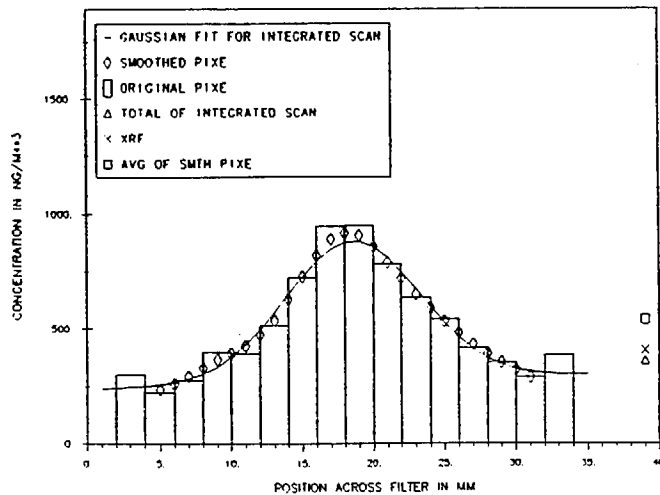
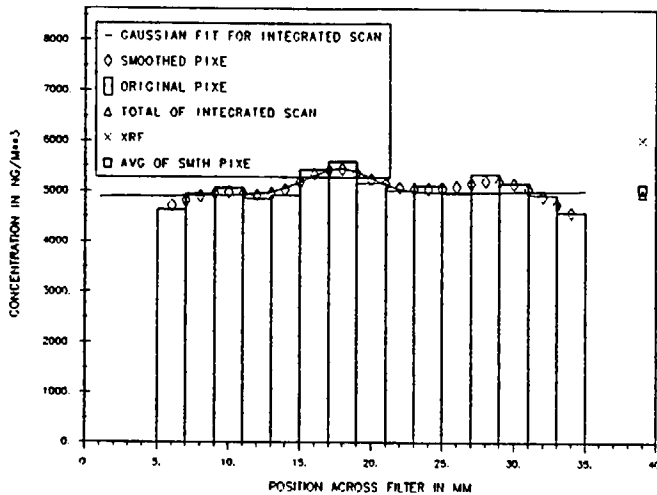
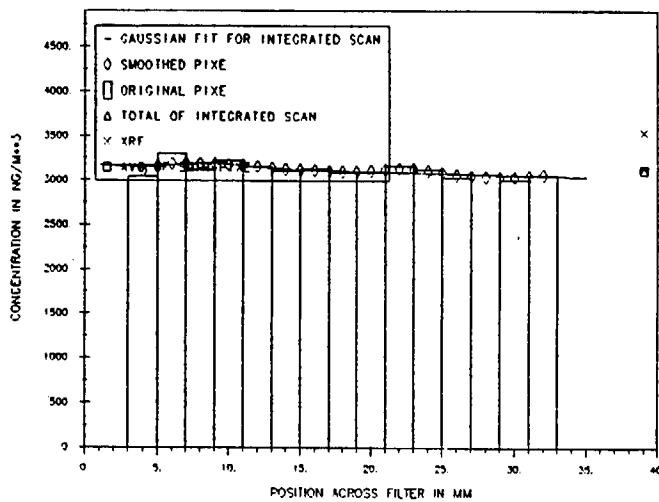


Figure 27

SCAQ5 PIXE SCANS FOR PM2.5 S : CHISO = 0.34  
 DOLA 8-072 JULIAN195 07-14-87 PERIOD3



SCAQ5 PIXE SCANS FOR PM2.5 S : CHISO = 0.02  
 AZUS 8-040 JULIAN195 07-14-87 PERIOD3



SCAQ5 PIXE SCANS FOR PM2.5 S : CHISO = 0.02  
 RUBI 8-104 JULIAN195 07-14-87 PERIOD3

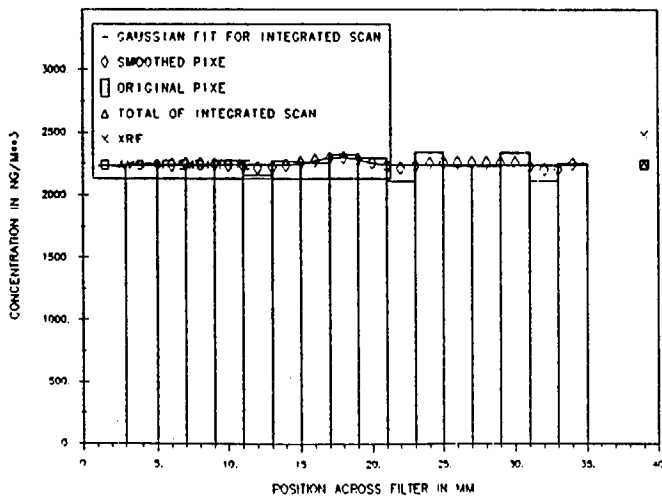
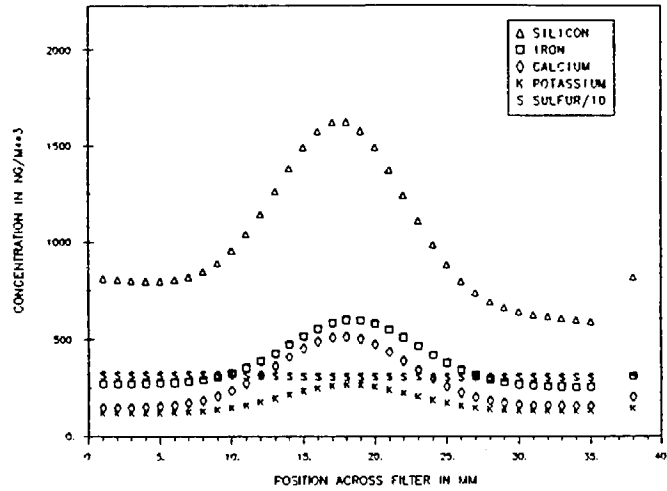
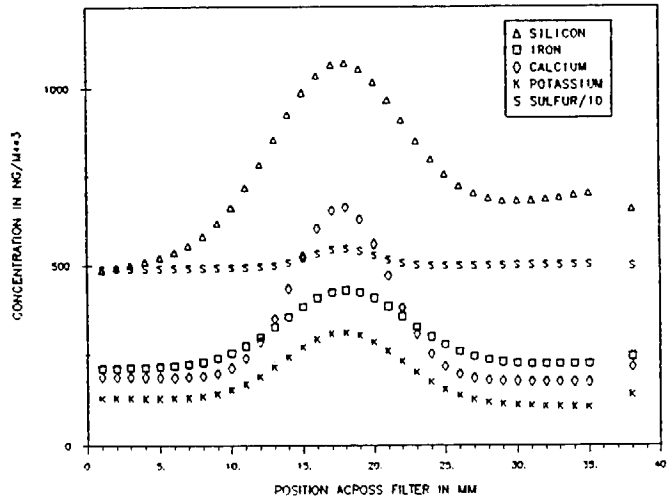


Figure 28

GAUSSIAN FITS OF SCAOS PIXE SCANS FOR PM2.5  
AZUS 8-040 JULIAN195 07-14-87 PERIOD3



GAUSSIAN FITS OF SCAOS PIXE SCANS FOR PM2.5  
DOLA 8-072 JULIAN195 07-14-87 PERIOD3



GAUSSIAN FITS OF SCAOS PIXE SCANS FOR PM2.5  
RUBI 8-104 JULIAN195 07-14-87 PERIOD3

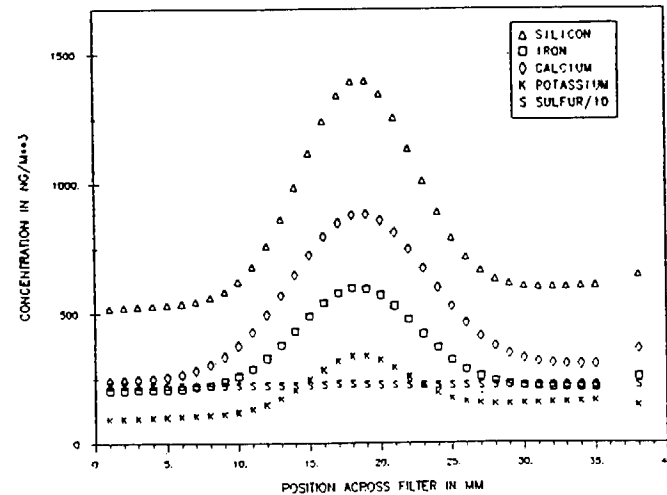
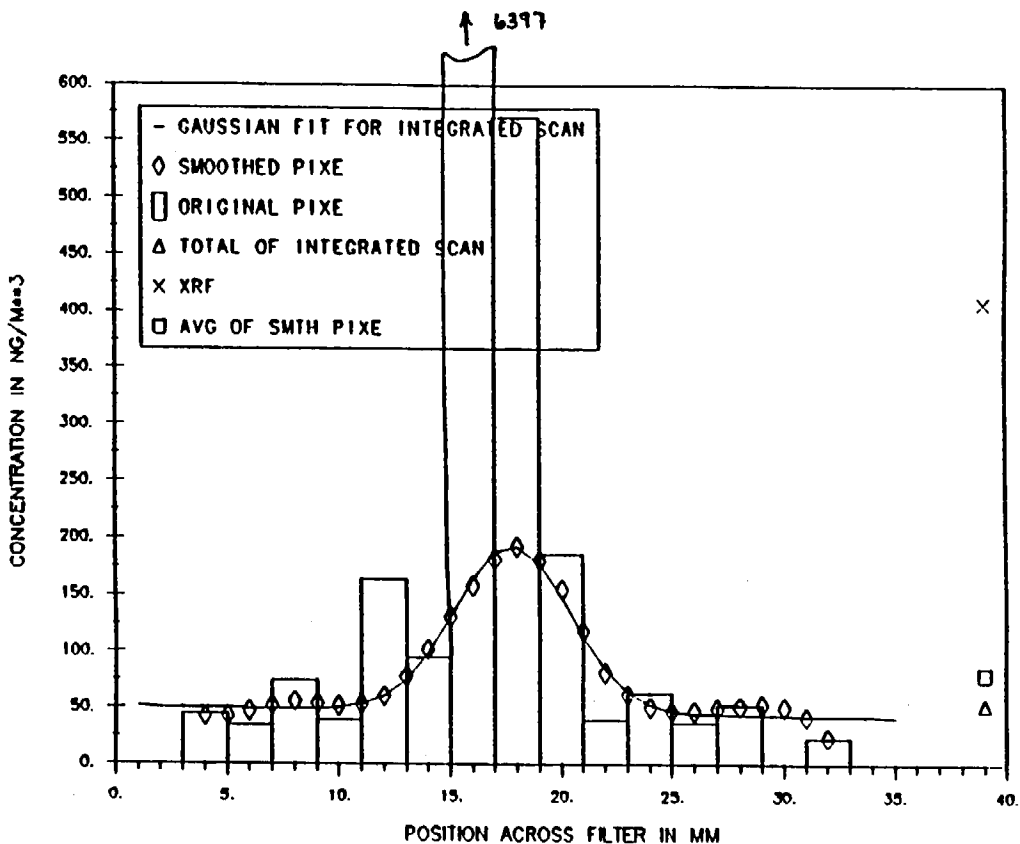


Figure 29

SCAOS PIXE SCANS FOR PM2.5 CU; CHISQ = 1.04  
DOLA 8-072 JULIAN195 07-14-87 PERIOD3



SCAOS PIXE SCANS FOR PM2.5 ZN; CHISQ = 0.28  
DOLA 8-072 JULIAN195 07-14-87 PERIOD3

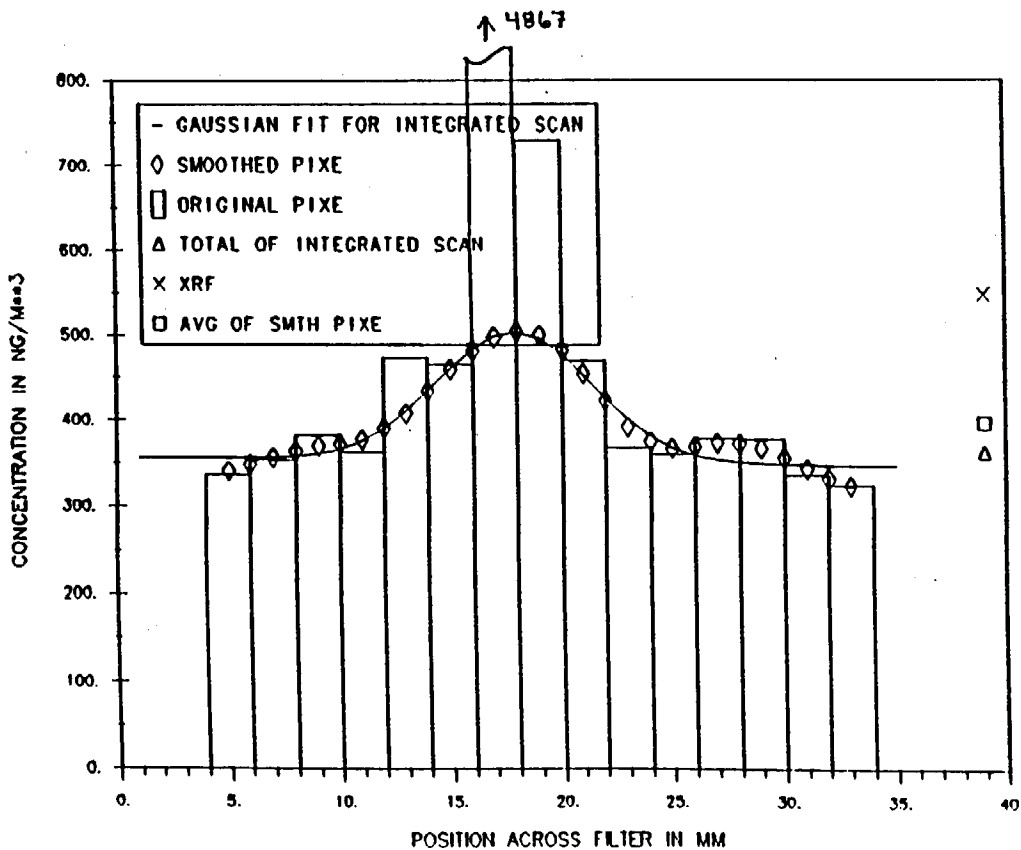
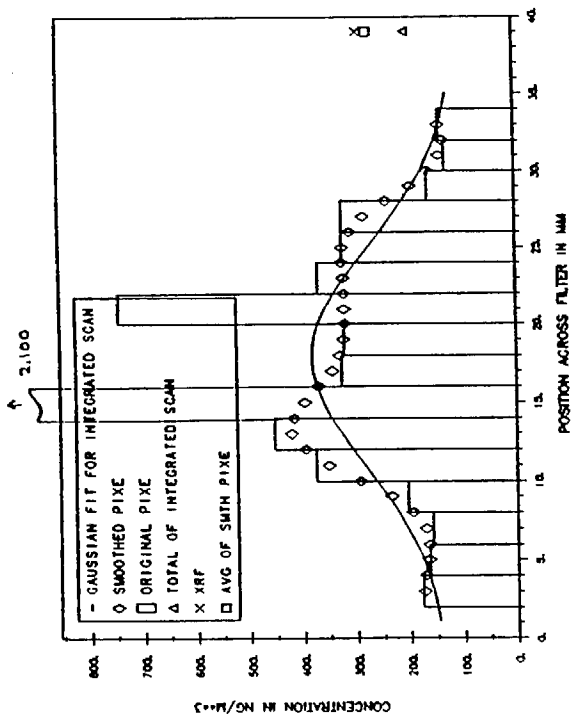
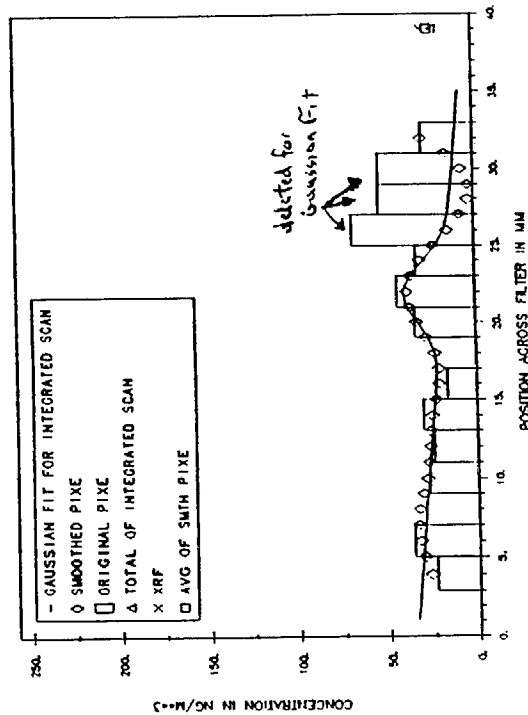


Figure 30

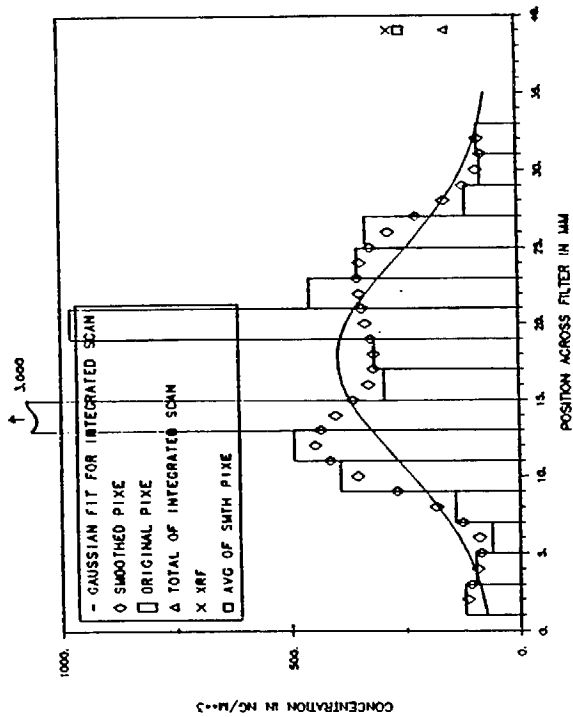
SCAOS PIXE SCANS FOR PM2.5 ZN: CHISO = 5.28  
 DOLA 8-450 JULIAN240 08-28-87 PERIOD3



SCAOS PIXE SCANS FOR PM2.5 BR: CHISO = 0.82  
 DOLA 8-215 JULIAN239 08-27-87 PERIOD3



SCAOS PIXE SCANS FOR PM2.5 CU: CHISO=12.66  
 DOLA 8-450 JULIAN240 08-28-87 PERIOD3



SCAOS PIXE SCANS FOR PM2.5 BR: CHISO = 0.18  
 DOLA 8-450 JULIAN240 08-28-87 PERIOD3

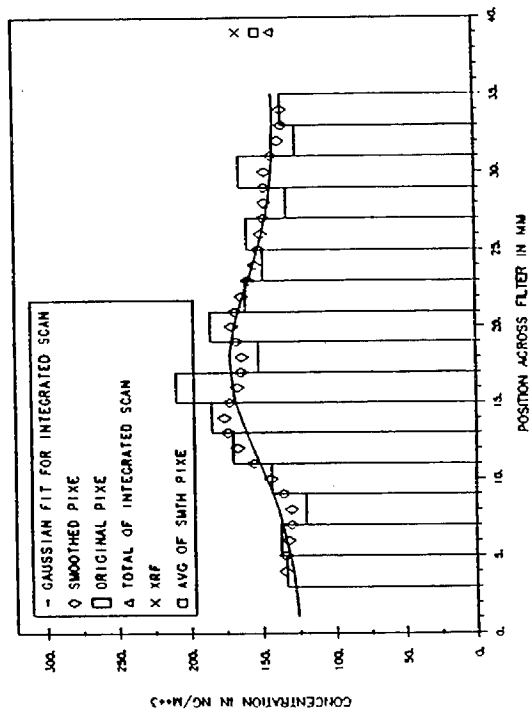


Figure 31

**PM 2.5 CORRELATION PLOTS, XRF VS PIXE - SUMMER**

With the results of the integrated scans we now have the true mean areal density of the filter. These can now be compared to the XRF results in order to find the equivalency factor to convert the XRF values to  $\text{ng}/\text{m}^3$  for PM 2.5 samples.

**Soil-Like Elements - Si, K, Ca, Ti, Fe**

Figure 32 shows the results for soils. On each graph is also a constrained line, marked "(CON)", forced through the origin. The best least squares fit give XRF/PIXE ratios of 1.36 (Si), 1.79 (K), 1.58 (Ca), and 1.33 (Fe); similar to the PM 10 values. However, there is usually a zero offset, large for Si ( $475 \text{ ng}/\text{m}^3$ ) and decreasing to Fe ( $47 \text{ ng}/\text{m}^3$ ). The constrained correlations, while poorer, are still reasonable and their slopes (constrained ratios) can be used to simplify the conversion factors (no offset). We can only speculate the reason for the offset, but refuse to do without further investigation. Later, we will combine the PM 2.5 fall data with the above summer data for better approximations.

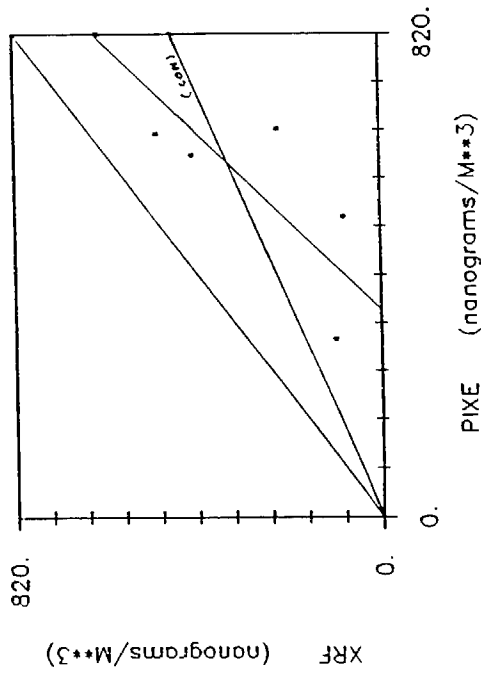
**Sulfur**

Figure 33 shows the correlation plot for sulfur, summer, all sites and all periods. An excellent  $r^2$  is achieved, 0.98, with a modest offset ( $\sim -5\%$ ), and a slope of 1.39 similar to PM 10 scans. Since almost all sulfur lies below 2.5 microns, the agreement between PM 10 and PM 2.5 was expected.

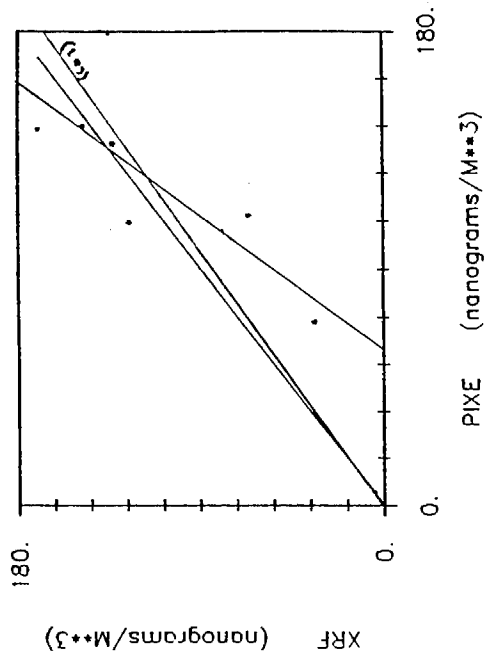
**Trace Elements - Mn, Cu, Zn, Pb, Br**

Figure 34 shows the correlation plot, summer, all sites, for copper; zinc; and bromine. Efforts were made (see Figures 30 and 31) to remove the artificial (brass) central peak, but still the results for copper are poor (only 2 data points). Zinc is better,  $r^2 = 0.77$ , slope = 1.31, offset =  $+3\%$ . Bromine is better yet, with a slope of 1.15 ( $2\%$  offset) but with limited data (only 2 data points).

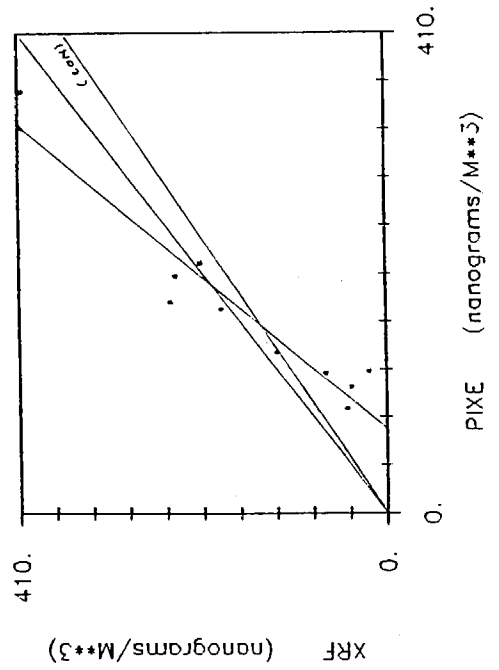
SCAQ5 PM2.5: SI FOR SUMMER



SCAQ5 PM2.5: K FOR SUMMER



SCAQ5 PM2.5: CA FOR SUMMER



SCAQ5 PM2.5: FE FOR SUMMER

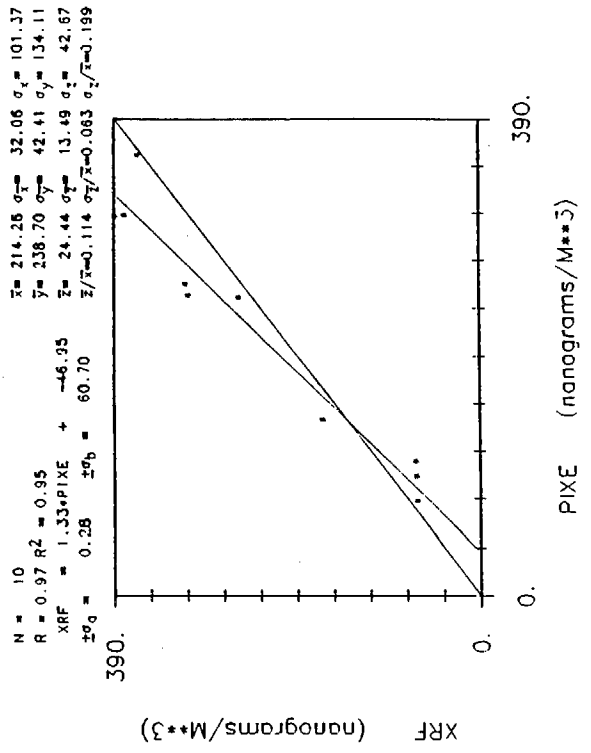


Figure 32

# SCAQs PM2.5: S FOR SUMMER

$\bar{x} = 3524.87$     $\sigma_{\bar{x}} = 538.15$     $\sigma_x = 1864.19$   
 $\bar{y} = 4320.25$     $\sigma_{\bar{y}} = 747.66$     $\sigma_y = 2589.98$   
 $\bar{z} = 795.38$     $\sigma_{\bar{z}} = 224.40$     $\sigma_z = 777.35$   
 $\bar{z}/\bar{x} = 0.226$     $\sigma_{\bar{z}}/\bar{x} = 0.064$     $\sigma_z/\bar{x} = 0.221$

$N = 12$   
 $R = 0.99$     $R^2 = 0.98$   
 $XRF = 1.39 * PIXE + -589.54$   
 $\pm \sigma_a = 0.15$     $\pm \sigma_b = 516.28$

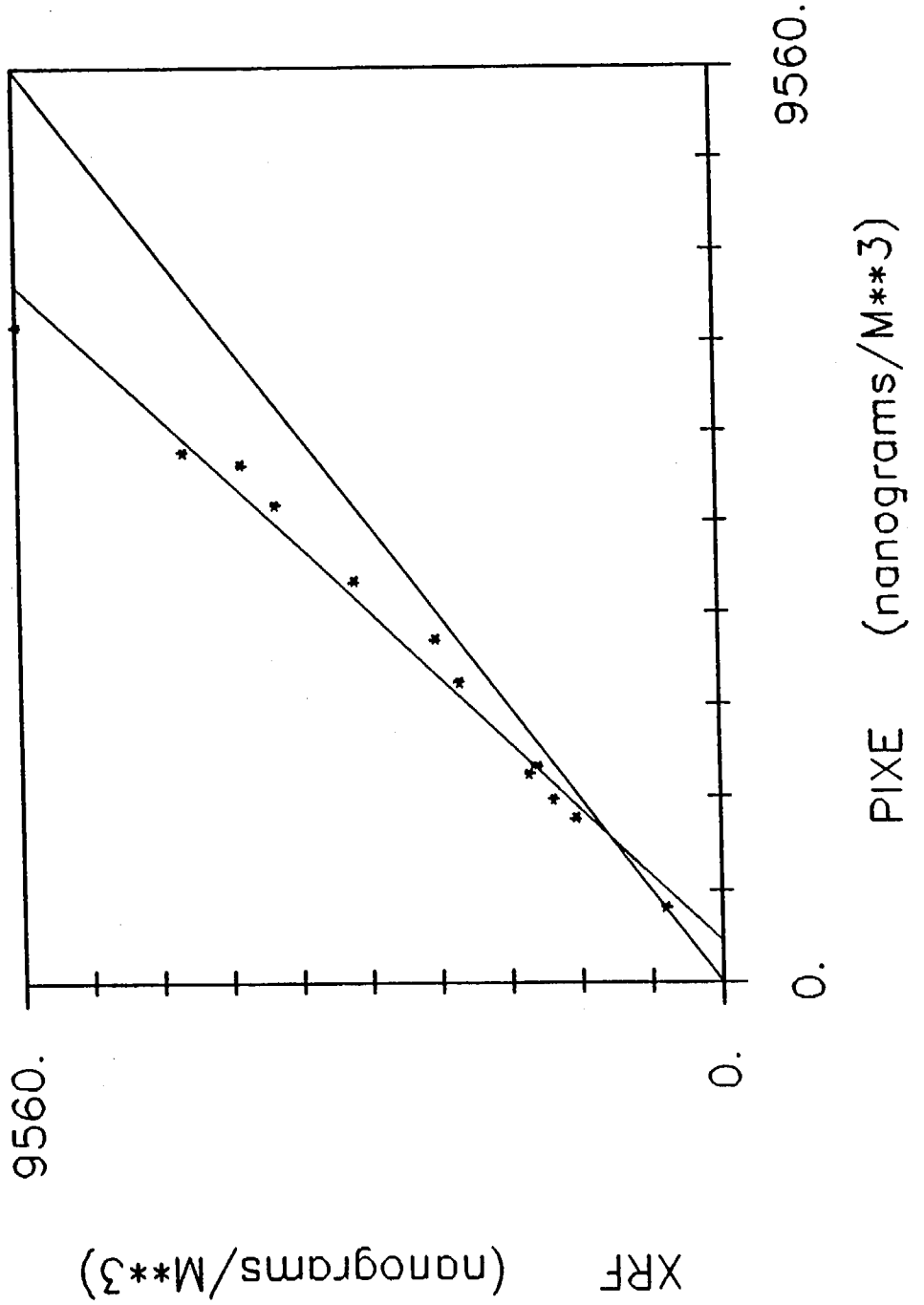
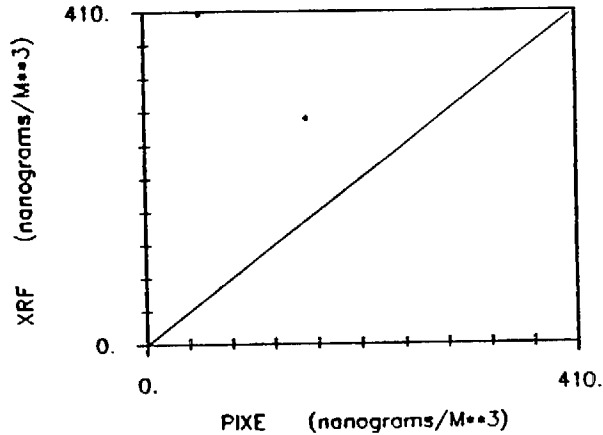


Figure 33

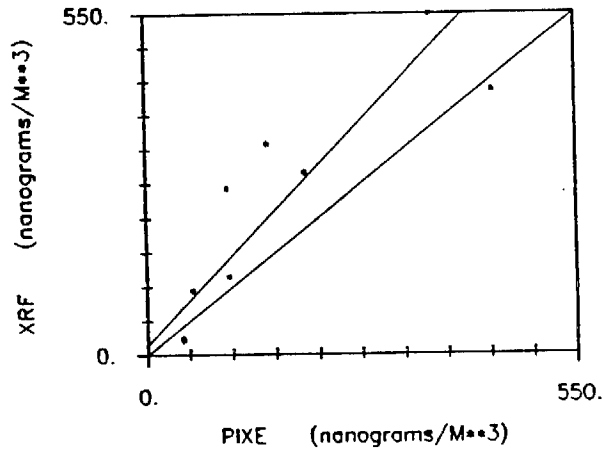
46  
SCAQ5 PM2.5: CU FOR SUMMER

$N = 2$   $\bar{x} = 103.37$   $\sigma_x = 50.64$   $\sigma_x = 71.82$   
 $R = \dots R^2 = 1.00$   $\bar{y} = 342.50$   $\sigma_y = 64.50$   $\sigma_y = 91.22$   
 $XRF = -1.27 \cdot PIXE + 474.16$   $\bar{x} = 239.13$   $\sigma_x = 115.14$   $\sigma_x = 162.83$   
 $\pm \sigma_a = 0.00$   $\pm \sigma_b = 100.57$   $\bar{x}/\bar{y} = 2.313$   $\sigma_x/\sigma_y = 1.114$   $\sigma_x/\sigma_y = 1.575$



SCAQ5 PM2.5: ZN FOR SUMMER

$N = 9$   $\bar{x} = 189.62$   $\sigma_x = 47.86$   $\sigma_x = 143.59$   
 $R = 0.68$   $R^2 = 0.77$   $\bar{y} = 238.56$   $\sigma_y = 60.89$   $\sigma_y = 182.67$   
 $XRF = 1.31 \cdot PIXE + 15.69$   $\bar{x} = 68.94$   $\sigma_x = 29.55$   $\sigma_x = 88.66$   
 $\pm \sigma_a = 0.68$   $\pm \sigma_b = 115.24$   $\bar{x}/\bar{y} = 0.408$   $\sigma_x/\sigma_y = 0.174$   $\sigma_x/\sigma_y = 0.523$



SCAQ5 PM2.5: BR FOR SUMMER

$N = 2$   $\bar{x} = 82.08$   $\sigma_x = 59.35$   $\sigma_x = 83.93$   
 $R = 1.00$   $R^2 = 1.00$   $\bar{y} = 97.00$   $\sigma_y = 68.00$   $\sigma_y = 96.17$   
 $XRF = 1.15 \cdot PIXE + 2.98$   $\bar{x} = 14.94$   $\sigma_x = 8.66$   $\sigma_x = 12.24$   
 $\pm \sigma_a = 0.00$   $\pm \sigma_b = 162.98$   $\bar{x}/\bar{y} = 0.182$   $\sigma_x/\sigma_y = 0.105$   $\sigma_x/\sigma_y = 0.149$

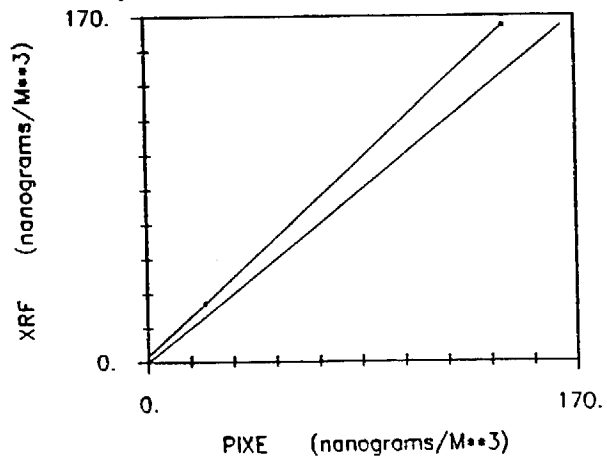


Figure 34

## PM 2.5 ELEMENTAL SCANS - FALL

### Soil-like Elements - Si, K, Ca, Ti, Fe

Figure 35 shows soil-like elements, Si, K, Ca, and Fe at Downtown Los Angeles (DOLA), while similar scans are shown for Long Beach (LOBE) and Burbank (BURB), for 11/12/87, in Figures 36 and 37.

The central peaking for Si, Ca, and Fe remain, similar to summer, but now potassium (K) shows a much flatter profile. This would be expected if there was significant wood smoke in the profile which was absent in summer.

### Sulfur

Figure 38 shows scans of sulfur for Los Angeles, Long Beach, and Burbank, 11/12/87, period 3. The results are similar to those of summer in all regards, showing little or no central peaking.

The above results are summarized in Figure 39 for all three sites, period 3, 11/12/87. Sulfur was divided by 10 to keep it on scale.

### Trace Elements

A major effort was made to gather enough data on trace elements to allow consistent ratios to be developed, XRF to PIXE. This effort was plagued by a lack of consistency in elemental profiles (site to site, period to period, element to element, etc.) unlike consistent profiles found for soil elements, sulfur, and carbon soot. Elemental amounts were also many times near or below minimum detectable limits for XRF and/or PIXE scans for trace elements thereby limiting the correction efforts with a lack of data. Thus, in this section, we will present examples of scans for each trace element species, all for fall, November and December.

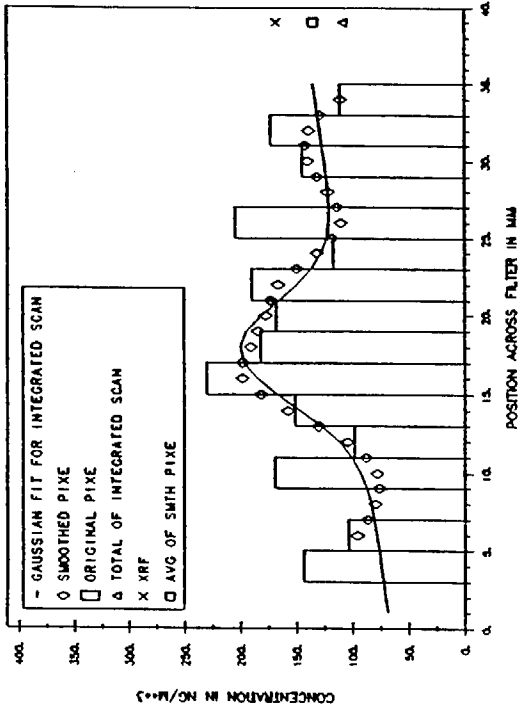
### Chlorine

Figure 40 shows a profile for chlorine at Anaheim in December. Since halogens are easily lost from acidic filters, especially in summer, chlorine was not regularly seen. The distribution in Figure 40 has a broadened central peaking that differs from soil-like particles, and the XRF value was far higher than the PIXE scans (see right margin of Figure 40). Thus, great caution must be exercised in applying correction factors for chlorine (and perhaps bromine - see later). A good deal of time had passed between particulate collection and the PIXE scans so an undetermined amount of chlorine may have been lost from each filter.

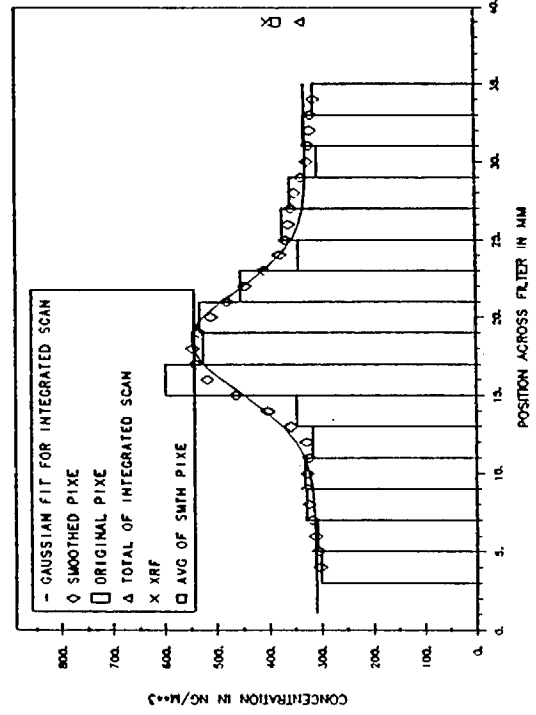
### Titanium

Figure 41 presents four separate scans for titanium. The variation versus site and time are great, from the soil-like coarse particulate behavior at Los Angeles, 11/12/87, period 5, to the virtually flat fine particulate behavior at Los Angeles, 12/11/87, period 3. Clearly, mixed sources are indicated, and thus correction factors will be uncertain.

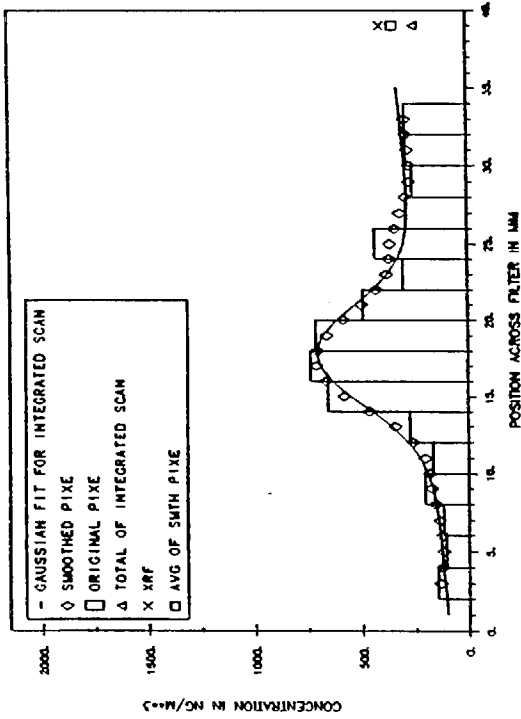
SCAQS PIXE SCANS FOR PM2.5 K; CHISO = 0.27  
 DOLA 8-691 JULIAN316 11-12-87 PERIOD3



SCAQS PIXE SCANS FOR PM2.5 FE; CHISO = 0.34  
 DOLA 8-691 JULIAN316 11-12-87 PERIOD3



SCAQS PIXE SCANS FOR PM2.5 SI; CHISO = 0.71  
 DOLA 8-691 JULIAN316 11-12-87 PERIOD3



SCAQS PIXE SCANS FOR PM2.5 CA; CHISO = 0.28  
 DOLA 8-691 JULIAN316 11-12-87 PERIOD3

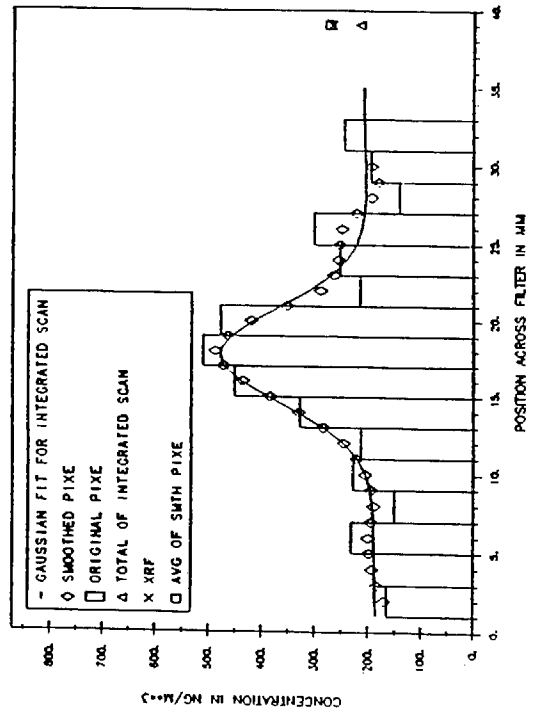
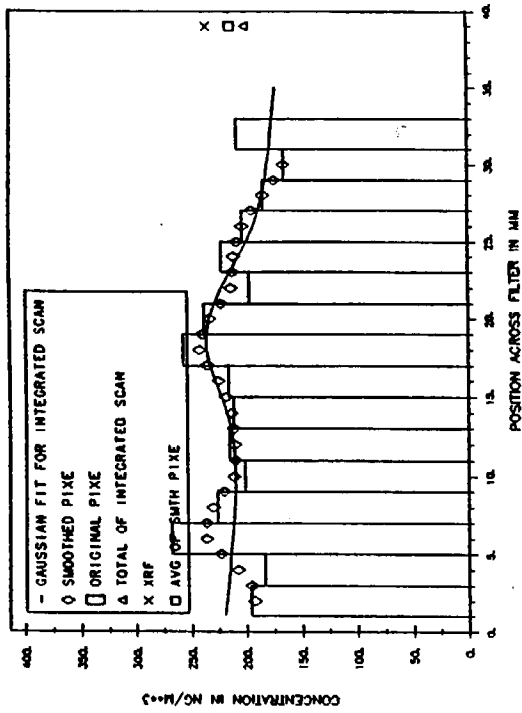
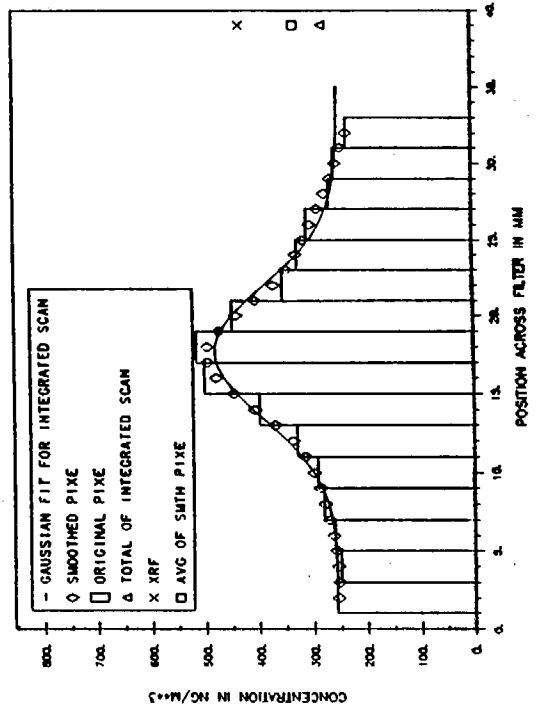


Figure 35

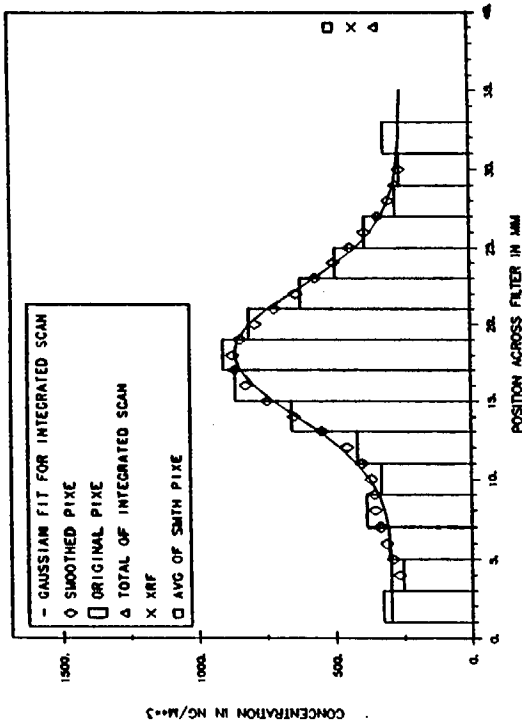
SCAOS PIXE SCANS FOR PM2.5 K; CHISO = 0.43  
LOBE 8-755 JULIAN316 11-12-87 PERIOD1



SCAOS PIXE SCANS FOR PM2.5 FE; CHISO = 0.33  
LOBE 8-755 JULIAN316 11-12-87 PERIOD1



SCAOS PIXE SCANS FOR PM2.5 SI; CHISO = 0.49  
LOBE 8-755 JULIAN316 11-12-87 PERIOD1



SCAOS PIXE SCANS FOR PM2.5 CA; CHISO = 0.08  
LOBE 8-755 JULIAN316 11-12-87 PERIOD1

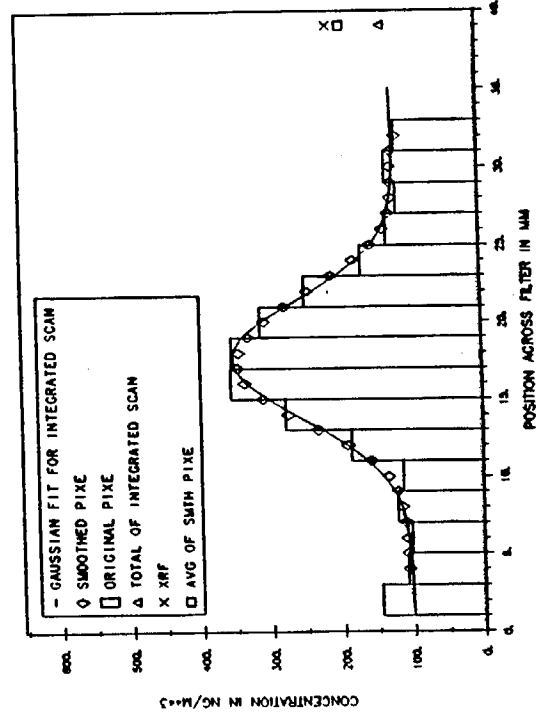
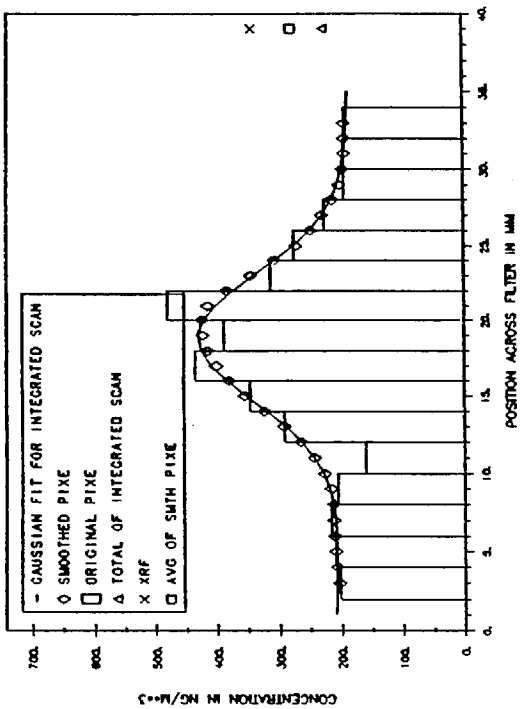
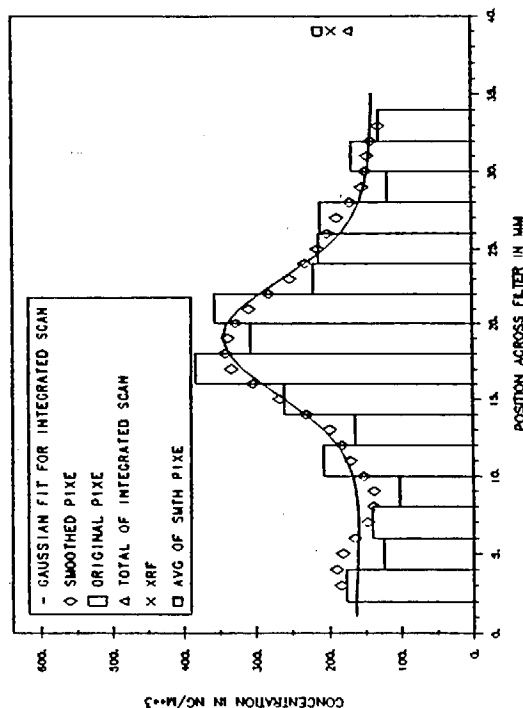


Figure 36

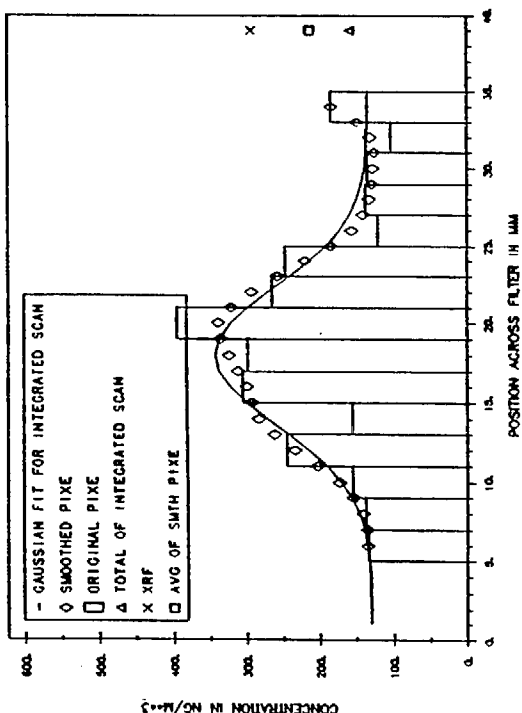
SCAOS PIXE SCANS FOR PM2.5 FE; CHISO = 0.05  
BURB 8-657 JULIAN316 11-12-87 PERIOD3



SCAOS PIXE SCANS FOR PM2.5 CA; CHISO = 0.19  
BURB 8-657 JULIAN316 11-12-87 PERIOD3



SCAOS PIXE SCANS FOR PM2.5 SI; CHISO = 0.56  
BURB 8-657 JULIAN316 11-12-87 PERIOD3



SCAOS PIXE SCANS FOR PM2.5 K; CHISO = 0.21  
BURB 8-657 JULIAN316 11-12-87 PERIOD3

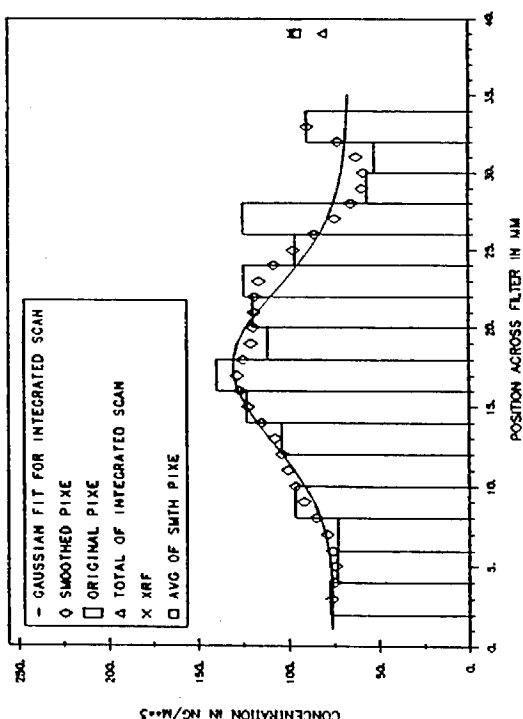
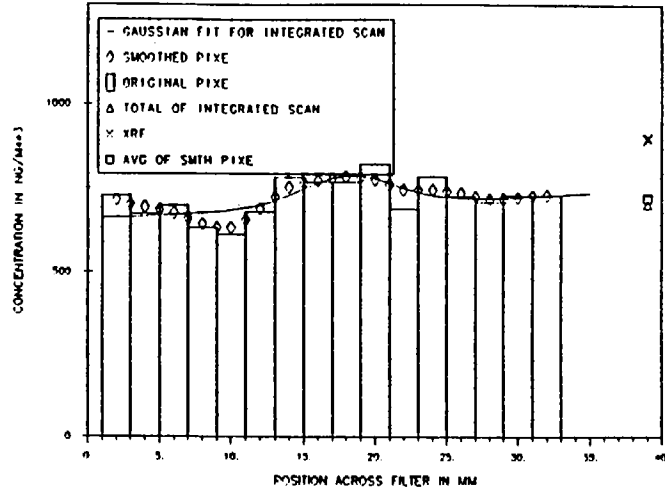
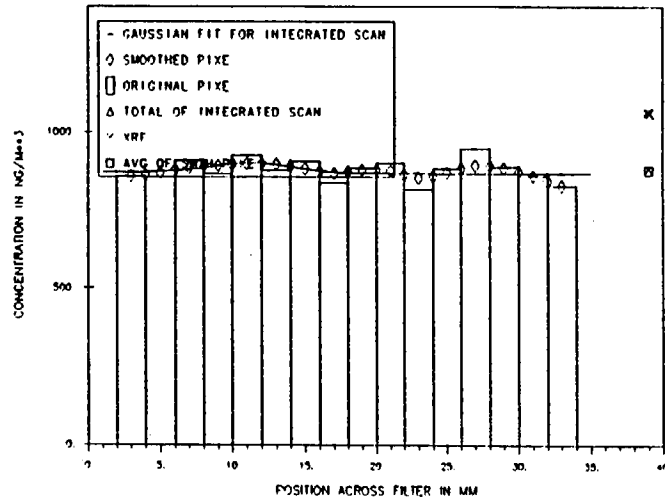


Figure 37

SCAQS PIXE SCANS FOR PM2.5 S : CHISO = 0.29  
 DOLA 8-691 JULIAN316 11-12-87 PERIOD3



SCAQS PIXE SCANS FOR PM2.5 S : CHISO = 0.07  
 LOBE 8-755 JULIAN316 11-12-87 PERIOD1



SCAQS PIXE SCANS FOR PM2.5 S : CHISO = 0.56  
 BURB 8-657 JULIAN316 11-12-87 PERIOD3

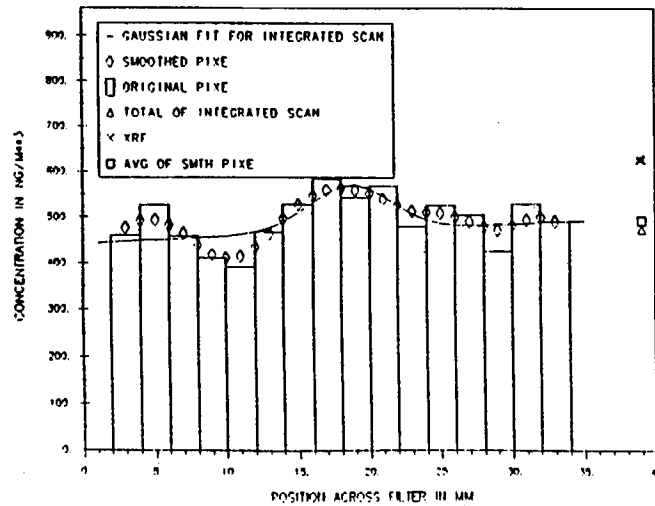
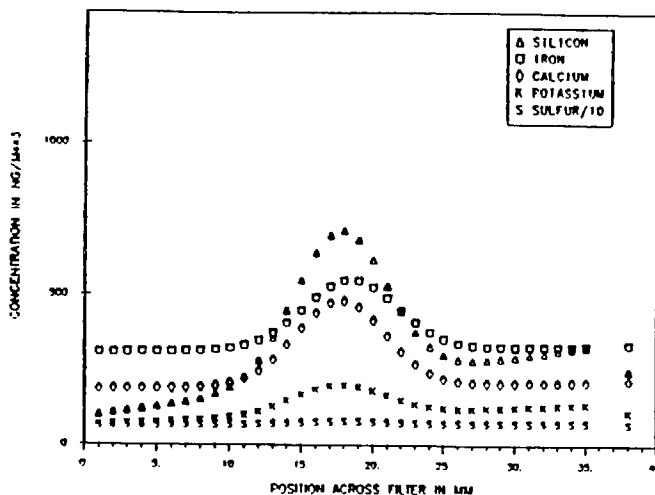
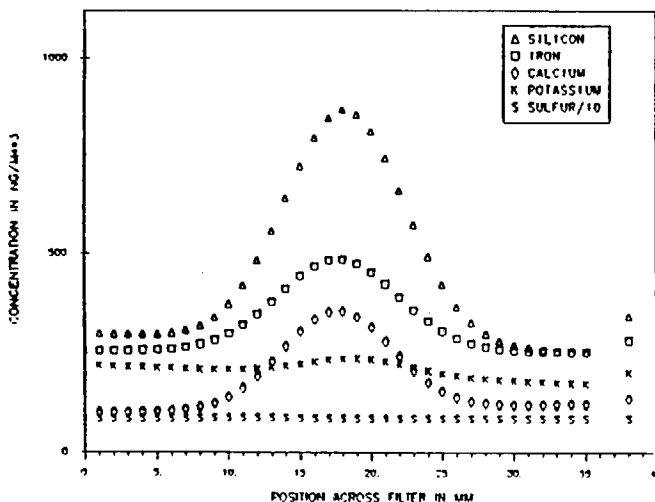


Figure 38

GAUSSIAN FITS OF SCAQS PIXE SCANS FOR PM2.5  
DOLA 8-691 JULIAN316 11-12-87 PERIOD3



GAUSSIAN FITS OF SCAQS PIXE SCANS FOR PM2.5  
LOBE 8-755 JULIAN316 11-12-87 PERIOD1



GAUSSIAN FITS OF SCAQS PIXE SCANS FOR PM2.5  
BURB 8-857 JULIAN316 11-12-87 PERIOD3

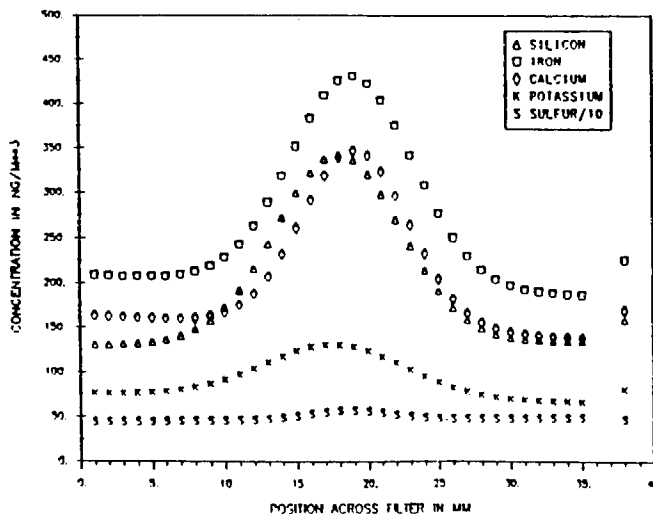


Figure 39

SCAQS PIXE SCANS FOR PM2.5 CL; CHISQ = 0.64  
 ANAH 8-641 JULIAN344 12-10-87 PERIOD3

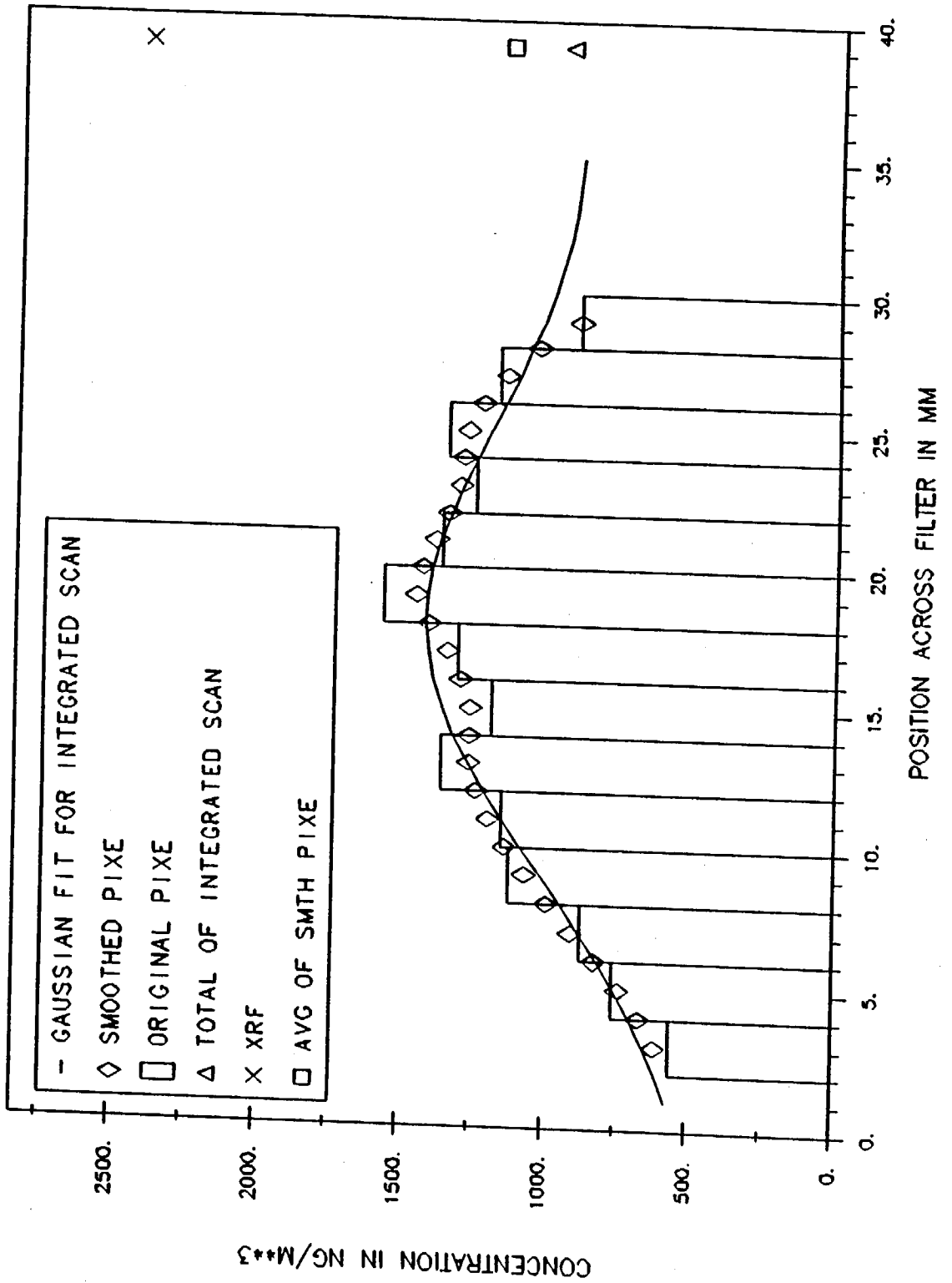
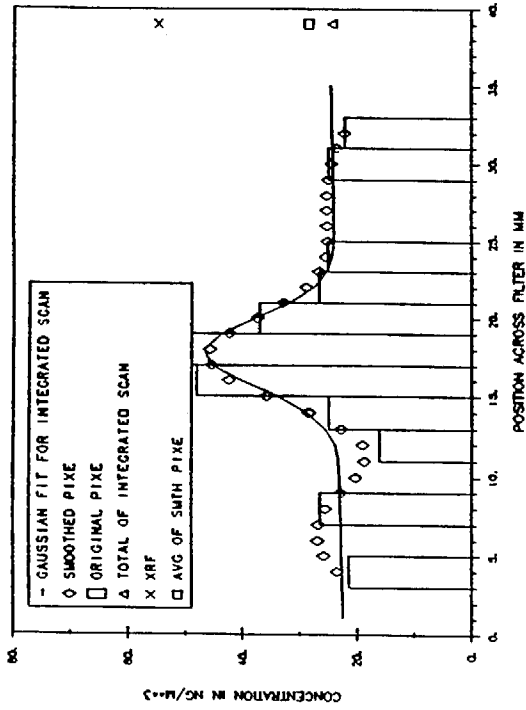
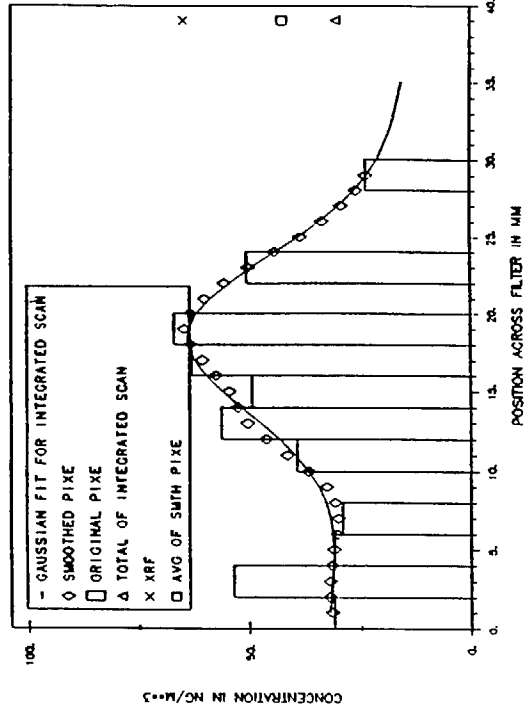


Figure 40

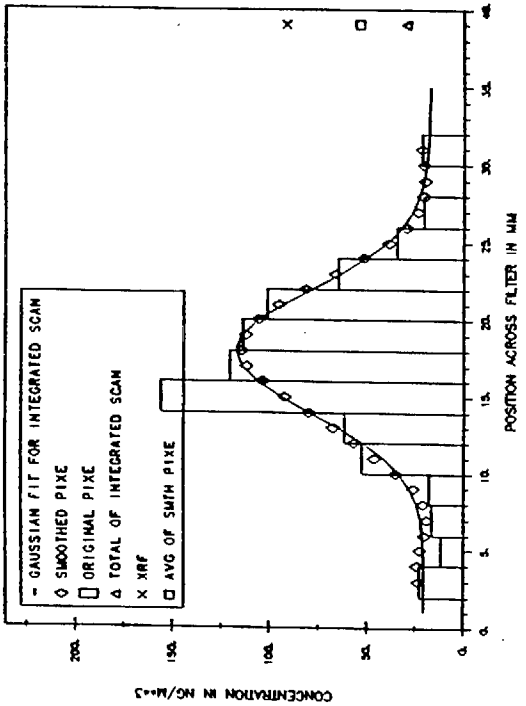
SCAQS PIXE SCANS FOR PM2.5 Tl; CHISO = 0.10  
 LOBE 8-755 JULIAN316 11-12-87 PERIOD1



SCAQS PIXE SCANS FOR PM2.5 Tl; CHISO = 0.01  
 ANAH 8-647 JULIAN345 12-11-87 PERIOD3



SCAQS PIXE SCANS FOR PM2.5 Tl; CHISO = 0.09  
 DOLA 8-893 JULIAN316 11-12-87 PERIOD5



SCAQS PIXE SCANS FOR PM2.5 Tl; CHISO = 0.20  
 DOLA 8-713 JULIAN345 12-11-87 PERIOD3

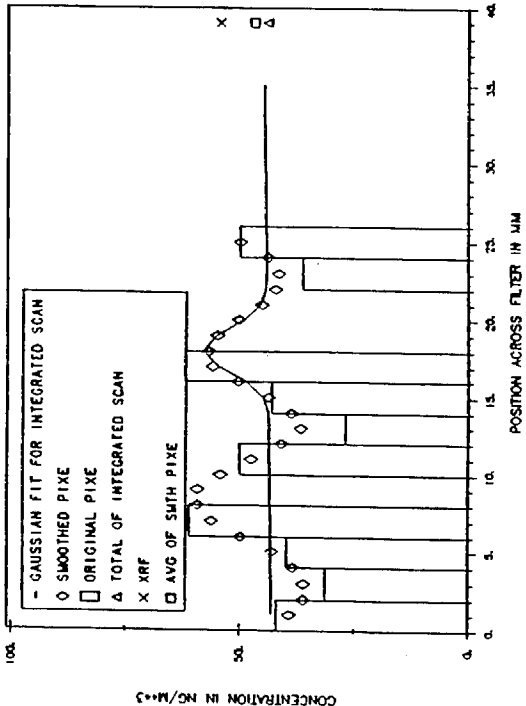


Figure 41

### Vanadium

Figure 42 shows a scan for vanadium at Hawthorne, 11/12/87, period 3. The low levels of this and some other tracers, such as nickel which tends to correlate with vanadium in this area, makes individual data points less firm statistically. However, the scan is consistent with a fine particulate source with only modest central peaking, and the XRF/PIXE ratio was close to 1.0.

### Manganese

Manganese, like titanium, is an element found in soils. Yet, unlike many titanium scans manganese shows little or no central peaking, indicating fine particulate behavior (Figure 43). This is not totally unexpected since the amount of manganese, though relatively low, greatly exceeds the expected Mn/Fe ratio from soil in filters we have scanned. We are unsure of the fine manganese source (maybe industrial).

### Copper and Zinc

These two elements will be handled together due to the brass-like anomalies seen on both PM 10 and PM 2.5 filters. The first set is shown in Figure 44 for Los Angeles, 11/12/87, period 1 and period 2. Figure 45 shows period 3 and period 5, also at Los Angeles on 11/12/87. In each sequential period, "brass-like" excursions appear, but at different locations and with different magnitudes. The PIXE integrated scans were done after removing these excursions, but clearly these filters are wildly non-uniform. If the XRF system observes a single such "brass-like" particle, the entire result could be inflated by a large factor. In period 2 and 3 the XRF excitation area did not overlap the "brass-like" particle, and the XRF/PIXE ratio is close to 1.0. In period 1, because the particle was centered on the filter, XRF/PIXE was close to 2.0, as might be expected. Period 5 shows a slightly off-center "brass-like" particle along with strong central peaking. Predictably, XRF/PIXE is now greater than 2.0. This behavior was seen on most filters, all sites, and all periods. A well behaved filter, such as that seen at Anaheim on 12/11/87, period 5 (bottom of Figure 46) was the exception, not the rule.

Ignoring the "brass-like" excursions, we still see differences site to site, period to period, in copper and zinc. Both have a major coarse particle, central peaking component, especially copper. Yet on many occasions, such as Los Angeles, 11/12/87, period 2; and 12/11/87, period 3 the central peaking is very weak, indicating an overwhelming dominance of very fine particles. Fortunately, except for the "brass-like" particles, XRF and PIXE are generally in good agreement when there is not strong central peaking.

### Bromine and Lead

Bromine and lead are also plotted together, since a source of these concentrations comes from the use of leaded gasoline, still commonly used in 1987. Figure 47 shows a rather typical spectrum, with a very flat lead profile, characteristic of fine particles for lead, but a slightly centrally peaked bromine profile. We compare Los Angeles and Long Beach for 11/12/87, period 5 and find more peaking for bromine at Los Angeles than Long Beach. Yet, the amount of bromine and lead is very similar at the two sites. A caution must be

SCAQ5 PIXE SCANS FOR PM2.5 V ; CHISQ = 0.03  
 HAWT 8-724 JULIAN316 11-12-87 PERIOD3

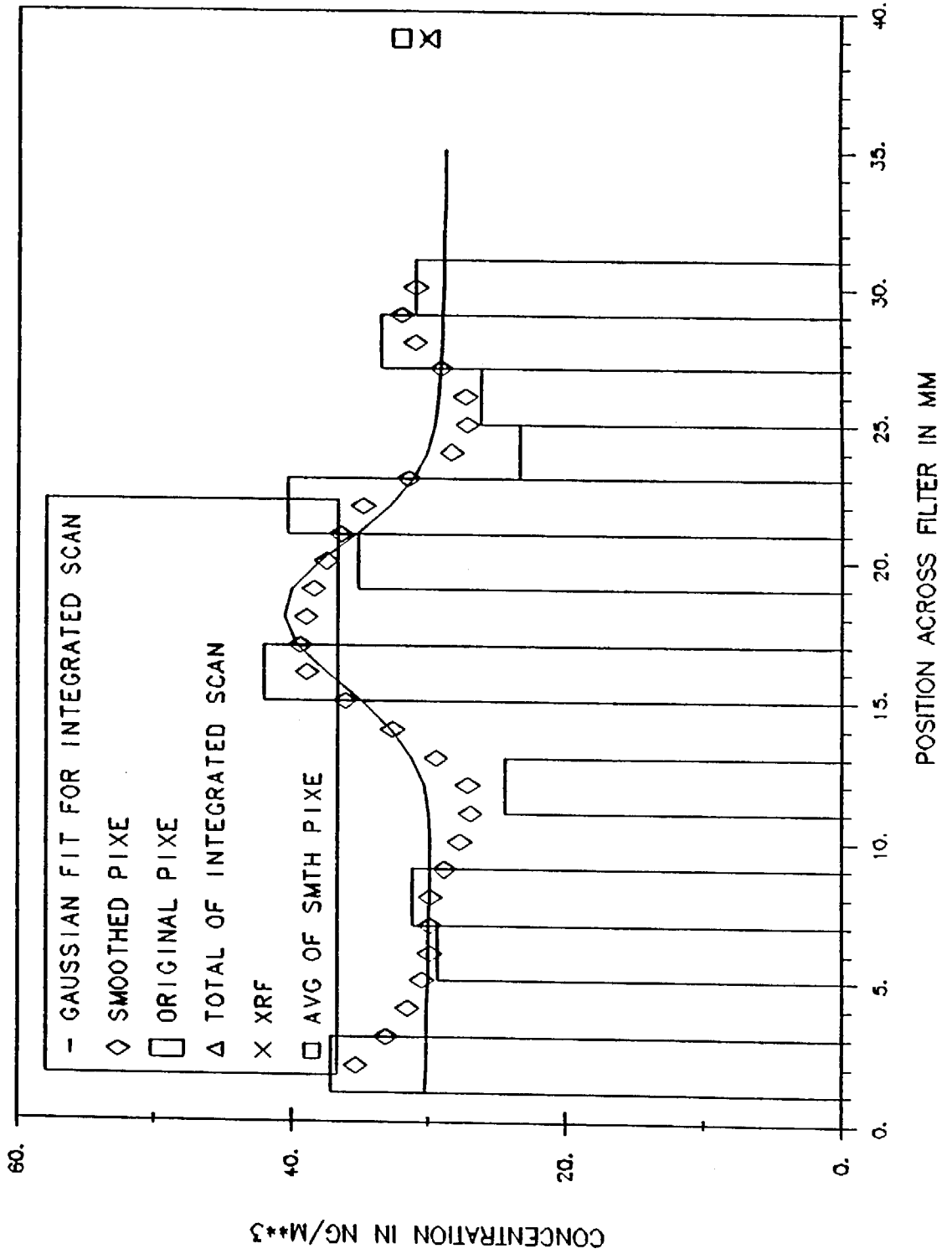
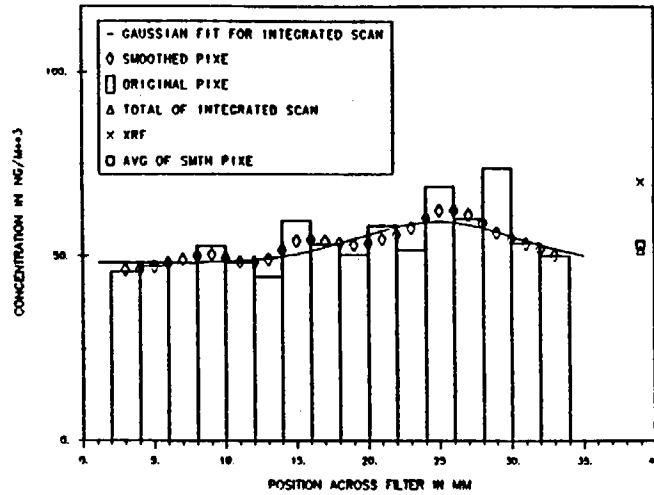
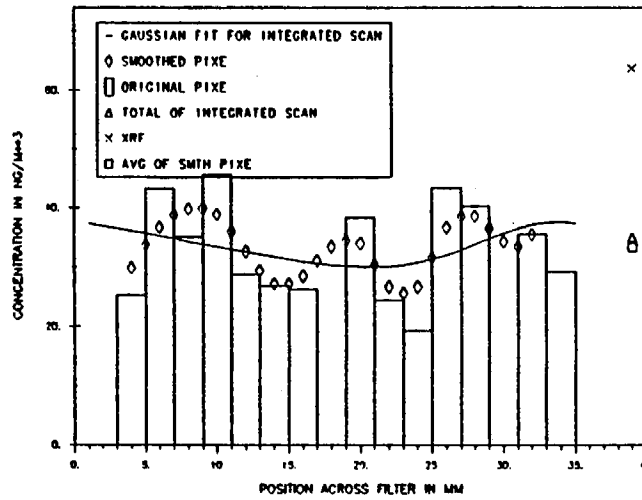


Figure 42

SCAQ5 PIXE SCANS FOR PM2.5 MN; CHISO = 0.12  
 LOBE 8-755 JULIAN316 11-12-87 PERIOD1



SCAQ5 PIXE SCANS FOR PM2.5 MN; CHISO = 0.38  
 DOLA 8-690 JULIAN316 11-12-87 PERIOD2



SCAQ5 PIXE SCANS FOR PM2.5 MN; CHISO = 0.42  
 DOLA 8-693 JULIAN316 11-12-87 PERIOD5

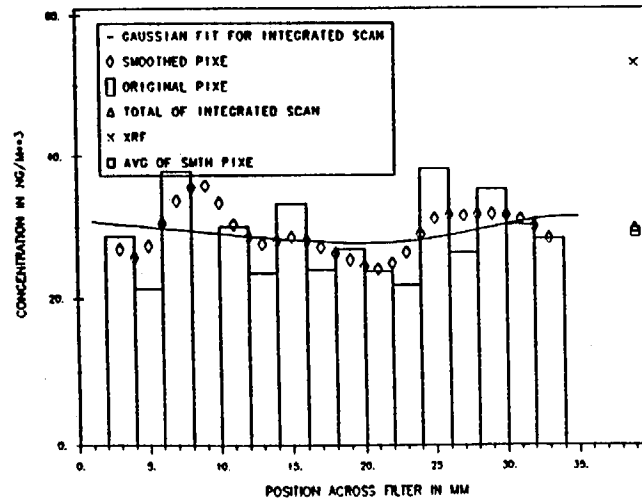
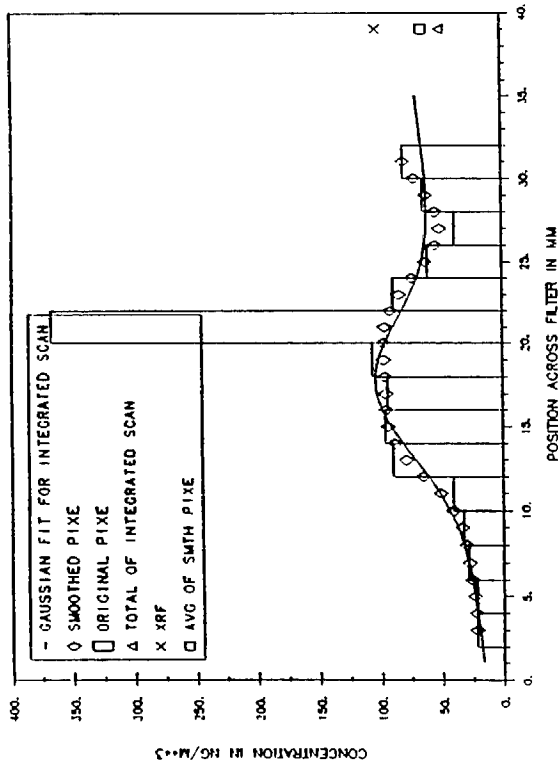
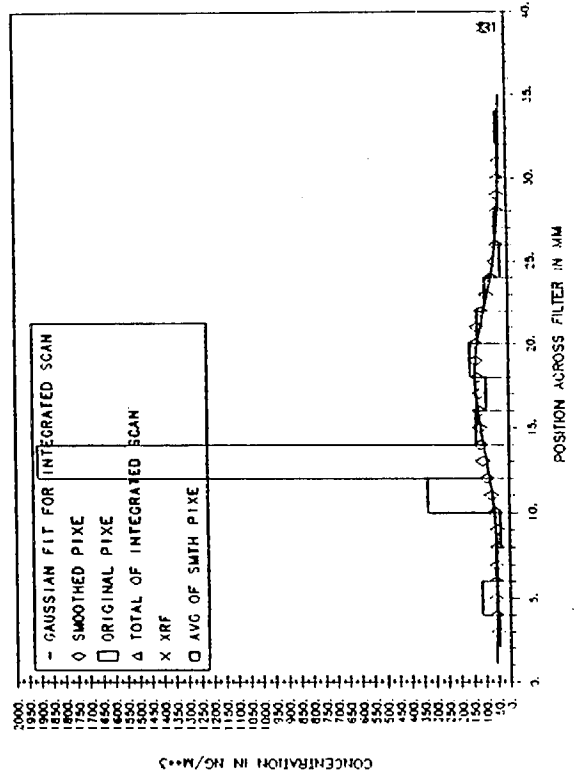


Figure 43

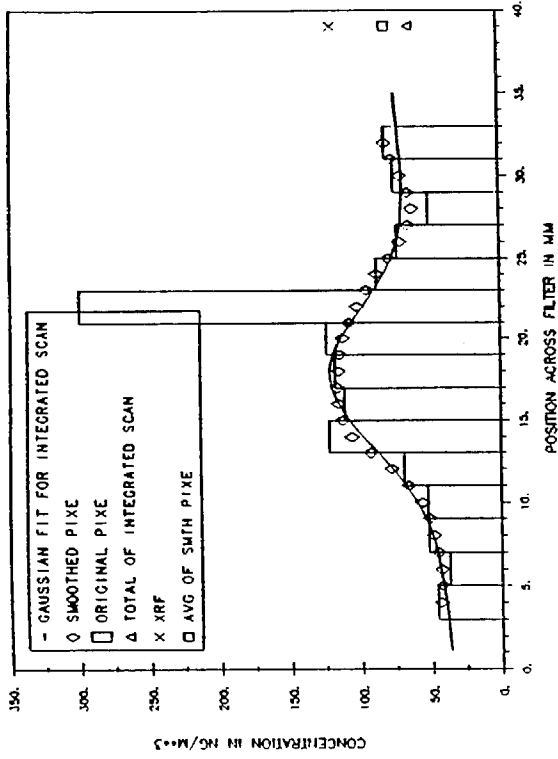
SCAOS PIXE SCANS FOR PM2.5 CU; CHISQ = 1.41  
 DOLA 3-689 JULIAN316 11-12-87 PERIOD1



SCAOS PIXE SCANS FOR PM2.5 CU; CHISQ = 1.15  
 DOLA 3-689 JULIAN316 11-12-87 PERIOD2



SCAOS PIXE SCANS FOR PM2.5 ZN; CHISQ = 0.63  
 DOLA 3-689 JULIAN316 11-12-87 PERIOD1



SCAOS PIXE SCANS FOR PM2.5 ZN; CHISQ = 0.35  
 DOLA 3-689 JULIAN316 11-12-87 PERIOD2

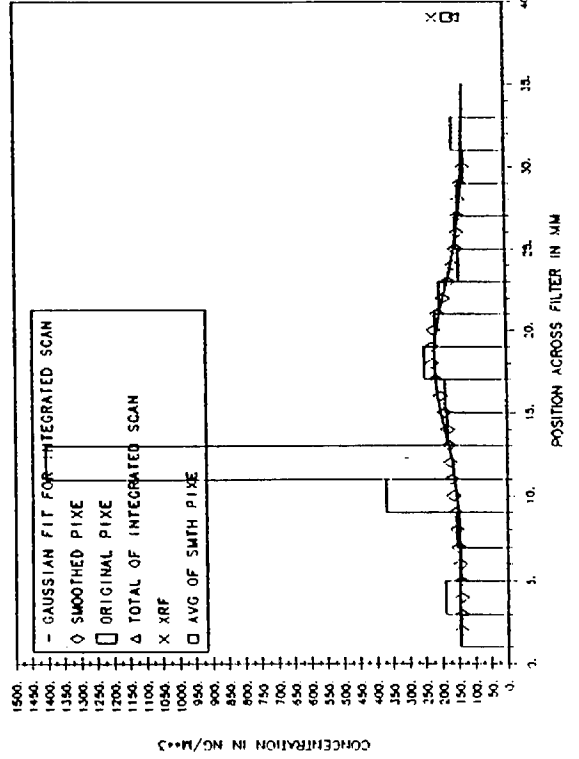
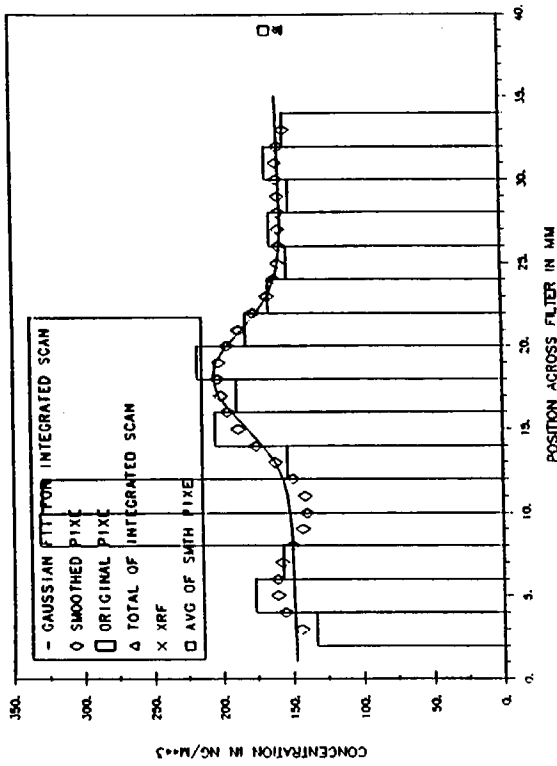
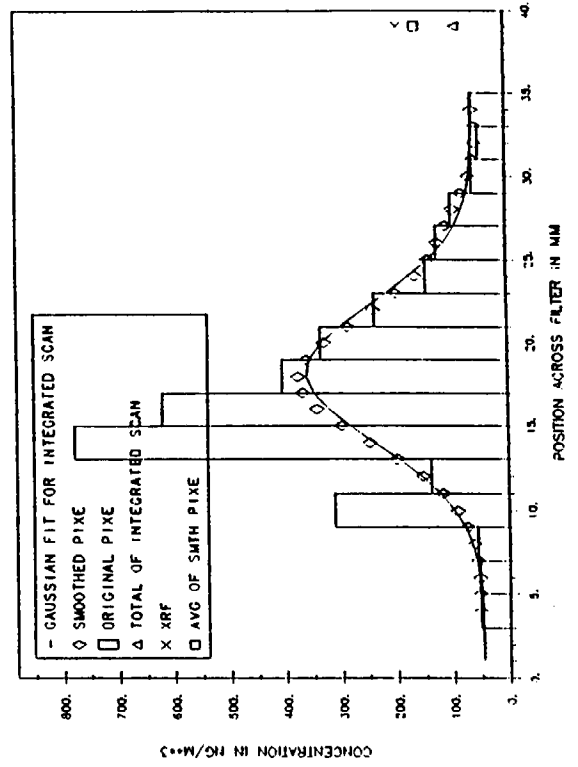


Figure 44

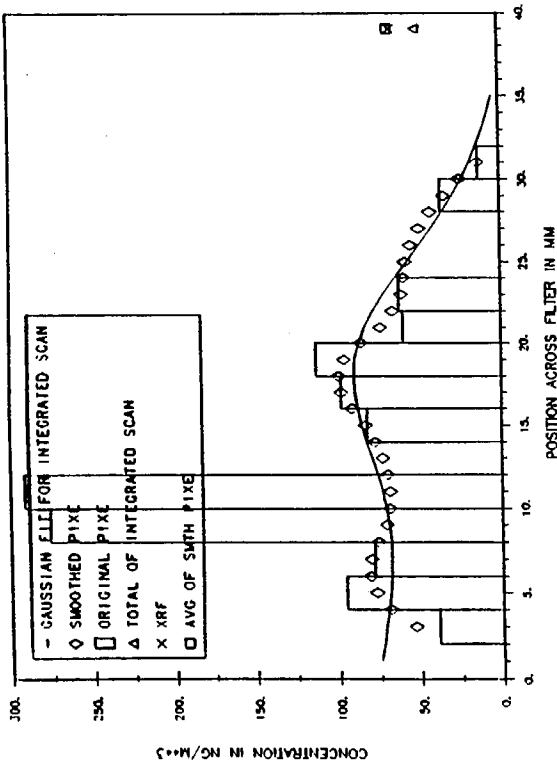
SCAQS PIXE SCANS FOR PM2.5 ZN; CHISO = 0.25  
DOLA 8-591 JULIAN316 11-12-87 PERIOD3



SCAQS PIXE SCANS FOR PM2.5 ZN; CHISO = 1.20  
DOLA 8-693 JULIAN316 11-12-87 PERIOD5



SCAQS PIXE SCANS FOR PM2.5 CU; CHISO = 0.92  
DOLA 8-591 JULIAN316 11-12-87 PERIOD3



SCAQS PIXE SCANS FOR PM2.5 CU; CHISO = 5.17  
DOLA 8-693 JULIAN316 11-12-87 PERIOD5

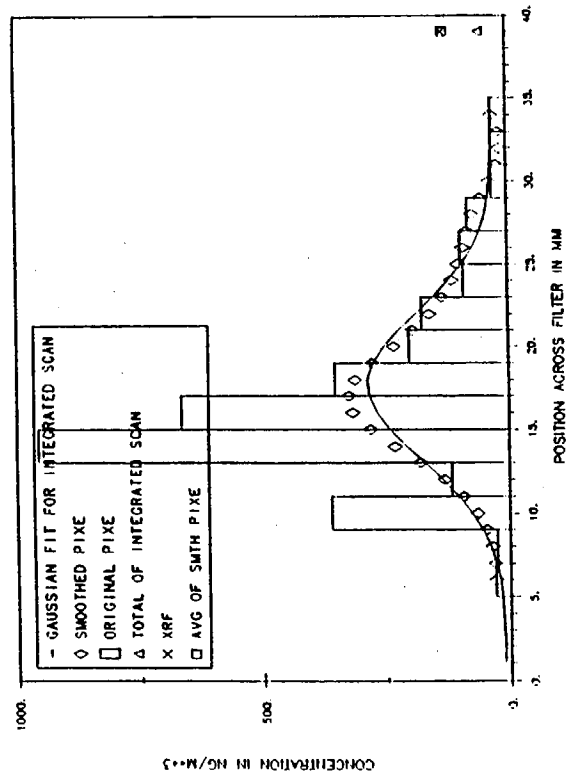
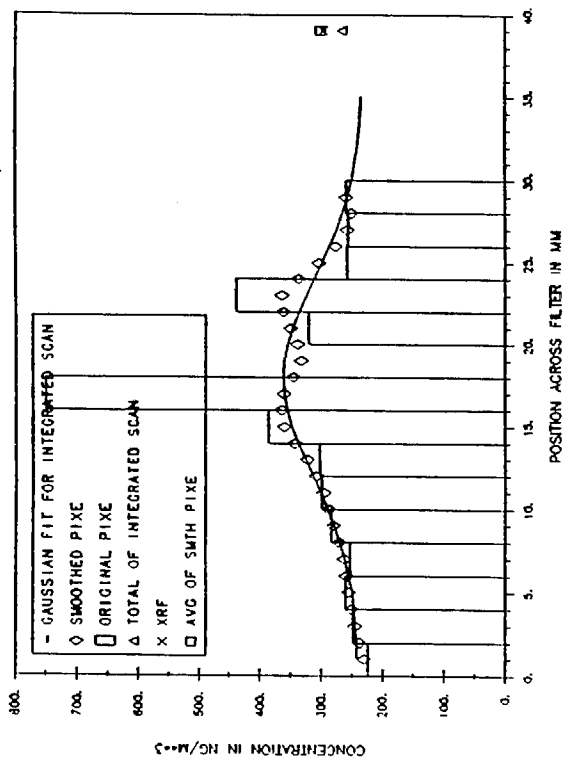
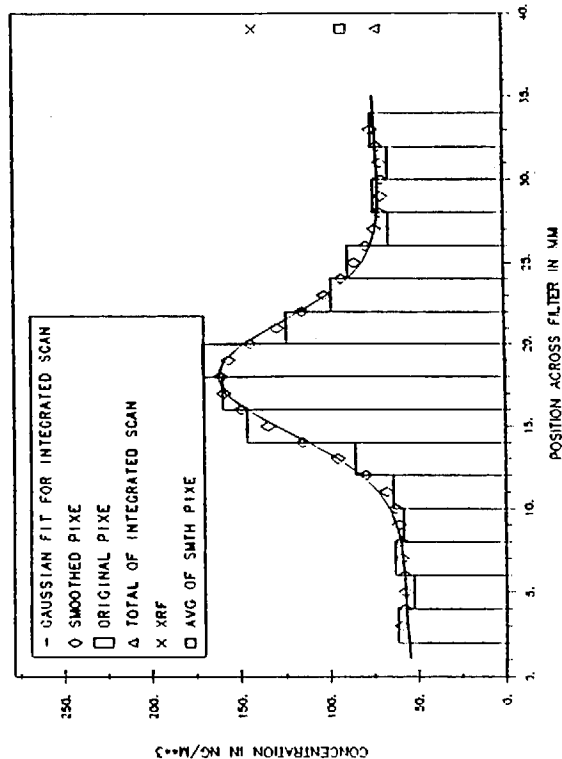


Figure 45

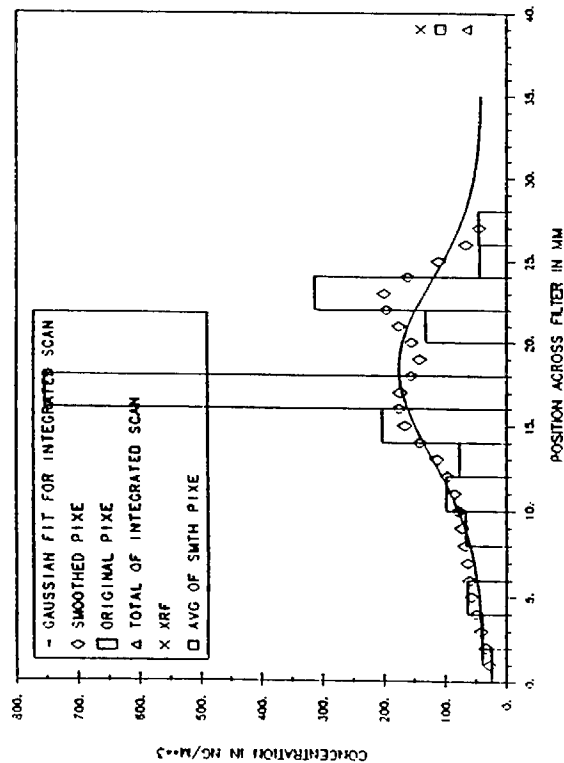
SCAQ5 PIXE SCANS FOR PM2.5 ZN; CHISO = 0.53  
DOLA 8-713 JULIAN345 12-11-87 PERIOD3



SCAQ5 PIXE SCANS FOR PM2.5 ZN; CHISO = 0.13  
ANAH 8-647 JULIAN345 12-11-87 PERIOD3



SCAQ5 PIXE SCANS FOR PM2.5 CU; CHISO = 3.84  
DOLA 3-713 JULIAN345 12-11-87 PERIOD3



SCAQ5 PIXE SCANS FOR PM2.5 CU; CHISO = 0.72  
ANAH 8-647 JULIAN345 12-11-87 PERIOD3

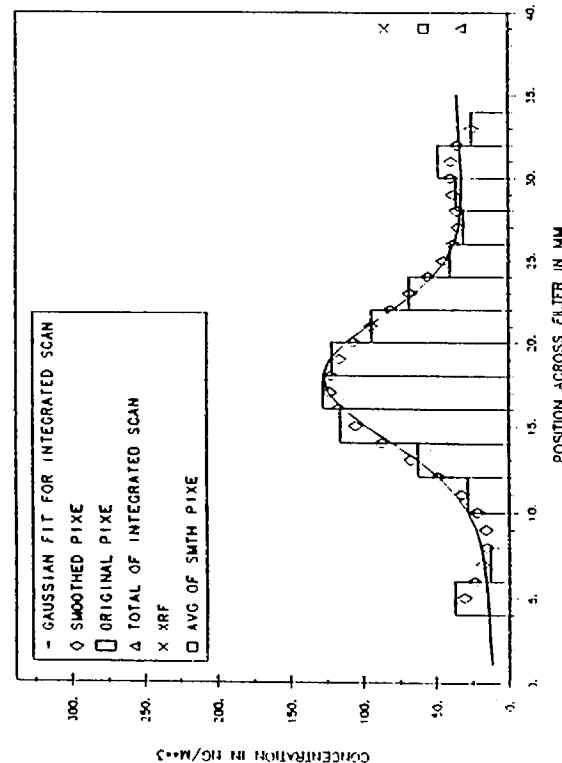
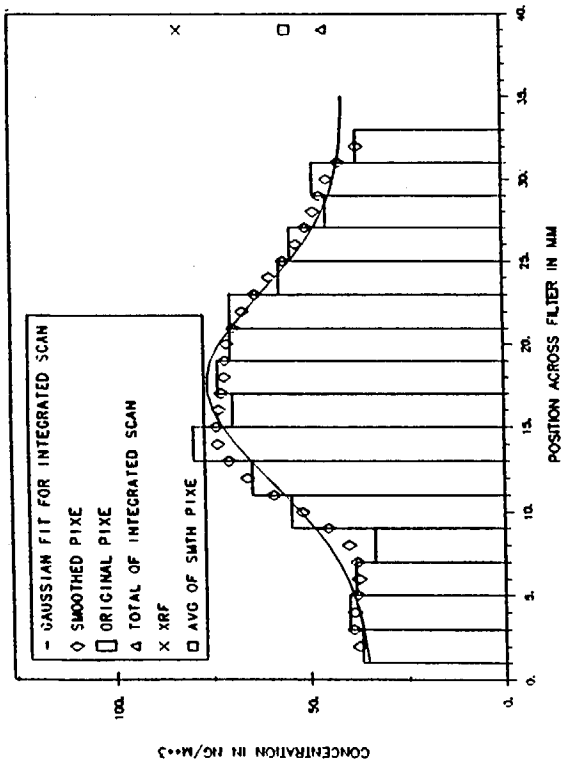
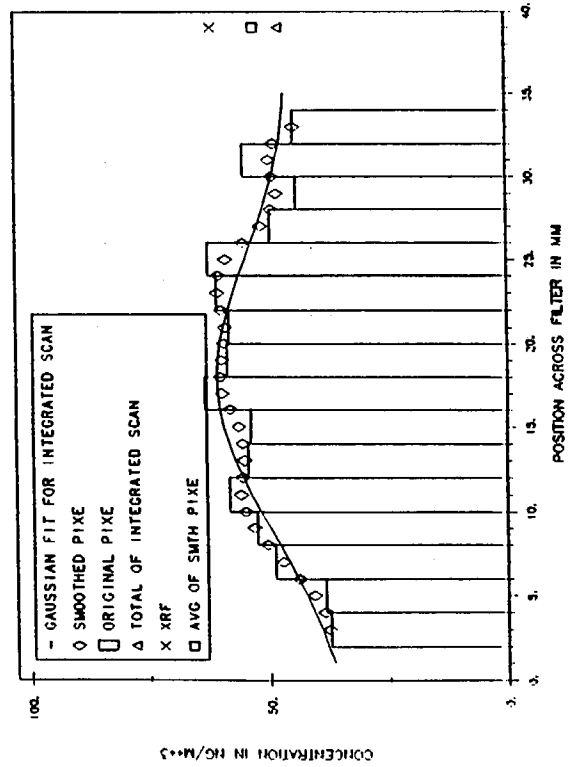


Figure 46

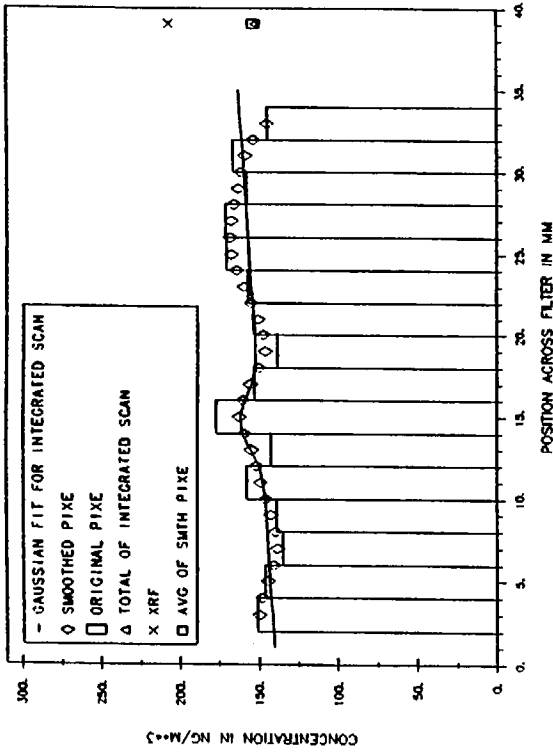
SCAOS PIXE SCANS FOR PM2.5 BR; CHISO = 0.26  
 DOLA 8-593 JULIAN316 11-12-87 PERIOD5



SCAOS PIXE SCANS FOR PM2.5 BR; CHISO = 0.13  
 LOBE 8-759 JULIAN316 11-12-87 PERIOD5



SCAOS PIXE SCANS FOR PM2.5 BR; CHISO = 0.27  
 DOLA 8-593 JULIAN316 11-12-87 PERIOD5



SCAOS PIXE SCANS FOR PM2.5 BR; CHISO = 0.27  
 LOBE 8-755 JULIAN316 11-12-87 PERIOD1

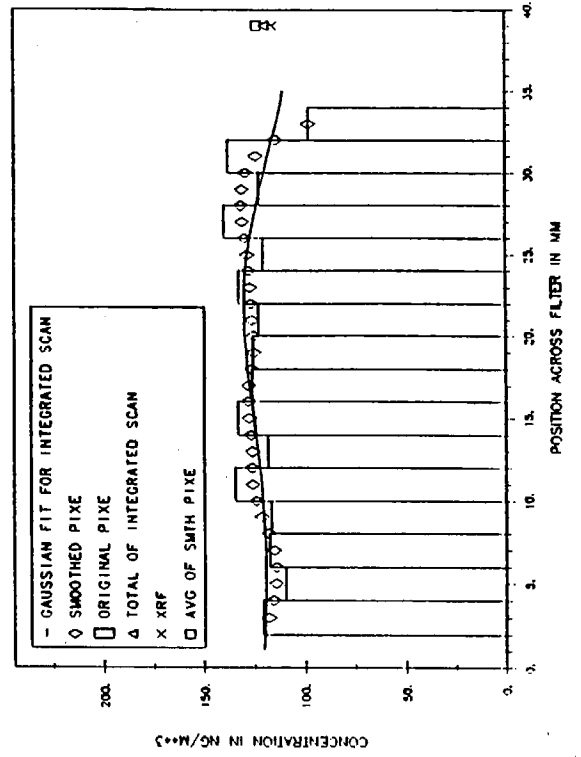
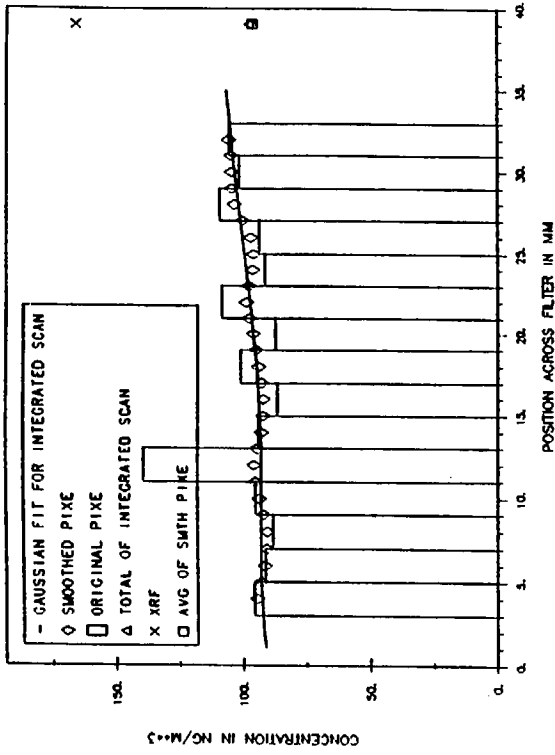


Figure 47

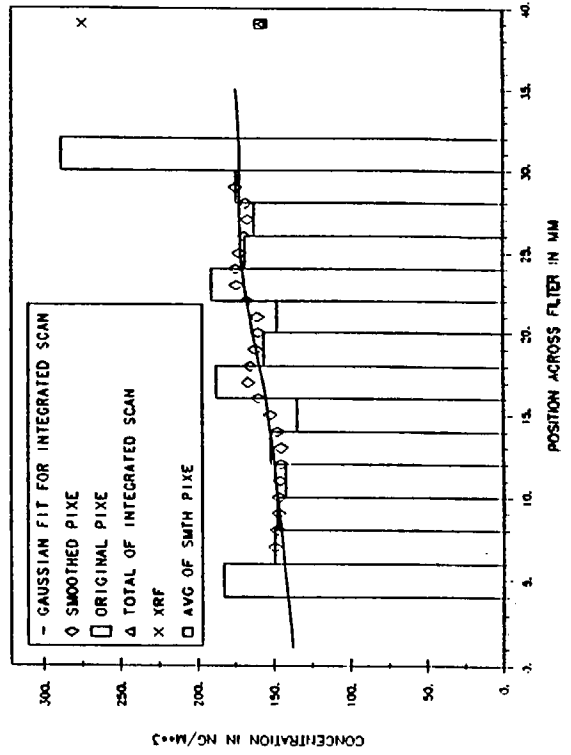
reiterated, however, the bromine central peaking resembles that of chlorine, far broader than seen for elements like copper or soils. It is conceivable that there have been post-sampling changes of the halogen profiles. In any case, the Br/Pb ratio is close to the 0.3 ratio in Pb Br Cl, favoring an automotive source at this site despite the central peaking. It is also a little surprising to see a high XRF/PIXE ratio at Los Angeles, compared to good agreement at Long Beach, for both bromine, with a central peak and lead, with no central peak. We can find no reason why such similar filters should have such variable XRF/PIXE ratios.

The study of bromine and lead is continued in Figure 48. The flat behavior at Los Angeles, 11/12/87, period 1 can be contrasted to the sloping behavior at Anaheim, for 12/10/87, period 3. Figure 49 shows a flat behavior for lead at Burbank, 11/12/87, period 3; and Long Beach, period 1; but some central peaking at Los Angeles, 11/12/87, period 3.

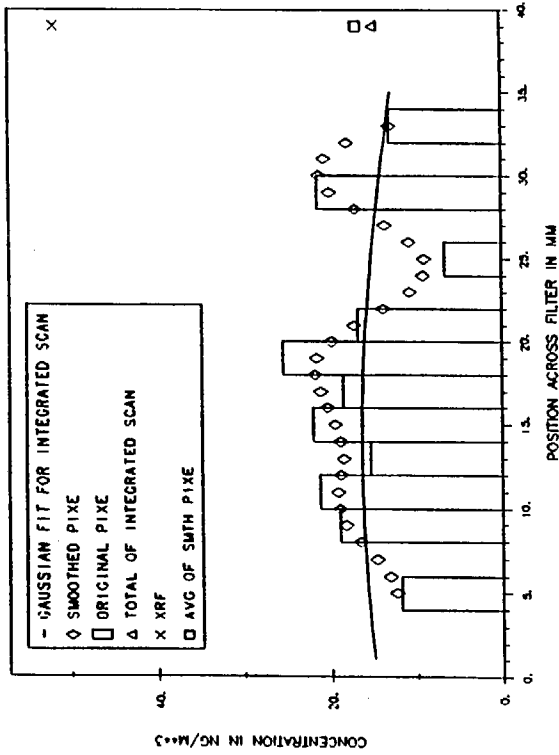
SCAOS PIXE SCANS FOR PM2.5 PB; CHISO = 0.03  
DOLA 8-689 JULIAN316 11-12-87 PERIOD1



SCAOS PIXE SCANS FOR PM2.5 PB; CHISO = 0.07  
ANAH 8-641 JULIAN344 12-10-87 PERIOD3



SCAOS PIXE SCANS FOR PM2.5 BR; CHISO = 1.68  
DOLA 8-689 JULIAN316 11-12-87 PERIOD1



SCAOS PIXE SCANS FOR PM2.5 BR; CHISO = 0.23  
ANAH 8-641 JULIAN344 12-10-87 PERIOD3

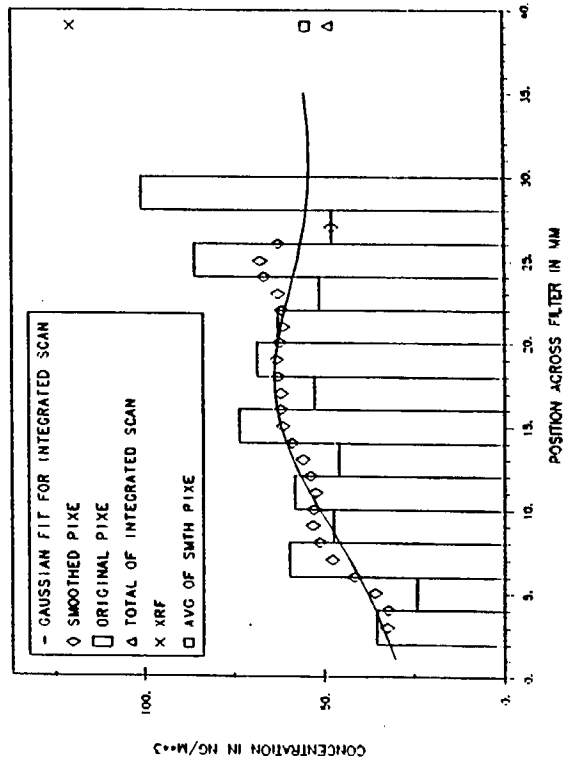
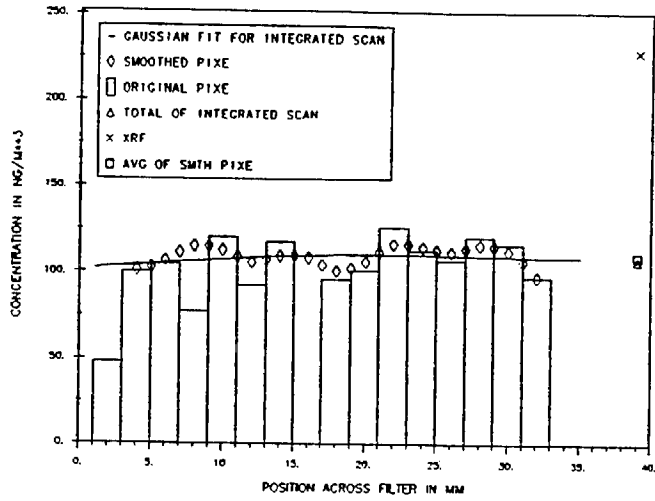
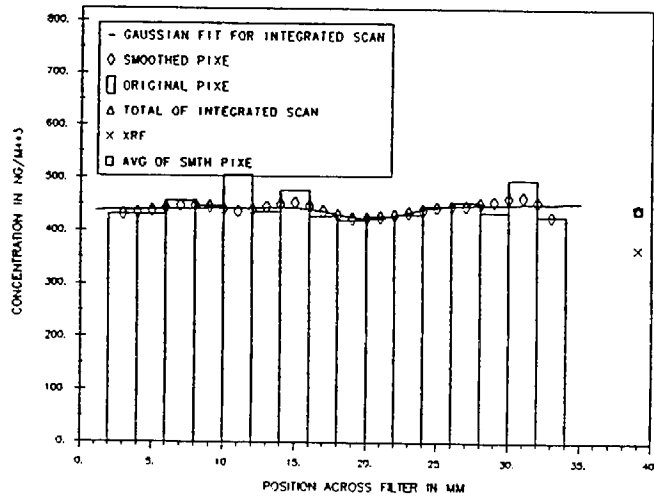


Figure 48

SCAQ5 PIXE SCANS FOR PM2.5 PB: CHISO = 0.10  
 BURB 8-657 JULIAN316 11-12-87 PERIOD3



SCAQ5 PIXE SCANS FOR PM2.5 PB: CHISO = 0.08  
 LOBE 8-755 JULIAN316 11-12-87 PERIOD1



SCAQ5 PIXE SCANS FOR PM2.5 PB: CHISO = 0.20  
 DOLA 8-691 JULIAN316 11-12-87 PERIOD3

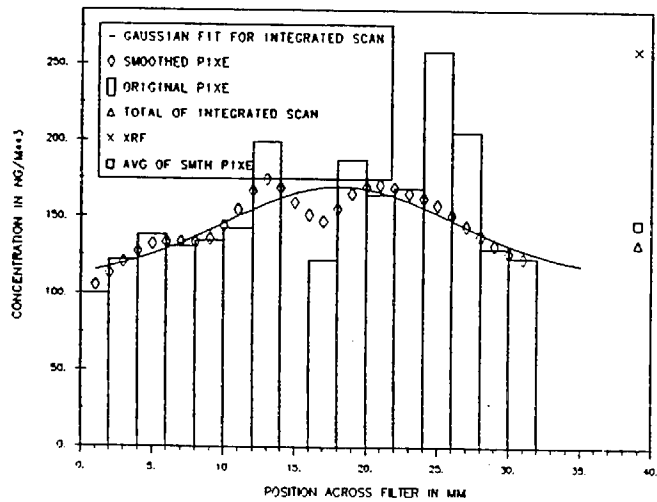


Figure 49

## PM 2.5 CORRELATION PLOTS, XRF VS PIXE - FALL AND SUMMER PLUS FALL

### Soil-like Elements - Si, K, Ca, Ti, Fe

XRF vs PIXE correlation plots for fine elements that are typically dominant in soil-derived aerosols are shown in Figure 50 for the fall sampling periods, November/December 1987. Correlations are fair to good;  $r^2 = 0.75$  (Si), 0.56 (K), 0.92 (Ca), and 0.66 (Fe), with generally small intercepts from zero. The exception is the intercept for Si, ~7% of full scale, but only a small loss of statistical significance occurs if the plot is forced through the origin. This was done for Si as marked "(CON)" for constrained in Figure 50. The slopes are ~1.2 (Si) (constrained fit or 1.11 unconstrained), 1.44 (K), 1.42 (Ca), and ~1.8 (Fe) (constrained fit or 1.94 unconstrained). In fact, these are similar in magnitude and trend for the PM 2.5 ratios, seen before in summer. Thus, in Figure 51 we combine PM 2.5 summer and fall scans for typically soil-dominated elements, while keeping in mind the relatively large fine particulate component of some species if comparing the results with PM 10 data.

Combining summer and fall data, the correlations are fair to good (Figure 51) from  $r^2 = 0.41$  (Si), 0.54 (K), 0.92 (Ca), and 0.74 (Fe), again with modest zero offset in most cases. The slopes are 1.17 (Si), 1.48 (Ca), 1.91 (Fe), and 1.74 (K) (1.60 for K if forced through zero). If we combine K, Ca, and Fe - summer and fall for PM 2.5, we obtain  $r^2 = 0.88$ , offset of about -3% of full scale, and a slope of 1.56 (Figure 52). In the same figure we show Ti, constrained through the origin, has a slope of about 1.8 ( $\pm 0.2$ ) but with little correlation indicating a high uncertainty. Thus, we propose an XRF/PIXE scaling factor of  $1.56 \pm 0.20$  for K, Ca, Ti, and Fe; and  $1.14 \pm 0.10$  for Si (and Al).

### Sulfur

XRF vs PIXE correlation plots for sulfur are shown in Figure 53 for fall only and summer and fall, for PM 2.5 particles, and summer and fall, PM 10 plus PM 2.5. The correlations are excellent,  $r^2 = 0.99$  for all cases, with zero offsets between 0.5% and 1.5% of full scale. The slopes are, as might be expected, highly consistent from 1.23 (fall only PM 2.5) to 1.30 (summer plus fall PM 2.5) to 1.26 (PM 10 plus PM 2.5, all periods). It is this latter value,  $1.26 \pm 0.05$ , that we propose for all sulfur particles.

### Trace Elements

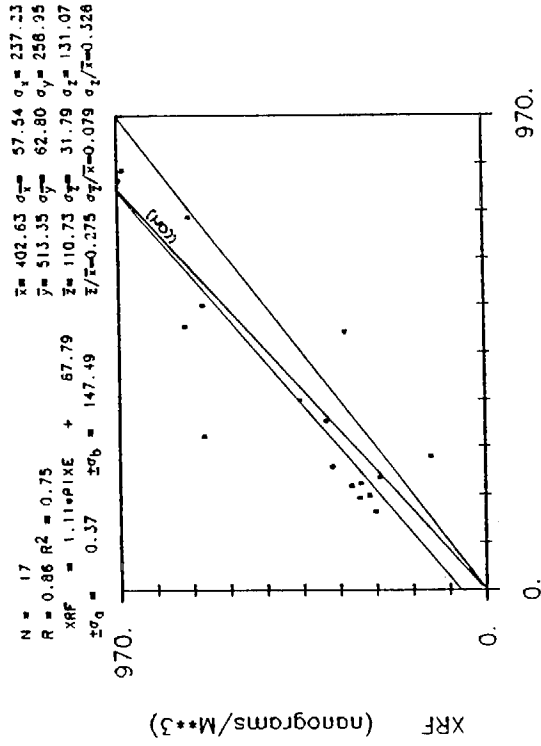
#### Chlorine, Titanium, Vanadium

Inadequate data exist for a statistically sound correlation plot for chlorine, so the ratio of  $2.5 \pm 1.0$  represents the proposed value for this element. Figure 54 shows a plot for titanium. The  $r^2$  is not good, ~0.4, and the slope is about  $1.9 \pm 0.3$  (least square fit forced through origin). This is not very different from soils (or in fact, chlorine). Inadequate data exist for a statistically sound correlation plot for vanadium, but the few values obtained give a ratio close to unity,  $1.0 \pm 0.2$ .

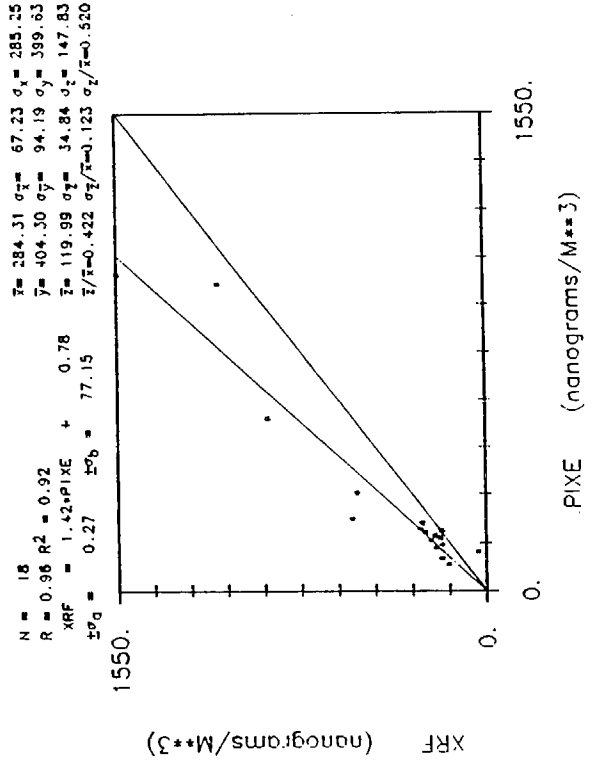
#### Manganese

Manganese was seen only in fall and a constrained fit through zero gives a slope of  $1.60 \pm 0.20$  (Figure 55).

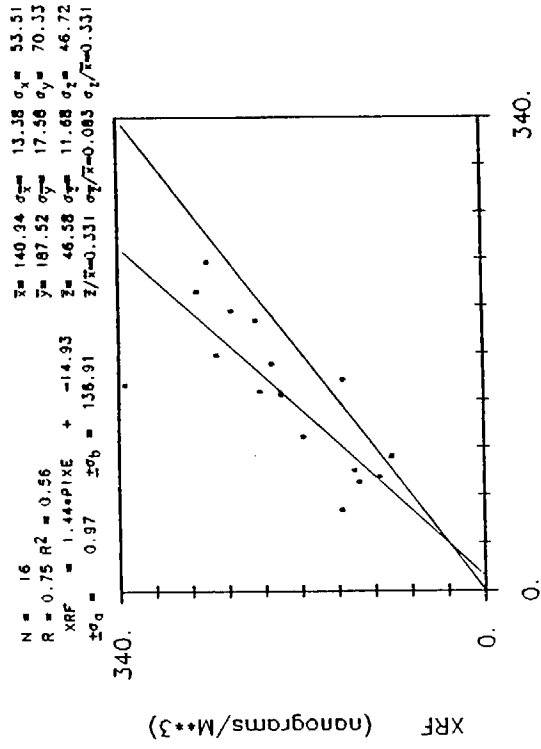
SCAQ5 PM2.5: SI FOR FALL



SCAQ5 PM2.5: CA FOR FALL



SCAQ5 PM2.5: K FOR FALL



SCAQ5 PM2.5: FE FOR FALL

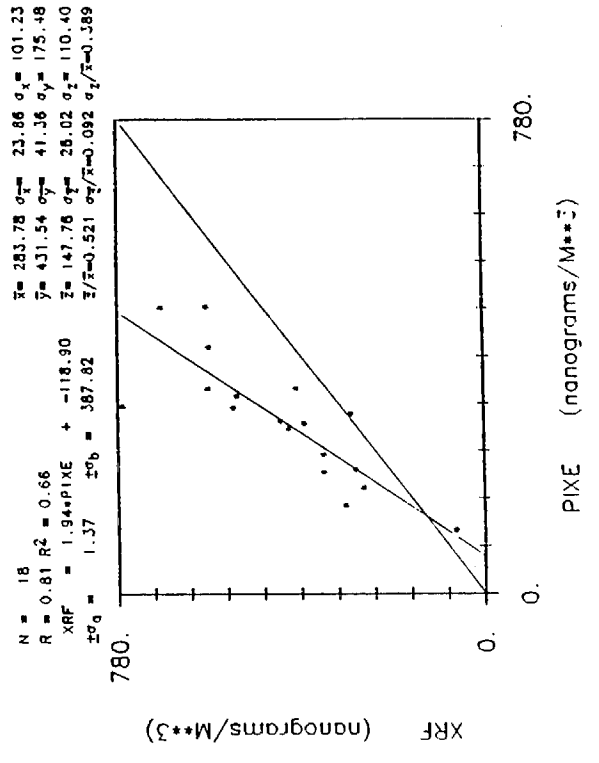
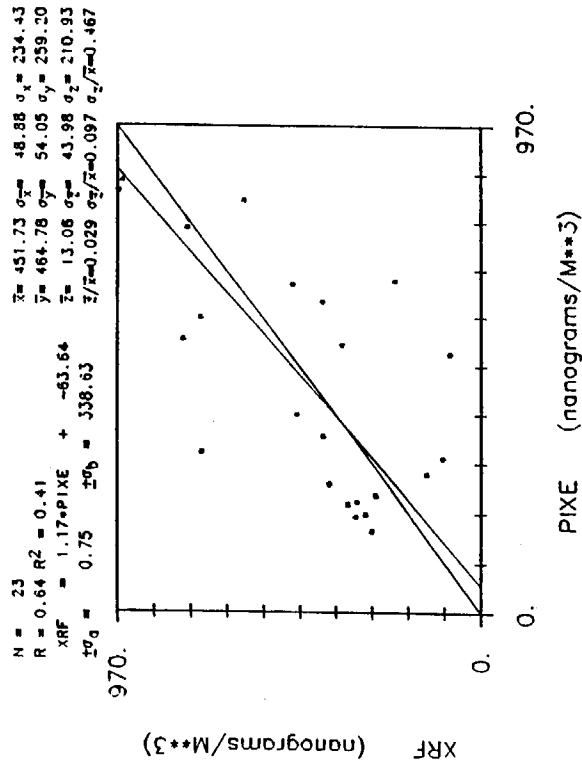
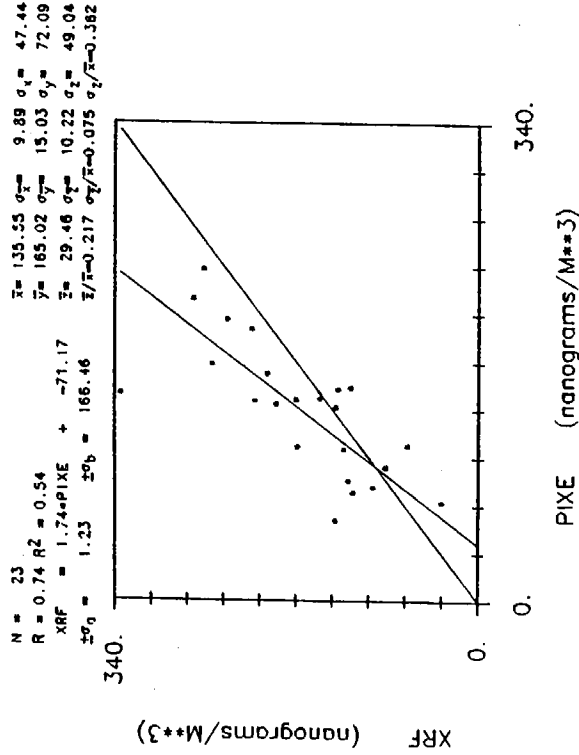


Figure 50

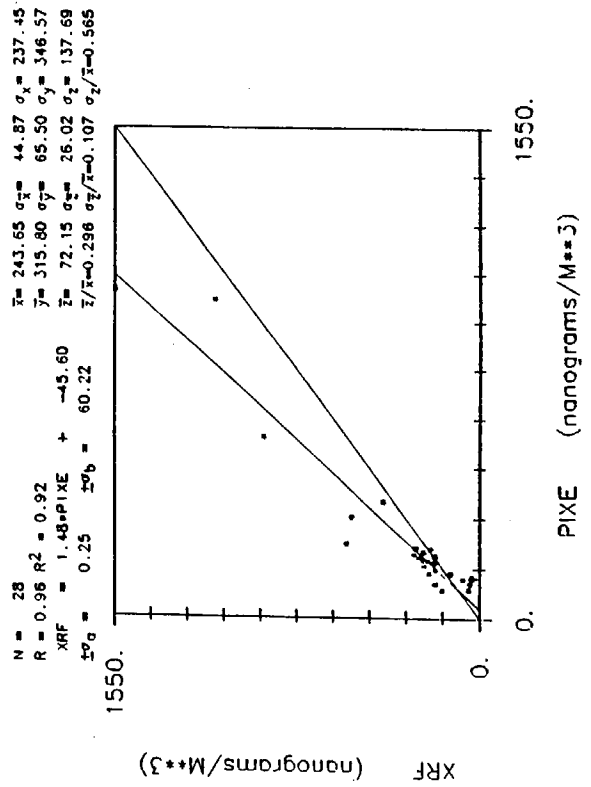
SCAQ5 PM2.5: SI FOR SUMMER AND FALL



SCAQ5 PM2.5: K FOR SUMMER AND FALL



SCAQ5 PM2.5: CA FOR SUMMER AND FALL



SCAQ5 PM2.5: FE FOR SUMMER AND FALL

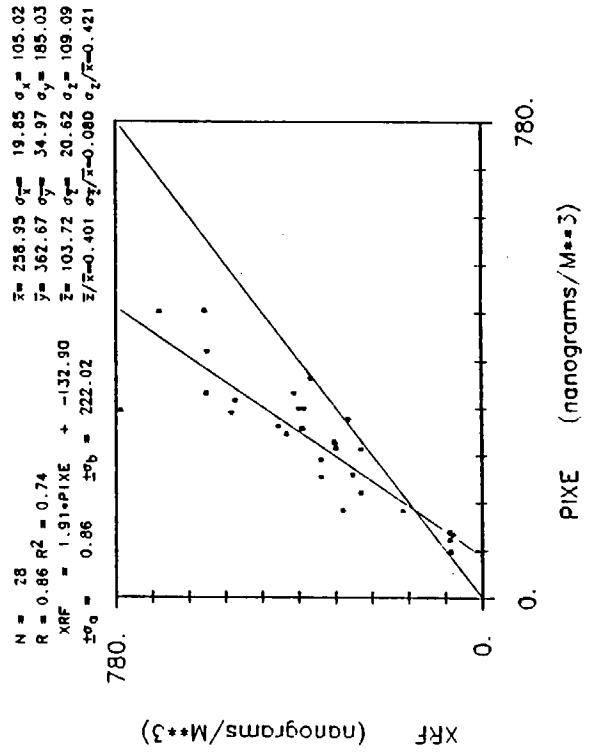
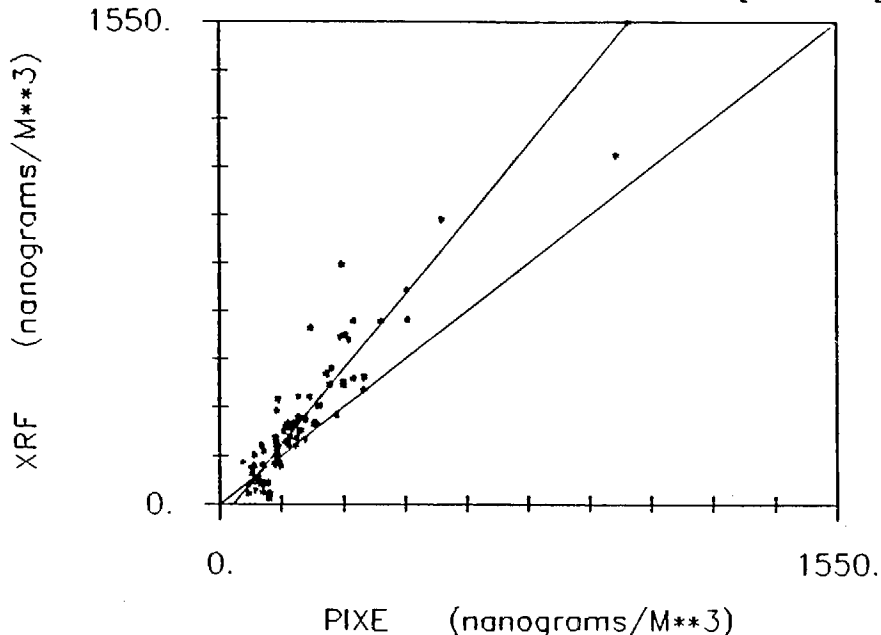


Figure 51

# SCAQ5 PM2.5: SOILS FOR SUMMER&FALL

$N = 79$   $\bar{x} = 217.60$   $\sigma_{\bar{x}} = 18.42$   $\sigma_x = 163.74$   
 $R = 0.94$   $R^2 = 0.88$   $\bar{y} = 288.51$   $\sigma_{\bar{y}} = 27.93$   $\sigma_y = 248.26$   
 $XRF = 1.56 \cdot PIXE + -50.19$   $\bar{z} = 70.91$   $\sigma_{\bar{z}} = 12.45$   $\sigma_z = 110.70$   
 $\pm\sigma_a = 0.20$   $\pm\sigma_b = 42.72$   $\bar{z}/\bar{x} = 0.326$   $\sigma_{\bar{z}/\bar{x}} = 0.057$   $\sigma_z/\bar{x} = 0.509$



# SCAQ5 PM2.5: TI FOR SUMMER AND FALL

$N = 7$   $\bar{x} = 36.42$   $\sigma_{\bar{x}} = 3.28$   $\sigma_x = 8.68$   
 $R = -.28$   $R^2 = 0.08$   $\bar{y} = 64.58$   $\sigma_{\bar{y}} = 5.90$   $\sigma_y = 15.61$   
 $XRF = -4.65 \cdot PIXE + 233.98$   $\bar{z} = 28.16$   $\sigma_{\bar{z}} = 7.51$   $\sigma_z = 19.87$   
 $\pm\sigma_a = 105.29$   $\pm\sigma_b = 3834.82$   $\bar{z}/\bar{x} = 0.773$   $\sigma_{\bar{z}/\bar{x}} = 0.206$   $\sigma_z/\bar{x} = 0.546$

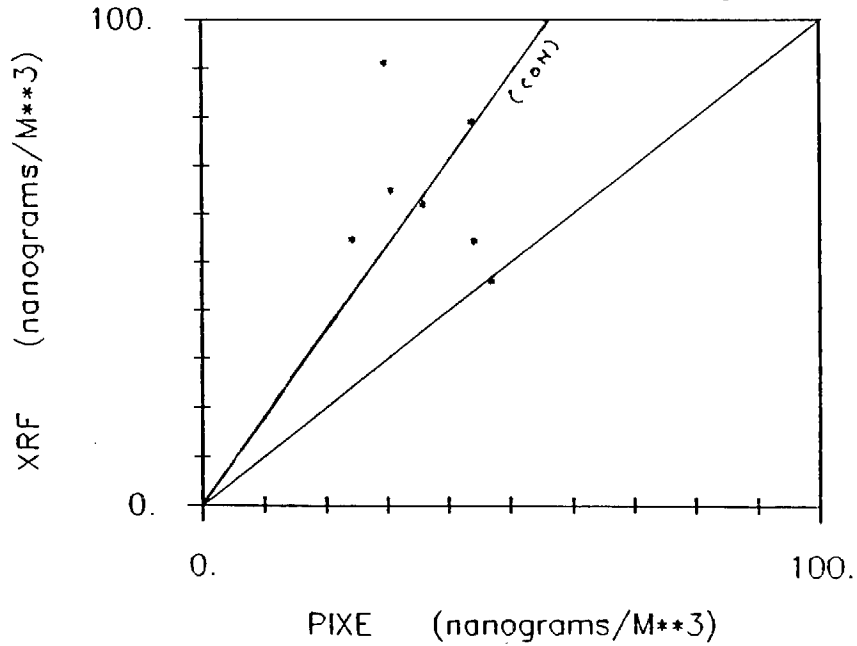
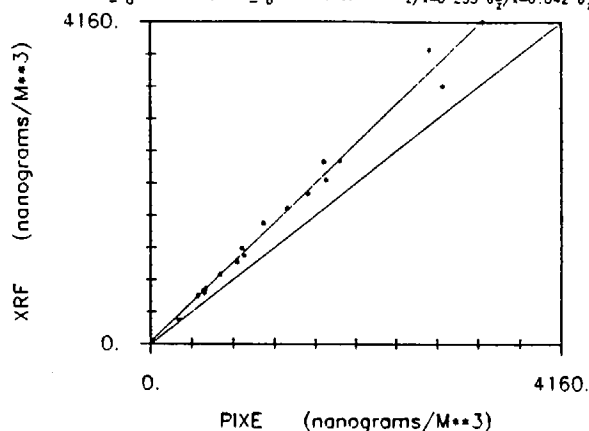


Figure 52

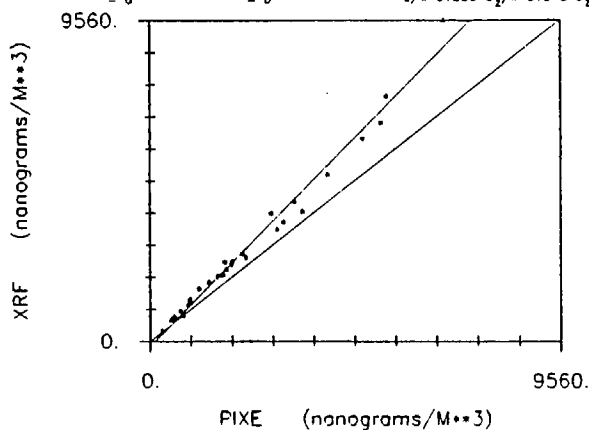
## SCAQ5 PM2.5: S FOR FALL

$N = 18$   $\bar{x} = 1362.95$   $\sigma_x = 217.58$   $\sigma_y = 923.13$   
 $R = 0.99$   $R^2 = 0.99$   $\bar{y} = 1708.18$   $\sigma_{\bar{y}} = 267.60$   $\sigma_y = 1135.32$   
 $XRF = 1.23 \cdot PIXE + 29.76$   $\bar{x} = 345.23$   $\sigma_x = 56.93$   $\sigma_z = 241.53$   
 $\pm\sigma_o = 0.08$   $\pm\sigma_b = 110.09$   $\bar{x}/\bar{y} = 0.255$   $\sigma_x/\sigma_y = 0.042$   $\sigma_z/\bar{y} = 0.177$



## SCAQ5 PM2.5: S FOR SUMMER AND FALL

$N = 30$   $\bar{x} = 2227.72$   $\sigma_x = 315.07$   $\sigma_y = 1725.73$   
 $R = 0.99$   $R^2 = 0.99$   $\bar{y} = 2753.01$   $\sigma_{\bar{y}} = 408.00$   $\sigma_y = 2234.72$   
 $XRF = 1.30 \cdot PIXE - 136.96$   $\bar{x} = 525.29$   $\sigma_x = 102.26$   $\sigma_z = 560.10$   
 $\pm\sigma_o = 0.07$   $\pm\sigma_b = 158.84$   $\bar{x}/\bar{y} = 0.236$   $\sigma_x/\sigma_y = 0.046$   $\sigma_z/\bar{y} = 0.251$



## SCAQ5 PM10 AND PM2.5: SULFUR

$N = 53$   $\bar{x} = 2420.92$   $\sigma_x = 256.46$   $\sigma_y = 1867.04$   
 $R = 1.00$   $R^2 = 0.99$   $\bar{y} = 2989.03$   $\sigma_{\bar{y}} = 322.29$   $\sigma_y = 2346.33$   
 $XRF = 1.26 \cdot PIXE - 56.61$   $\bar{x} = 568.11$   $\sigma_x = 71.53$   $\sigma_z = 520.74$   
 $\pm\sigma_o = 0.04$   $\pm\sigma_b = 98.28$   $\bar{x}/\bar{y} = 0.235$   $\sigma_x/\sigma_y = 0.030$   $\sigma_z/\bar{y} = 0.215$

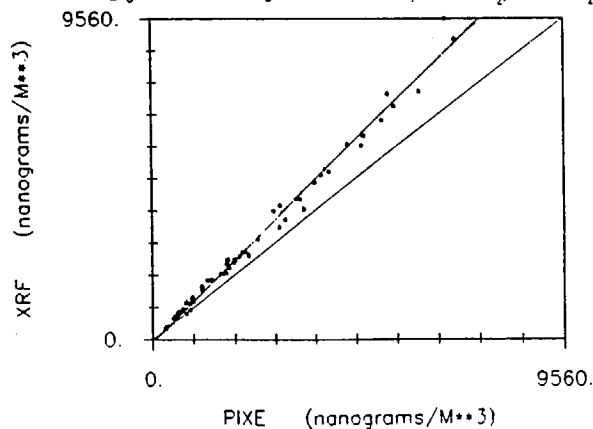


Figure 53

## SCAQs PM2.5: T1 FOR FALL

$N = 5$                        $\bar{x} = 35.07$     $\sigma_{\bar{x}} = 4.40$     $\sigma_x = 9.85$   
 $R = -.51$     $R^2 = 0.26$                        $\bar{y} = 62.21$     $\sigma_{\bar{y}} = 7.81$     $\sigma_y = 17.46$   
 $XRF = -2.73 * PIXE + 157.90$                        $\bar{z} = 27.15$     $\sigma_{\bar{z}} = 10.75$     $\sigma_z = 24.04$   
 $\pm \sigma_a = 16.96$     $\pm \sigma_b = 594.86$                        $\bar{z}/\bar{x} = 0.774$     $\sigma_{\bar{z}/\bar{x}} = 0.307$     $\sigma_{z/\bar{x}} = 0.685$

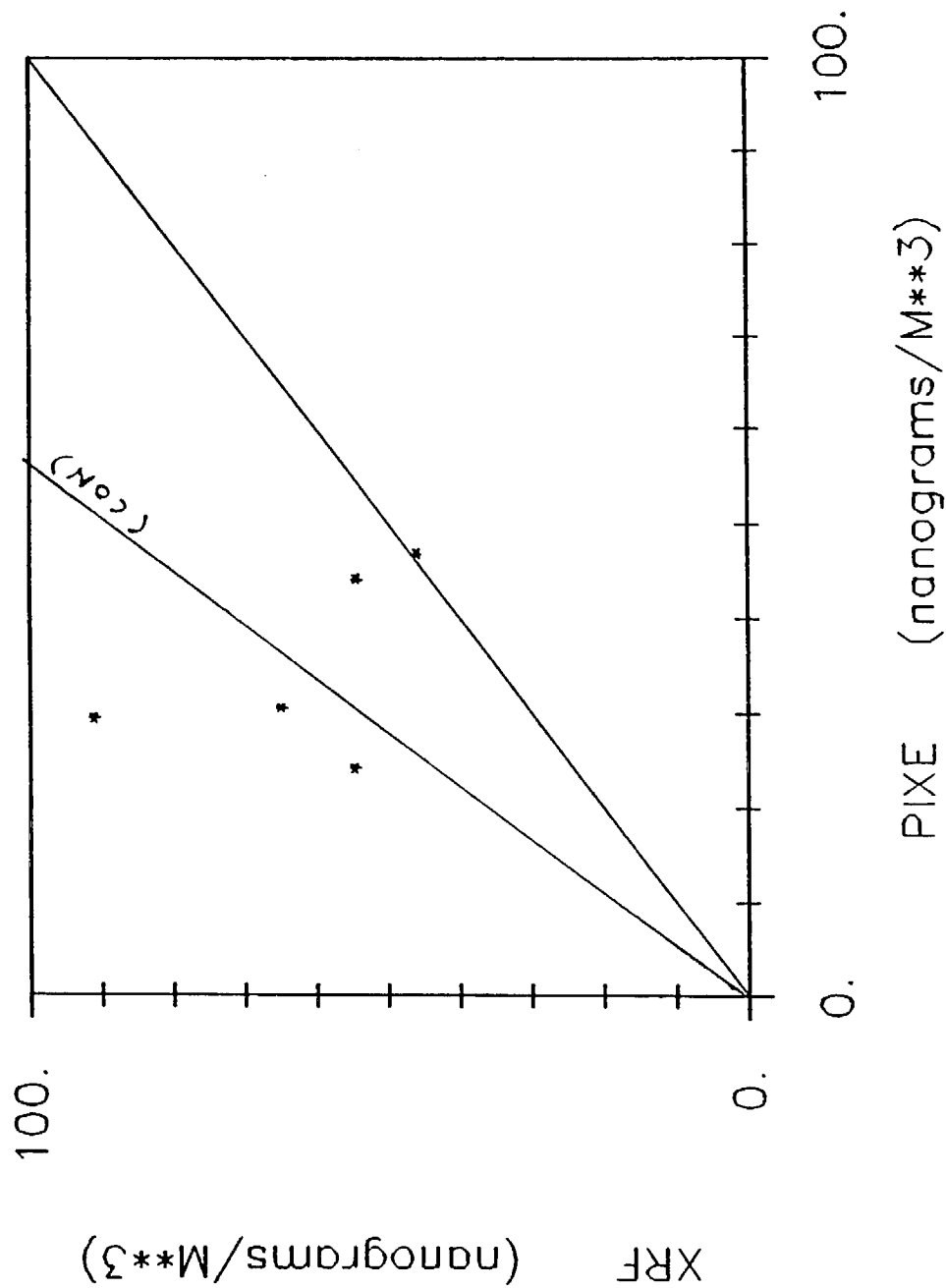


Figure 54

# SCAQ5 PM2.5: MN FOR SUMMER AND FALL

$N = 3$   
 $R = 0.90$   $R^2 = 0.82$   
 $XRF = 0.73 * PIXE + 34.04$   
 $\pm \sigma_a = 0.65$   $\pm \sigma_b = 30.79$   
 $\bar{x} = 38.85$   $\sigma_{\bar{x}} = 6.58$   $\sigma_x = 11.39$   
 $\bar{y} = 62.31$   $\sigma_{\bar{y}} = 4.93$   $\sigma_y = 8.54$   
 $\bar{z} = 23.46$   $\sigma_{\bar{z}} = 2.98$   $\sigma_z = 5.16$   
 $\bar{z}/\bar{x} = 0.604$   $\sigma_{\bar{z}/\bar{x}} = 0.077$   $\sigma_z/\sigma_x = 0.133$

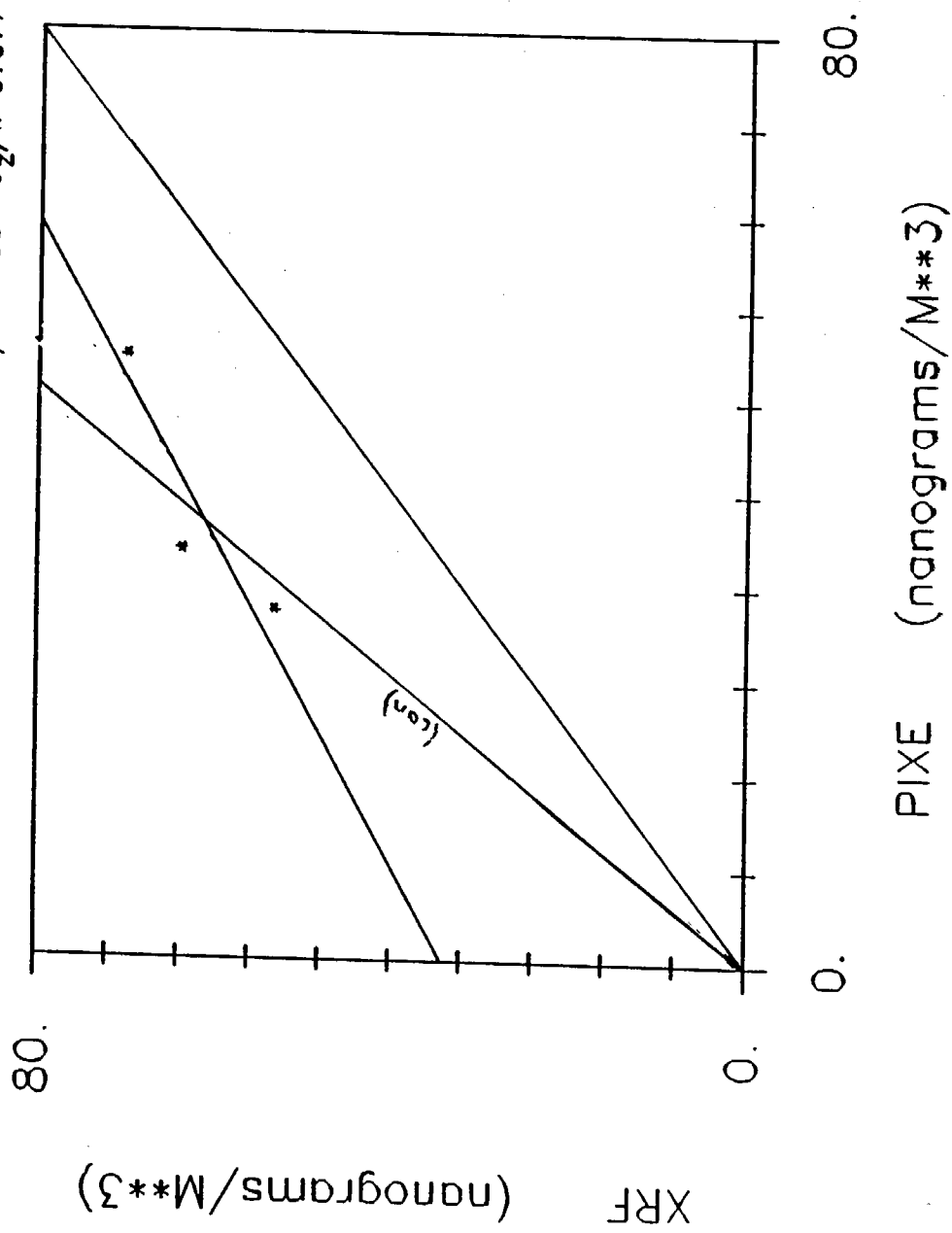


Figure 55

### Copper and Zinc

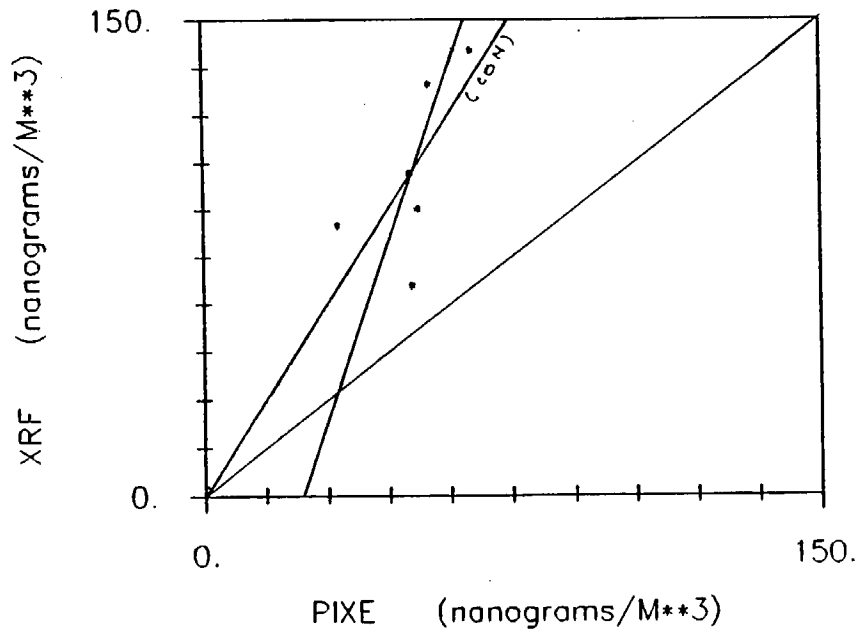
Figure 56 shows copper and zinc PM 2.5, fall; while Figure 57 shows copper and zinc PM 2.5, summer and fall. The constrained fit for copper gives a slope of  $2.1 \pm 0.3$  for fall, which is consistent with summer and fall PM 2.5 (1.7) if one excludes one very high ratio. Recall, however, the difficulty in extracting the "brass-like" particles from the scans. For zinc, this problem is less severe. It is still surprising, however, that the XRF/PIXE ratio is so different, about 1.2 for fall only constrained through the origin; 1.27 summer plus fall PM 2.5 unconstrained and with small zero offset +2.5% of full scale. The  $r^2$  of 0.79 for the combined zinc scans is also acceptable. Finally, we attempted to combine PM 10 and PM 2.5 data for zinc, since zinc was also seen commonly in PM 10 samples. Figure 58 gives the combined result  $r^2 = 0.87$ , slope of 1.13, and an intercept under 5%. The fit constrained through zero gives a slope of about 1.15.

### Bromine and Lead

XRF vs PIXE correlation plots for bromine and lead, PM 2.5 for fall are shown in Figure 59. Little or nothing was gained by combining summer and fall in this case. For bromine and lead, poor correlations and huge zero offsets merely reflect the inconsistent results shown in the lateral scan plots earlier. For fits constrained through zero, an XRF/PIXE ratio of about  $1.4 \pm 0.3$  is obtained for bromine,  $1.1 \pm 0.3$  for lead. However, if one deletes a single filter's data, very different ratios are obtained. XRF/PIXE is then about 1.9 for lead and bromine, both with a much better  $r^2$ .

## SCAQS PM2.5: CU FOR FALL

$N = 6$   $\bar{x} = 51.03$   $\sigma_{\bar{x}} = 4.32$   $\sigma_x = 10.58$   
 $R = 0.65$   $R^2 = 0.42$   $\bar{y} = 102.10$   $\sigma_{\bar{y}} = 11.48$   $\sigma_y = 28.11$   
 $XRF = 3.77 \cdot PIXE + -90.22$   $\bar{z} = 51.06$   $\sigma_{\bar{z}} = 9.26$   $\sigma_z = 22.69$   
 $\pm\sigma_a = 19.37$   $\pm\sigma_b = 988.51$   $\bar{z}/\bar{x} = 1.001$   $\sigma_{\bar{z}}/\bar{x} = 0.182$   $\sigma_z/\bar{x} = 0.445$



## SCAQS PM2.5: ZN FOR FALL

$N = 15$   $\bar{x} = 106.70$   $\sigma_{\bar{x}} = 18.29$   $\sigma_x = 70.83$   
 $R = 0.88$   $R^2 = 0.78$   $\bar{y} = 141.60$   $\sigma_{\bar{y}} = 19.00$   $\sigma_y = 73.59$   
 $XRF = 1.04 \cdot PIXE + 30.19$   $\bar{z} = 34.90$   $\sigma_{\bar{z}} = 9.07$   $\sigma_z = 35.11$   
 $\pm\sigma_a = 0.33$   $\pm\sigma_b = 34.76$   $\bar{z}/\bar{x} = 0.327$   $\sigma_{\bar{z}}/\bar{x} = 0.085$   $\sigma_z/\bar{x} = 0.329$

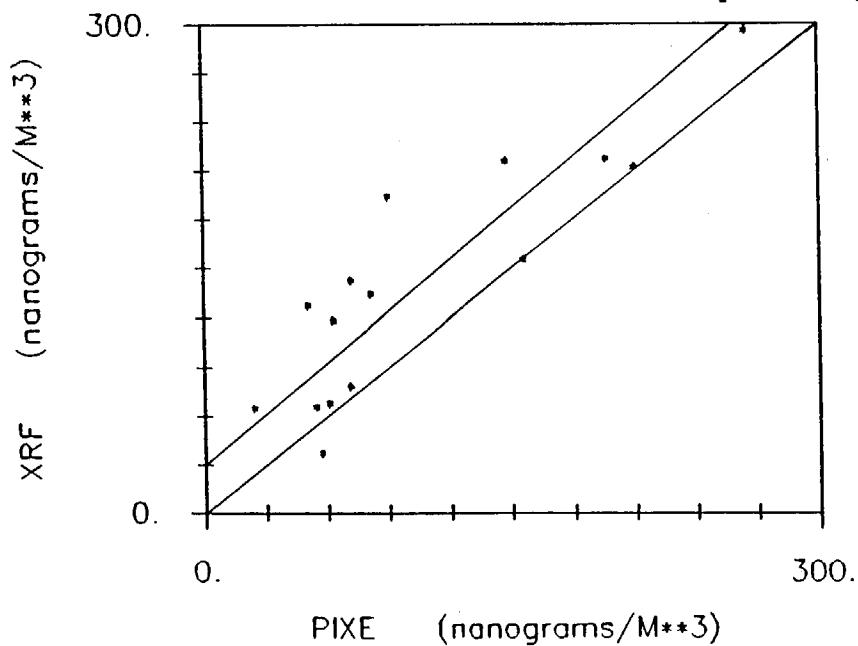
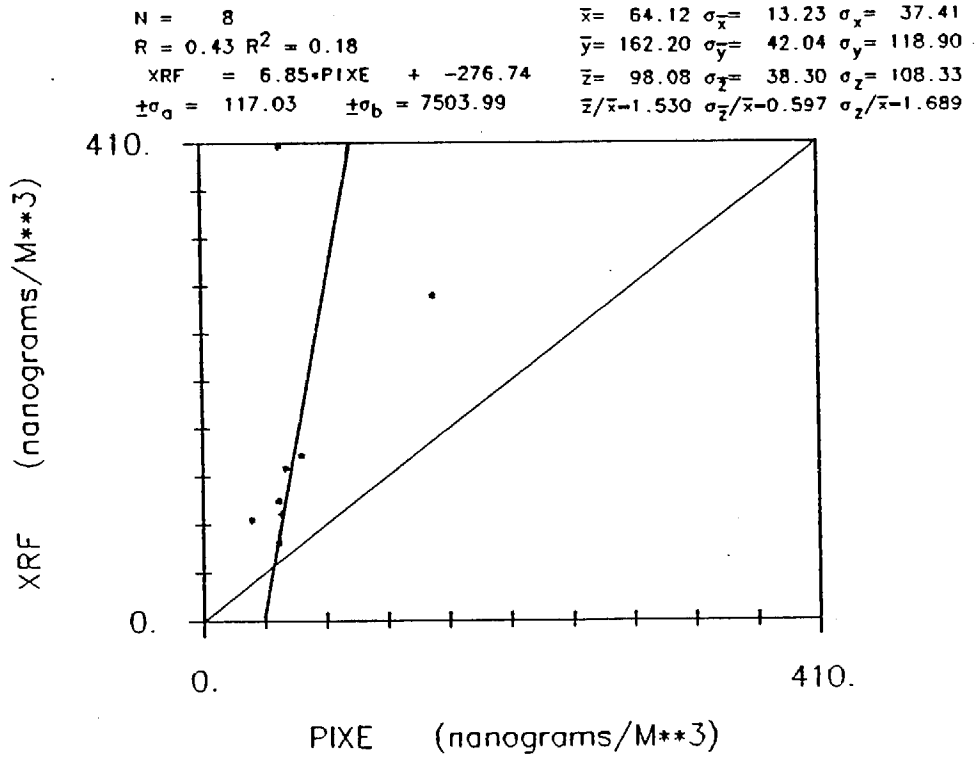


Figure 56

## SCAQ5 PM2.5: CU FOR SUMMER AND FALL



## SCAQ5 PM2.5: ZN FOR SUMMER AND FALL

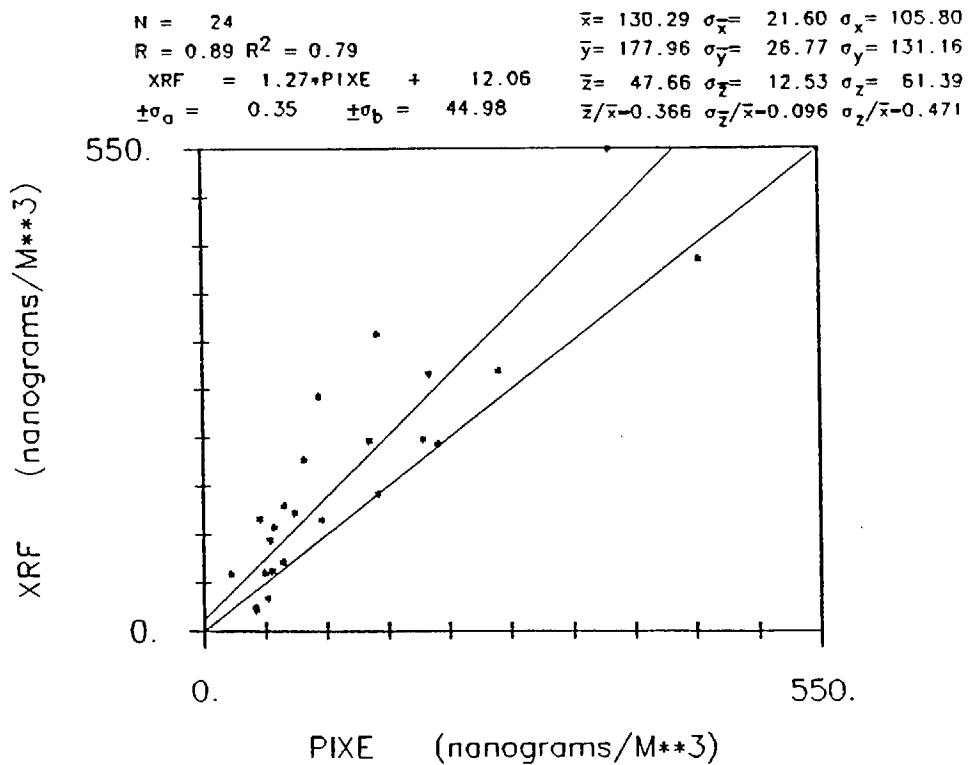


Figure 57

# SCAQ5 PM2.5 & PM10: ZINC

$N = 41$   
 $R = 0.93$   $R^2 = 0.87$   
 $XRF = 1.13 * PIXE + 31.56$   
 $\pm \sigma_a = 0.15$   $\pm \sigma_b = 24.31$   
 $\bar{x} = 160.44$   $\sigma_{\bar{x}} = 21.50$   $\sigma_x = 137.70$   
 $\bar{y} = 212.33$   $\sigma_{\bar{y}} = 24.04$   $\sigma_y = 153.93$   
 $\bar{z} = 51.90$   $\sigma_{\bar{z}} = 8.66$   $\sigma_z = 55.47$   
 $\bar{z}/\bar{x} = 0.323$   $\sigma_{\bar{z}/\bar{x}} = 0.054$   $\sigma_{z/\bar{x}} = 0.346$

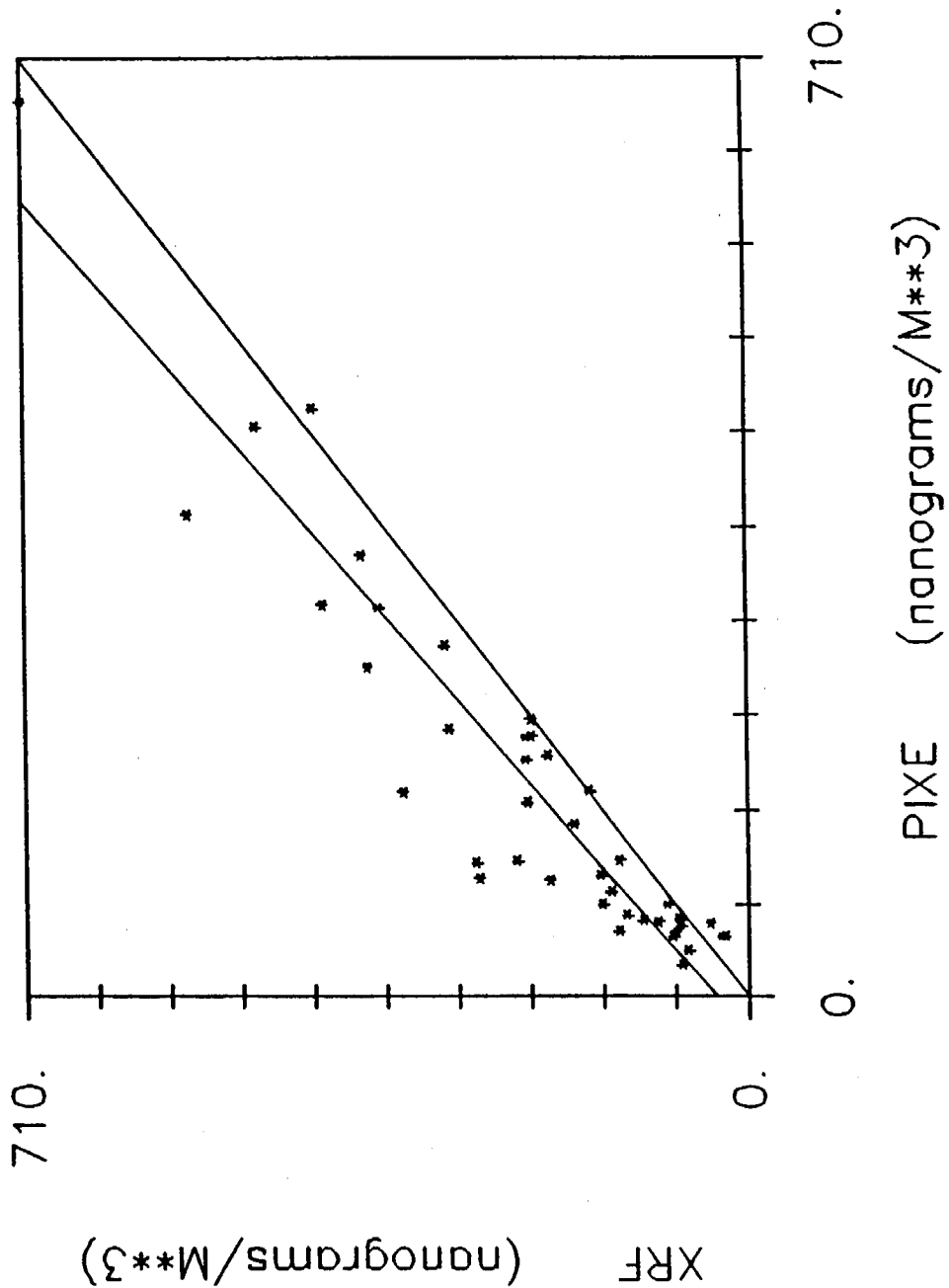
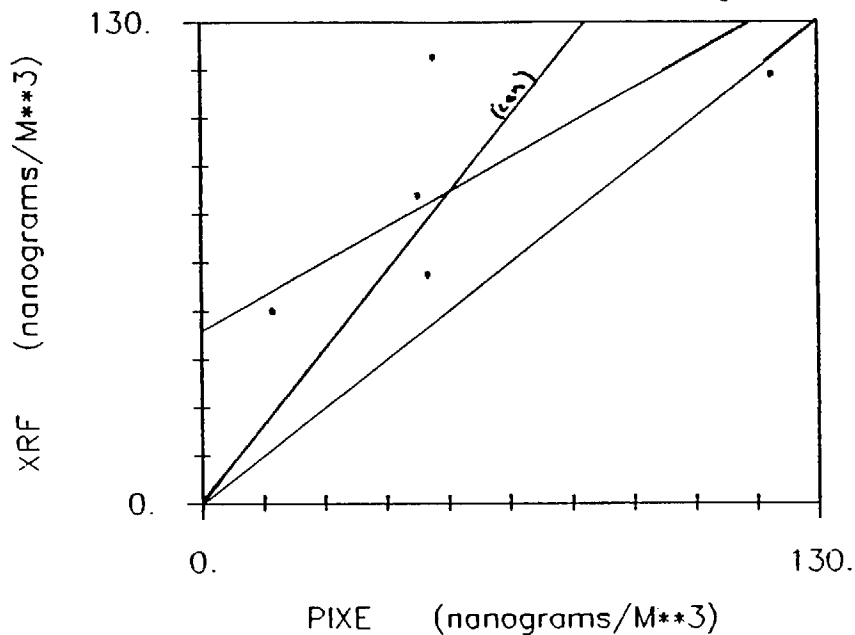


Figure 58

## SCAQS PM2.5: BR FOR FALL

$N = 5$   $\bar{x} = 55.42$   $\sigma_{\bar{x}} = 17.35$   $\sigma_x = 38.80$   
 $R = 0.69$   $R^2 = 0.47$   $\bar{y} = 86.51$   $\sigma_{\bar{y}} = 13.84$   $\sigma_y = 30.96$   
 $XRF = 0.72 \cdot PIXE + 46.52$   $\bar{z} = 31.10$   $\sigma_{\bar{z}} = 12.77$   $\sigma_z = 28.55$   
 $\pm\sigma_a = 0.89$   $\pm\sigma_b = 49.32$   $\bar{z}/\bar{x} = 0.561$   $\sigma_{\bar{z}}/\bar{x} = 0.230$   $\sigma_z/\bar{x} = 0.515$



## SCAQS PM2.5: PB FOR FALL

$N = 6$   $\bar{x} = 182.18$   $\sigma_{\bar{x}} = 53.35$   $\sigma_x = 130.68$   
 $R = 0.88$   $R^2 = 0.77$   $\bar{y} = 250.64$   $\sigma_{\bar{y}} = 28.15$   $\sigma_y = 68.96$   
 $XRF = 0.49 \cdot PIXE + 161.63$   $\bar{z} = 68.46$   $\sigma_{\bar{z}} = 31.67$   $\sigma_z = 77.58$   
 $\pm\sigma_a = 0.27$   $\pm\sigma_b = 48.99$   $\bar{z}/\bar{x} = 0.376$   $\sigma_{\bar{z}}/\bar{x} = 0.174$   $\sigma_z/\bar{x} = 0.426$

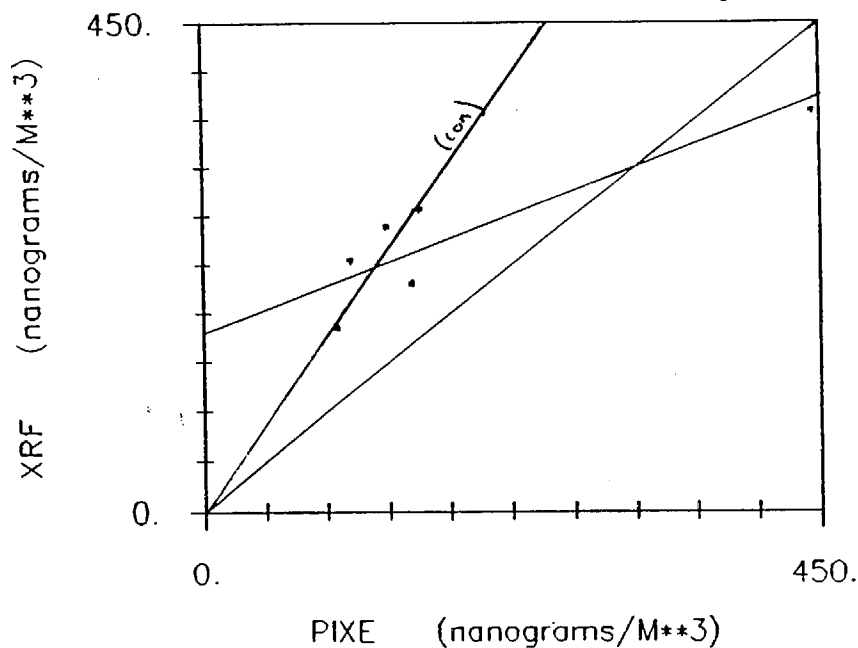


Figure 59

### STATISTICAL REDUCTION OF THE DATA

Tables 1, 2, 3, and 4 contain results on the degree of central peaking and the XRF/PIXE integrated scan conversion factor. The former values are taken from the PIXE elemental scan data, as the mean of the two highest PIXE values at the center divided by the mean of the three lowest values at the edges of the filter. It is merely a relative parameter by which to compare filter profiles. For PM 10 (Table 1), sulfur is fairly flat, center/edge ratio of 1.245 and soils very centrally peaked,  $5.30 \pm 0.80$ . Surprisingly, trace elements are also centrally peaked and more variable,  $2.39 \pm 0.38$  with the exception of Mn and Pb, fall, which are much flatter. Since these particles are typically combustion-derived and thus much finer than soils, we expected values similar to those of PM 2.5 aerosols. However, no systematic difference was seen site to site or season to season in PM 10 profiles.

The situation for PM 2.5 filters (Table 3) showed, as expected, less central peaking; sulfur  $1.15 \pm 0.02$ , soils  $2.78 \pm 0.67$ , and trace elements  $1.87 \pm 0.38$ ; ignoring some extreme values seen in Cu, Zn, and Br. Again, we were surprised by the degree of central peaking seen in almost all trace elements.

Tables 2 and 4 give statistically derived mean XRF/PIXE integrated scan ratios. These will be discussed later in combination with the correlation plots due to the extreme sensitivity of the statistical values to outliers.

Complete values are given in Appendix F for PM 10 scans and Appendix G for PM 2.5 scans.

Table 1. Degree of Central Peaking of PM 10 Filters  
(average of 2 highest / average of 3 lowest)

	#	<u>Summer</u>	#	<u>Fall</u>	<u>All</u>
Sulfur	(10)	$1.21 \pm 0.12$	(13)	$1.28 \pm 0.14$	$1.245 \pm 0.035$
Al	(--)	NA	(--)	NA	
Si	(10)	$5.19 \pm 1.43$	(13)	$5.41 \pm 1.85$	
K	(09)	$5.10 \pm 0.60$	(13)	$4.17 \pm 1.07$	
Ca	(10)	$6.50 \pm 1.94$	(13)	$5.45 \pm 2.00$	
Ti	(08)	$6.76 \pm 2.41$	(12)	$4.91 \pm 1.52$	-- $5.30 \pm 0.80^*$
Mn	(03)	$4.97 \pm 1.44$	(07)	$2.03 \pm 0.30$	
Fe	(10)	$5.51 \pm 0.81$	(13)	$4.26 \pm 1.34$	
Cl		NA	(01)	3.31	
V		NA		NA	
Cr	(01)	2.39		NA	
Cu	(07)	$2.57 \pm 0.85$	(09)	$2.56 \pm 0.85$	
Zn	(09)	$2.04 \pm 0.07$	(13)	$2.24 \pm 0.85$	-- $2.39 \pm 0.38^{**}$
Br	(01)	2.59	(04)	$1.74 \pm 0.37$	
Pb	(06)	$2.96 \pm 0.12$	(07)	$1.38 \pm 0.14$	

\* - Except Mn, Fall

\*\* - Except Pb, Fall

NA - Not available, no data or estimate

Table 2. Mean ratios of XRF to PIXE Integrated Scan Concentrations for PM 10 Filters

	#	<u>Summer</u>	#	<u>Fall</u>	<u>All</u>
Sulfur	(10)	1.20 ± 0.07	(13)	1.27 ± 0.08	1.235 ± 0.035
Al	(--)	NA	(--)	NA	
Si	(10)	1.11 ± 0.29	(13)	1.31 ± 0.15	1.21 ± 0.10
K	(09)	2.03 ± 0.21	(13)	1.77 ± 0.25	
Ca	(10)	2.08 ± 0.35	(13)	1.80 ± 0.44	
Ti	(08)	2.67 ± 0.51	(12)	2.12 ± 0.60 --	2.06 ± 0.28
Mn	(03)	NA	(07)	1.87 ± 0.04	
Fe	(10)	2.23 ± 0.58	(13)	1.95 ± 0.33	
Cl	(--)	NA	(01)	3.44	
V	(--)	NA		NA	
Cr	(01)	NA		NA	
Cu	(--)	NA	(09)	2.06 ± 1.92	NA
Zn	(09)	1.19 ± 0.18	(13)	1.57 ± 0.50	
Br	(01)	1.91	(04)	1.01  --	1.39 ± 0.31
Pb	(06)	1.53 ± 0.78	(04)	1.12 ± 0.17	

NA - Not available, no data or estimate

Table 3. Degree of Central Peaking of PM 2.5 Filters  
(average of 2 highest / average of 3 lowest)

	#	<u>Summer</u>	#	<u>Fall</u>	<u>All</u>
Sulfur	(12)	1.13 ± 0.06	(18)	1.17 ± 0.09	1.15 ± 0.02
Al	(--)	NA	(--)	NA	
Si	(06)	2.83 ± 1.13	(17)	3.99 ± 2.36	
K	(07)	2.50 ± 0.49	(16)	2.63 ± 1.49	
Ca	(12)	3.31 ± 0.82	(18)	3.68 ± 2.05 --	2.78 ± 0.67
Ti	(02)	1.91 ± 0.26	(05)	2.79 ± 1.66	
Mn	(--)	NA	(07)	1.75 ± 0.43	
Fe	(11)	2.70 ± 0.85	(18)	2.51 ± 1.03	
Cl	(--)	NA	(01)	2.14	
V	(--)	NA	(02)	1.82 ± 0.53	
Cr	(--)	NA		NA	
Cu	(03)	5.74 ± 0.80	(08)	6.09 ± 5.38	NA
Zn	(12)	2.03 ± 0.66	(16)	2.33 ± 1.44	2.18 ± 0.15
Br	(02)	4.72 ± 4.79	(06)	1.96 ± 0.61	
Pb	(06)	1.69 ± 0.33	(14)	1.33 ± 0.21 --	1.51 ± 0.18

NA - Not available, no data or estimate

Table 4. Mean ratios of XRF to PIXE Integrated Scan Concentrations  
for PM 2.5 Filters

	#	<u>Summer</u>	#	<u>Fall</u>	<u>All</u>
Sulfur	(12)	1.18 ± 0.11	(18)	1.26 ± 0.09	1.22 ± 0.04
Al	(--)	NA	(--)	NA	
Si	(06)	0.51 ± 0.26	(17)	1.39 ± 0.44	
K	(07)	0.89 ± 0.27	(16)	1.39 ± 0.41	
Ca	(12)	0.81 ± 0.39	(18)	1.44 ± 0.45	
Ti	(02)	1.77 ± 0.05	(05)	1.93 ± 0.84 --	1.30 ± 0.44
Mn	(--)	NA	(03)	1.65 ± 0.26	
Fe	(11)	1.05 ± 0.23	(18)	1.51 ± 0.41	
Cl	(--)	NA	(01)	2.53	
V	(--)	NA	(01)	1.01	
Cr	(--)	NA	(--)	NA	
Cu	(02)	4.76 ± 4.18	(06)	2.03 ± 0.46	
Zn	(19)	1.40 ± 0.69	(16)	1.50 ± 0.60	
Br	(02)	1.22 ± 0.08	(05)	2.00 ± 1.00 --	1.63 ± 0.33
Pb	(--)	NA	(06)	1.62 ± 0.47	

NA - Not available, no data or estimate

## INTERPRETATION

The aerosol deposits on the SCAQS filters tested by lateral PIXE scans showed a daunting lack of uniformity. We anticipate that given further testing, similar results would be repeated while other sorts of behavior could be uncovered. A larger data set with more PIXE scans would be statistically better and give an improved understanding of the non-uniformities in SCAQS filters.

Table 5 gives the results of the XRF to PIXE integrated scan correlation plots. The results are coded as follows. A "C" code indicates the fit was forced through the origin. A "D" code indicates that one data point has been deleted in the fit. The "E" code indicates that, based upon other data, an estimate can be made of the conversion ratio. For example, the "E" value for aluminum is based on silicon values and the tight Al/Si ratios seen for XRF,  $0.341 \pm 0.047$ , despite a lack of an Al calibration for the PIXE scan. A "S" code indicates that a single conversion factor was derived by including several soil-like elements in one correlation plot. The resulting slope was then used as the conversion factor for each individual soil element. All values marked "NA" require a close look at the raw data because of detectable limit problems (XRF and/or PIXE), extreme variability, etc.

Table 5. Conversion Factors (XRF/PIXE Scan) as Derived from Correlation Plots

<u>Element</u>	<u>PM 10</u>	<u>PM 2.5</u>	<u>PM 10 &amp; 2.5</u>
Na, Mg	NA	NA	NA
Al	1.13E	1.14E	1.13E
Si	1.13	1.17	1.13
P	NA	NA	NA
S	1.22	1.30	1.26
Cl	NA	$2.5 \pm 1.0C$	NA
K	2.07/2.09S	1.6C/1.56S	NA
Ca	2.02/2.09S	1.48/1.56S	NA
Ti		1.9C	NA
V	NA	$1.0 \pm 0.2C$	1.0E
Cr, Co	NA	NA	NA
Mn	1.91	$1.60 \pm 0.2C$	$1.78 \pm 0.18$
Fe	2.30/2.09S	1.91/1.56S	NA
Ni		$1.2 \pm 0.2E$	1.2 E
Cu	1.25C	1.7 C, D	1.47
Zn	1.16C	1.27	1.13
Br	1.60C	$1.4 \pm 0.3$	1.35
Sr, Zr	2.09E	1.56E	NA
Pb	1.28C	$1.1 \pm 0.3$	$1.2 \pm 0.2$

Code: C - Fit constrained through origin  
 D - One datum deleted  
 NA - Not available, no data or estimate  
 E - Estimate, no data  
 S - Soil conversion factor

With the full knowledge that any global attempt to correct the XRF values for filter non-uniformity is impossible without scanning each and every filter, we will present here our "best estimate" of what such a global correction factor might be.

Table 6. Global Conversion Factors (XRF/PIXE Scan) as Derived from Correlation Plots and Ratios

	Correlations	Ratios
1. XRF/PIXE Standards	1.038	1.038
2. PM 10 Soils, (Na, Mg, Al, Si)	1.13	1.21 ± 0.10
PM 10 Soils, (K, Ca, Ti, Fe, Sr, Zn)	2.09	2.06 ± 0.28
3. PM 10 Sulfur	1.22	1.25 ± 0.04
4. PM 10 Combustion-derived aerosols (Mn, Cu, Zn, Br, Pb, V, Ni)	1.30	1.39 ± 0.31
5. PM 2.5 Soils, (Na, Mg, Al, Si)	1.14	1.30* ± 0.44
PM 2.5 Soils, (K, Ca, Ti, Fe, Sr, Zr)	1.56	1.30* ± 0.44
6. PM 2.5 Sulfur	1.30	1.22 ± 0.07
7. PM 2.5 Combustion-derived aerosols (Mn, Cu, Zn, Br, Pb, V, Ni)	1.30	1.63 ± 0.33
* All Soils:	0.82 ± 0.23 Summer	
	1.55 ± 0.21 Fall	

It is our opinion that the values derived from correlation plots are the most reliable, since individual outlying points and extreme behavior such as seen in Cu (and to a lesser extent, Zn and other trace elements), can be evaluated. On the other hand, the mean ratios (XRF/PIXE scan) give uncertainties that show the high degree of variability between some of the filter results.

However, statistically - speaking, one can derive a global average for the XRF vs PIXE integrated scan comparisons. Only PM 10 soils (K, Ca, Ti, Fe) and chlorine (sea salt) are inconsistent with a global correction factor,  $1.31 \pm 0.17$ , for all secondary aerosols (sulfur) and combustion derived trace elements. For the PM 10 soils (K and heavier) and sea salt, a value of  $2.1 \pm 0.28$  is preferred. Light PM 10 soils have a value of  $1.21 \pm 0.10$  consistent with fine aerosols, despite the strong central peak of coarse aerosols. The reason for this is unknown to us. All corrections factors were calculated ignoring the slight difference in calibration, XRF/PIXE scans =  $1.038 \pm 0.045$ .

It is not our contention that application of such factors will solve the dauntingly complex spatial uniformity and contamination problems of the SCAQS

filters. But application of these factors, plus a dose of skepticism about "outlier" values such as seen in Cu and Zn, will result in an improved data set.

## SELECTED REFERENCES

1. Fitz, D., Zwicker, J.. 1988. Design and Testing of the SCAQS Sampler for the SCAQS Study 1987, ARB Contract No. A6-077-32.
2. Fujita, E.M., J.F. Collins. 1989. Quality assurance for the southern california air quality study. Presented at the 82nd Annual Meeting of the Air and Waste Management Association, Anaheim, Calif., June 25 - 30, 1989.
3. Cahill, T.A.. 1989. Particle induced x-ray emission. Metals Handbook Ninth Edition.
4. Cahill, T.A., P.J. Feeney, R.A. Eldred. 1987. Size-time profile of aerosols using the DRUM sampler. Nuclear Instruments and Methods in Physics Research B22: 344-348.
5. Cahill, T.A., Y. Matsuda, D.J. Shadoan, R.A. Eldred, P.J. Feeney and B.H. Kusko. 1984. Complete elemental analysis of aerosols: PIXE, FAST, LIPM, and Mass. Nuclear Instruments and Methods B3: 291-295.
6. Campbell, D., S. Copeland, T.A. Copeland, R.A. Eldred, C., Cahill, and J. Vesenska. 1989. The coefficient of optical absorption from particles deposited on filters: integrating plate, integrating sphere, and coefficient of haze measurements. Presented at the 82nd Annual Meeting of the Air and Waste Management Association, Anaheim, Calif., June 25 - 30, 1989.
7. Collins, J., E.F. Fujita. 1989. Fax transmittal of XRF data from EPA.

\*00001959\*



ASSET